The ecological structure of *Laminaria hyperborea* kelp forests along the North Sea coast of the United Kingdom.

Volume 1/1

Harrison John Norman Catherall

Thesis submitted to the School of Natural and Environmental Sciences in fulfilment for the requirements of the degree of Doctor of Philosophy.

December 2024

Abstract

While kelp forests play a crucial role in coastal ecosystems, providing habitat, supporting biodiversity, and contributing to carbon sequestration, their response to environmental perturbations, such as pollution, is not well understood. This thesis investigated the structure and ecological function of *Laminaria hyperborea* kelp forests along the understudied UK North Sea coastline, with a focus on the impacts of historic coal mine waste on kelp growth, productivity, and associated biodiversity (including microbiome).

Field surveys were conducted to assess the structural characteristics and carbon standing stock of kelp forests in northeast England and southeast Scotland. The results indicate significant variation in kelp forest structure across depth gradients and small spatial scales. Kelp density, biomass, and length decreased with depth, while carbon standing stock varied across sites, highlighting the influence of local environmental factors. This work provides a baseline for kelp forests in understudied regions of the UK's North Sea and gives evidence to suggest they are structured and function similarly to *L hyperborea* forests at similar latitudes.

To investigate the effects of coal mine waste on kelp forests ecosystems, comparative studies were conducted between polluted and non-polluted sites. The results show that kelp forests affected by historic coal mine waste have largely recovered, with growth patterns and carbon contributions similar to unpolluted sites. However, holdfast-associated fauna exhibited reduced abundance and diversity in polluted areas. Whilst this was predominantly an effect of habitat volume, it suggests that there could be lingering ecological impacts that may be affecting broader ecosystem dynamics. Additionally, examination of the effects of historic pollution on the kelp microbiome showed that while bacterial taxa adapted to polluted sites were more abundant, the overall diversity, structure, and abundance of surface microbiomes were similar between polluted and non-polluted kelp forests.

This research advances understanding of both natural and pollution-driven variability in *L. hyperborea* forests, demonstrating that while the structural recovery of kelp forests impacted by mining activities has been successful, biodiversity in some areas remains compromised. These findings underscore the resilience of kelp ecosystems but also highlight the ongoing need for conservation and management to protect these valuable habitats from historic and future environmental stressors.

Acknowledgements

I would like to express my thanks to my supervisors, Prof. Pippa Moore and Dr. Heather Sugden, whose excellent guidance and support over the last four years have been instrumental in the completion of this thesis. Without their mentorship, I would not be in the position of finalising a PhD thesis today. Pip, your support has been unparalleled, spanning nearly a decade—from receiving a handwritten letter of encouragement for my undergraduate application, to teaching and supporting me during my undergraduate thesis, and finally guiding me through my PhD journey. I am deeply grateful for the countless opportunities you've created for me throughout this time. These opportunities have taken me to new continents, enabled me to gain invaluable experiences, and helped me achieve qualifications I could never have imagined. Heather, my heartfelt thanks go to you for being a source of clarity and encouragement during the more challenging periods of this journey. Your guidance during times of slow progress and high stress was crucial in helping me push through those moments and move steadily toward the end goal.

I would also like to extend my gratitude to the Dove Marine Laboratory community. From starting in a quiet building in 2021 to finishing in a vibrant hub, it has been a privilege to see the Dove community grow and flourish. I wish the research group and the broader community all the best in continuing to build a strong and dynamic society in the years to come. I am especially grateful for everyone's assistance with fieldwork over the years, particularly Hannah Earp, who endured the brutally cold and challenging campaigns that were essential to my research. These are some of my fondest memories of the PhD experience.

Finally, I would also like to acknowledge my family for their support. My parents provided the foundation for my studies, supporting my early education and encouraging my ensuing endeavours, which has allowed me to reach this stage. For this, I am deeply grateful. And to Lucy - thank you for being by my side throughout this journey. You have been my sounding board, my source of unwavering support, and my constant companion throughout the process. I am incredibly grateful for everything you have done to help me reach this point.

Table of Contents

Abstract ii
Acknowledgements iii
Table of Contents iv
List of figures vi
List of tables viii
List of abbreviations and acronyms x
Chapter 1 . General introduction 1
1.1 Introduction to kelp forests globally 1
1.2 Introduction to *Laminaria hyperborea* 2
1.3 Kelp forest productivity 5
1.4 Anthropogenic influences affecting kelp forests 6
1.5 Coal mining in the United Kingdom 7
1.6 Aims and hypotheses 15
Chapter 2 . Regional-scale variability in the structure and carbon standing stock of *Laminaria hyperborea* forests across gradients of depth in the North Sea. 17
2.1 Introduction 17
2.2 Methods 19
2.2.1 Kelp forest structure and depth distribution 19
2.2.2 Carbon standing stock 22
2.2.3 Environmental data 22
2.2.4 Statistical analysis 23
2.3 Results 24
2.3.1 Spatial variability in the structure of *L. hyperborea* forests 24
2.3.2 Environmental drivers 27
2.3.3 Depth distribution of kelp forests in NE England and SE Scotland 27
2.3.4 Carbon standing stock 31
2.4 Discussion 32
Chapter 3 . Growth and productivity of kelp forests along a historically industrialised coastline 40
3.1 Introduction 40
3.2 Methods 43
3.2.1 Study design and location 43
3.2.2 Kelp forest structure 44
3.2.3 Biomass accumulation and loss 46
3.2.4 Statistical analysis 48
3.3 Results 49

3.3.1 Kelp forest structure 49
3.3.2 Biomass accumulation and loss 52
3.4 Discussion 56
Chapter 4 . Variability in macroinvertebrate assemblages associated with *Laminaria hyperborea* stipes and holdfasts along a historically industrialised coastline. 61
4.1 Introduction 61
4.2 Methods 64
4.2.1 Study design 64
4.2.2 Statistical analysis 66
4.3 Results 67
4.4 Discussion 74
Chapter 5 . Patterns in *Laminaria hyperborea* bacterial microbiome community structure across a range of spatial scales along a historically industrialised coastline 80
5.1 Introduction 80
5.2 Methods 83
5.2.1 Sampling 83
5.2.2 Sequence processing 85
5.2.3 Statistical analysis 86
5.3 Results 87
5.3.1 Shared ASVs 88
5.3.2 Diversity and assemblage structure 90
5.3.3 Core assemblage 92
5.4 Discussion 99
Chapter 6 . General discussion 106
6.1 Overview 106
6.2 Recovery of kelp forests and persistent impacts of historical mine wastes 108
6.3 Limitations of thesis and suggestions for future work 110
6.4 Conclusions 112
References 114
Supplementary materials 129

List of figures

Figure 1.1. Coal mine waste on the shores of Durham with two different methods of disposal shown. Top image shows Easington (site C2) in 1992. Bottom image shows Blackhall Rocks (year unknown). Credit/Durham Heritage Coast. 9
Figure 1.2. Blast Beach, County Durham, 1974 (top) and present day (bottom) demonstrating the significant quantity of mine waste deposited. Credit/DM Allen (bottom image). Red arrows indicate the location of sampling at site C1 in Chapters 3-5 of this thesis, which was buried under coal spoil during the mining period. 11
Figure 1.3. Minewater discharge at Blackhall Rocks on the County Durham coast, 1974. Credit/Catherine Smith. 13
Figure 1.4. The 'coal shelf' at Blast Beach (Site C1), County Durham, showing present day evidence of historic coal mining waste disposal. 14
Figure 2.1. Study regions across the United Kingdom: (A) NE England, (B) SE Scotland, (C) N Scotland, (D) W Scotland, (E) SW Wales, (F) SW England. Small maps indicate locations of study sites within each region. Regions A and B are new survey regions sampled in the present study. Data for the previously sampled regions of C-F are from Smith et al. (2022). 21
Figure 2.2. Structure of Laminaria hyperborea populations at sites within regions A (NE England) and B (SE Scotland) at a depth of 5 m BCD. Bars represent mean values ± SE. Points represent raw data values. (n ≥ 6 for quadrat-level variables: A, B & F; n ≥ 9 for plant-level variables: C, D, E & G). FW: Fresh Weight. Ind.: Individual. See Figure 2.1 for study site locations. 25
Figure 2.3. Structure of Laminaria hyperborea populations at sites within regions A (NE England) and B (SE Scotland) at depths of 2 m, 5 m and 7-10 m BCD. Bars represent mean values ± SE. Points represent raw data values. (n ≥ 6 for quadrat-level variables: A, B & F; n ≥ 9 for plant-level variables: C, D, E & G). FW: Fresh Weight. Ind.: Individual. See Figure 2.1 for study site locations. 29
Figure 2.4. Estimated *Laminaria hyperborea* canopy carbon standing stock (g C m^{-2}) at study sites around the United Kingdom. Bars represent mean values ± SE, n = 8-10. See Figure 2.1 for study site locations. 31
Figure 3.1. Study area (a) showing the position of the two sites (1 and 2) within each of three sampling locations (A, B and C) (b). Sampling locations A and C represent areas impacted by mining waste, while B was unaffected. 44
Figure 3.2. Structure of Laminaria hyperborea forests at sites affected (locations A & C) and unaffected (location B) by historic coal mine waste disposal in northeast England. Bars represent mean values ± SE (n=10). Points represent raw data values. FW: Fresh Weight. Ind.: Individual. Site and locations can be seen in Figure 3.1. 51
Figure 3.3. Carbon standing stock of Laminaria hyperborea forests at sites in northeast England affected (locations A and C) and unaffected (location B) by historic coal mine waste disposal. Bars represent mean values ± SE. Ind.: Individual. Sites and locations can be seen in Figure 3.1. 52
Figure 3.4. Annual pattern of biomass accumulation (a), biomass loss through erosion (b) and biomass loss through whole plant dislodgement (c) occurring in Laminaria hyperborea forests at sites in northeast England affected (locations A and C) and unaffected (location B) by historic coal mine waste disposal. Points represent mean values ± SE. Dashed lines between points where data was not collected in consecutive months. Ind.: Individual. Sites and locations can be seen in Figure 3.1. 54
Figure 4.1. Study area (a) showing the position of the two sites (1 and 2) within each of three sampling locations (A, B and C) (b). With locations A and C (green points) representing sites impacted by mining waste and location B (yellow points) not affected by mining waste. 65

Figure 4.2. Proportion of macroinvertebrate phyla associated with Laminaria hyperborea (a) holdfasts and (b) stipes. Sites and locations can be seen in Figure 4.1. Lack of data for stipe fauna at site C2 was due to no organisms being present on stipes. 68
Figure 4.3. Univariate metrics of holdfast associated macroinvertebrate assemblages: (a) species richness, (b) abundance, (c) Shannon-Weiner diversity (H') and (d) Pielou's evenness (J'). Values represent means ± 1 SE. n=5. Sites and locations can be seen in Figure 4.1. 69
Figure 4.4. Univariate metrics of stipe associated macroinvertebrate assemblages: (a) species richness, (b) abundance, (c) Shannon-Weiner diversity (H') and (d) Pielou's evenness (J'). Values represent means ± 1 SE. n=5. Sites and locations can be seen in Figure 4.1. 70
Figure 4.5. Non-metric MDS plot of holdfast associated macroinvertebrate assemblage structure of Laminaria hyperborea individuals at sites subjected to coal waste dispersal (Locations A & C) and sites not directly exposed to such pollution (Location B). Sites and locations can be seen in Figure 4.1. Point size indicates holdfast volume (ml). Data based on modified Gower similarity derived from square root transformed abundance data. Each point represents a single holdfast. 71
Figure 4.6. Non-metric MDS plot of stipe associated macroinvertebrate assemblage structure of Laminaria hyperborea individuals at sites subjected to coal waste dispersal (Locations A & C) and sites not directly exposed to such pollution (Location B). Sites and locations can be seen in Figure 4.1. Data based on modified Gower similarity derived from square root transformed abundance data. Each point represents a single stipe. 72
Figure 4.7. Taxa contributing to the average dissimilarity between holdfast associated macroinvertebrate assemblages at sites subjected to coal waste dispersal (Locations A & C) and sites not directly exposed to such pollution (Location B) as determined by SIMPER analysis performed on square root transformed data. Bubble size indicates relative abundance of taxa at each site after standardisation by holdfast volume. Site locations can be seen in Figure 4.1. See Table S4.2 for full SIMPER tables. 73
Figure 4.8. Taxa contributing to the average dissimilarity between stipe associated macroinvertebrate assemblages at sites subjected to coal waste dispersal (Locations A & C) and sites not directly exposed to such pollution (Location B) as determined by SIMPER analysis performed on square root transformed data. Bubble size indicates relative abundance of taxa at each site. No taxa were recorded at site C2. Sites and locations can be seen in Figure 4.1. See Table S4.3 for full SIMPER tables. 74
Figure 5.1. Before (1992) (A) and after (2010) (B) the 'Turning The Tide' project undertook remediation of coal mining waste on the foreshore at Easington, County Durham, UK (site C2 – Site locations can be seen in Figure 5.2). (Image A: Durham Heritage Coast. Image B: Durham Heritage Coast/Credit Mike Smith) 82
Figure 5.2. Study area (a) showing the position of the two sites (1 and 2) within each of three sampling locations (A, B and C) (b). With A and C representing sites impacted by mining waste disposal and site C not affected by mining waste disposal 84
Figure 5.3. Relative abundance of bacterial microbiome classes found on the surface microbiome of Laminaria hyperborea blade and holdfast tissues, rock biofilms and seawater controls from two sites within each of three locations. Sites and locations can be seen in Figure 5.2. Classes contributing to <1% abundance were merged into a single category. 88
Figure 5.4. Overlap of bacterial ASVs from the surface microbiome of Laminaria hyperborea blade (a) and holdfast (b) tissue samples from polluted and non-polluted sites. Total abundance of Venn diagram segments for blade samples (c) and holdfast samples (d) standardised by number of regions represented in each Venn diagram segment. 89
Figure 5.5. Bacterial microbiome alpha diversity metrics (Chao1 (top) and Shannon-Weiner (bottom)) sampled from Laminaria hyperborea holdfast and blade tissues, and rock biofilms and seawater controls from two sites within each of three locations. Site locations can be seen in Figure 5.2. 92

Figure 5.6. Bacterial microbiome assemblage structure associated with Laminaria hyperborea (a), as well as for blade (b), holdfast (c), rock biofilms (d) and seawater controls (e) from two sites within each of three locations. Sites and locations can be seen in Figure 5.2. Data based on Bray-Curtis similarity. Each point represents a sample taken from an individual kelp, rock biofilm or water sample. 94
Figure 5.7. Relative abundance of the bacteria within the core bacterial surface microbiome of Laminaria hyperborea blade and holdfast tissues, rock biofilms and seawater controls from two sites within each of three locations. Sites and locations can be seen in Figure 5.2. Core bacterial assemblages are defined as taxa present in >95% of samples at a relative abundance of >0.1%. Taxonomic classification given as precursor (f_ = Family, o_ = Order) in the legend. Where no precursor is given, taxonomic classification is to genus or species level. Where "sp." is given, taxonomic classification is to genus level. Abundance is relative to whole bacterial assemblage. 96
Figure 5.8. Core bacterial microbiome alpha diversity metrics (Chao1 (top) and Shannon-Weiner (bottom)) from Laminaria hyperborea holdfast and blade tissues, rock biofilms and seawater controls from two sites within each of three locations. Sites and locations can be seen in Figure 5.2. Core bacterial assemblages are defined as taxa present in >95% of samples at a relative abundance of >0.1%. 97
Figure 5.9. Core bacterial microbiome assemblage structure associated with Laminaria hyperborea (a), as well as for blade (b), holdfasts (c), rock biofilms (d) and seawater controls (e) from two sites within each of three locations. Sites and locations can be seen in Figure 5.2. Core bacterial assemblages are defined as taxa present in >95% of samples at a relative abundance of >0.1%. Each point represents a sample taken from an individual kelp, rock or water sample. 97
Figure 6.1. Coal mine waste washed ashore in Northumberland near to location B. Locations can be seen in Figure 5.2. 109

List of tables

Table 2.1. Environmental drivers of kelp forest structure at six study sites within two regions of NE England and SE Scotland. Mean annual sea surface temperature (SST) and chlorophyll a values were extracted from Bio-ORACLE (Assis et al., 2018) for the years 2000 to 2014. Wave fetch values are extracted from Burrows (2020). Urchin density is the average number of Echinus esculentus recorded in 5-8 replicate 1 m^2 quadrats at a range of sampling depths at each site. Site locations can be seen in Figure 2.1. 26
Table 2.2. Univariate permutational ANOVAs to test for variability in population and individual level kelp metrics between regions and sites at a depth of 5 m BCD. Significant values ($p < 0.05$) are indicated in **bold**. Significance values followed by a '†' are derived from Monte Carlo simulations. Variables per m^2 and per canopy-forming individual tested between two study regions (A and B), carbon standing stock tested between all six regions (A-F: Figure 2.1). 26
Table 2.3. Univariate permutational ANOVAs to test for variability in population and individual level kelp metrics between regions, sites and depths for two regions in the UK (A and B; Figure 2.1). Significant values ($p < 0.05$) are indicated in **bold**. Significance values followed by a '†' are derived from Monte Carlo simulations. 30
Table 3.1. Univariate permutational ANOVAs to test for variability in population and individual level kelp metrics between time points, levels of pollution and sites (nested in pollution). Models were run using 9,999 permutations based on similarity matrices derived from Euclidian distances, with 'Time'

(where applicable) as a fixed factor, 'Pollution' as a fixed factor and 'Site' as a random factor nested within 'Pollution'. Significant values ($p < 0.05$) are indicated in **bold**. Significance values followed by a '†' are derived from Monte Carlo Simulations due to the low number of unique permutations. p-values underlined indicate a significant result of PERMDISP tests and therefore a significance threshold reduction to $p < 0.01$. '-' indicates the term was not included in the statistical model. 55
Table 3.2. Univariate permutational ANOVAs to test for variability in biomass accumulation, biomass loss through erosion and biomass loss through whole plant dislodgement between months (where applicable), levels of pollution and sites (nested in pollution). Models were run using 9,999 permutations based on similarity matrices derived from Euclidian distances, with 'Month' as a fixed factor, 'Pollution' as a fixed factor and 'Site' as a random factor nested within 'Pollution'. Significant values ($p < 0.05$) are indicated in **bold**. Significance values followed by a '†' are derived from Monte Carlo Simulations due to the low number of unique permutations, and p-values underlined indicate a significant result of PERMDISP tests and therefore a significance threshold reduction to $p < 0.01$. '-' indicates the term was not included in the statistical model. 55
Table 4.1. Univariate PERMANOVA testing variation in holdfast and stipe associated macroinvertebrate faunal abundance and diversity metrics between levels of pollution and sites (nested in pollution). Holdfast volume was used as a covariate in tests of holdfast abundance and diversity metrics. Results indicated with 'ŧ' are derived from Monte-Carlo simulations due to a low number of unique permutations. Significant results are indicated in **bold**. 72
Table 4.2. Multivariate PERMANOVA testing variation in holdfast and stipe associated macroinvertebrate assemblage structure between levels of pollution and sites (nested in pollution). Holdfast volume was used as a covariate for comparisons of holdfast assemblage structure. Results indicated with 'ŧ' are derived from Monte-Carlo simulations due to a low number of unique permutations. Significant results are indicated in **bold**. 73
Table 5.1. Univariate PERMANOVA testing variation in bacterial microbiome alpha diversity indices (Chao1 and Shannon-Weiner) between tissue types, different levels of pollution and sites nested within pollution. Results indicated with 'ŧ' are derived from Monte-Carlo simulations due to the low number of unique permutations. Significant results are indicated in **bold.** 93
Table 5.2. Multivariate PERMANOVA testing variation in bacterial microbiome assemblage structure between tissue types, level of pollution and sites nested in pollution. Results indicated with 'ŧ' are derived from Monte-Carlo simulations due to the low number of unique permutations. Significant results are indicated in **bold.** 93
Table 5.3. Multivariate PERMANOVA testing variation in core bacterial microbiome assemblage structure between tissue type, level of pollution and site nested in pollution. Results indicated with 'ŧ' are derived from Monte-Carlo simulations due to the low number of unique permutations. Significant results are indicated in **bold.** 98
Table 5.4. Univariate PERMANOVA testing variation in core bacterial microbiome alpha diversity indices (Chao1 and Shannon-Weiner) between tissue types, levels of pollution and sites nested within pollution. Results indicated with 'ŧ' are derived from Monte-Carlo simulations due to the low number of unique permutations. Significant results are indicated in **bold.** 98

List of abbreviations and acronyms

ASV – Amplicon sequence variant

BCD – Below chart datum

cm – centimetre

DW – Dry weight

FW – Fresh weight

HDS – High density sludge

Ind. – Individual

km – kilometre

L. hyperborea – *Laminaria hyperborea*

m – metre

N – North

NE – Northeast

SAC – Special area of conservation

SCUBA – Self-contained underwater breathing apparatus

SE (followed by geographic region) – Southeast

SE (in numerical context) – Standard error

SPA – Special protection area

SST – Sea surface temperature

SSSI – Site of special scientific interest

SW – Southwest

UK – United Kingdom

Chapter 1. General introduction

1.1 Introduction to kelp forests globally

Kelps are a group of large, canopy forming macroalgae belonging to the order Laminariales. Globally there are approximately 112 species belonging to 33 genera (Bolton, 2010) that are distributed along ~36% of global coastlines (Jayathilake and Costello, 2021). Confined to areas of temperate and subpolar rocky reef, kelp often form dense stands referred to as forests. Kelp forests are ecologically, and in some regions commercially important biogenic habitats that provide a range of ecosystem goods and services (Beaumont et al., 2008; Smale et al., 2013). Through high primary productivity they underpin marine food webs and support a diverse range of associated assemblages (Dayton, 1985; Duarte and Cebrián, 1996; Rassweiler et al., 2018; Elliott Smith and Fox, 2022). The organisms they support range from small invertebrates (Zahn et al., 2016; King et al., 2021) and algae (Leliaert et al., 2000) to fish (Pérez-matus et al., 2007; Jackson-Bue et al., 2023) and large mammals (Steneck et al., 2002), some of which are commercially important (Smale et al., 2022). As well as supporting high levels of macroorganism biodiversity, they also support a high diversity of associated microorganisms, such as bacteria that form part of their microbiome (Singh and Reddy, 2016; Ramírez-Puebla et al., 2022). In addition, the physical structure of kelp contributes to a range of coastal processes including carbon storage (Pessarrodona et al., 2018), nutrient cycling (Pfister, Altabet and Weigel, 2019), nearshore sedimentation (Connell, 2005) and coastal protection through wave attenuation (Pinsky, Guannel and Arkema, 2013), making kelp 'true' ecosystem engineers (Steneck et al., 2002).

The degree to which kelp forests contribute to coastal processes is strongly influenced by their structure and spatial extent. Numerous physical factors interact to determine the structure and extent of kelp forests, including temperature (Smith et al., 2022; Wernberg et al., 2015), wave exposure (Harrold, Watanabe and Lisin, 1988; Norderhaug et al., 2012; Pedersen et al., 2012) and light availability (Desmond et al., 2015; Smith et al., 2022). Additionally, biological factors such as herbivory (Watanabe and Harrold, 1991; Hjorleifsson, Kassa and Gunnarsson, 1995; Scheibling, Hennigar and Balch, 1999) and competition (Arkema, Reed and Schroeter,

2009) also influence kelp forest structure and in some cases, can lead to complete losses of kelp forest habitat (Sivertsen, 1997). However, rapidly changing environmental conditions and increasing anthropogenic influences on marine environments have had negative impacts on the structure and functioning of kelp forests globally and are likely to pose a threat into the future (Ling et al., 2009; Arnold et al., 2016; Provost et al., 2017; Wernberg et al., 2024). One such example is the effect of climate change, which, through increased sea surface temperatures has induced shifts in species distributions (Smale et al., 2020), and marine heatwaves which are responsible for the alteration and collapse of kelp forests across multiple continents (Tyler-Walters, 2007; Arafeh-Dalmau et al., 2019; Smale et al., 2019; Wernberg, 2021). Alongside changing environmental conditions, human activities on land, such as coastal development and agricultural practices, can result in the degradation and loss of kelp forests through the reduction of water quality and an increase in light attenuation (Krumhansl et al., 2016). With climate change and human population growth predicted to increase in future years (United Nations, 2022; IPCC, 2023), anthropogenic stressors are likely to intensify, and further degradation of kelp forest habitats is expected.

1.2 Introduction to *Laminaria hyperborea*

The coastal waters of the United Kingdom are occupied by seven species of kelp, of which *Laminaria hyperborea* is the dominant canopy forming species on moderately to fully wave exposed coastlines (Smale et al., 2016). Found in rocky subtidal habitats, its range extends from northern Portugal (Pinho et al., 2016) to northern Norway (Sjøtun et al., 1993) and across the Barents Sea to northwest Russia (Schoschina, 1997; Müller et al., 2009). Whilst it has been recorded at depths of >40 m in clear waters off St Kilda, Scotland (Hiscock, 1992; Tyler-Walters, 2007), it is more typically found at depths of 15 to 20 m, particularly around much of the UK coastline (Smith et al., 2022) and extends right up to the shallow subtidal zone. Research conducted by Kain and Jones provided early insights into the biology and life history of *L. hyperborea,* examining aspects such as physical structure (Kain and Jones, 1963), patterns of growth (Kain and Jones, 1976), interactions with environmental factors (Kain and Jones, 1977) and reproductive mechanisms (Kain, 1971). This body of work described *L. hyperborea* as a stipitate kelp, distinguished by its characteristically large holdfast that provides habitat to a diverse assemblage of macroinvertebrates, and a long epiphyte covered stipe that holds the

photosynthetic blades towards the light. Growth in *L. hyperborea* occurs from the meristematic junction, the transition zone between the stipe and blade. It is from this meristematic junction that both stipe elongation and blade growth occur (Kain and Jones, 1976). Simultaneously, tissue loss via erosion takes place at the blade tips, defined as 'conveyor-belt' growth in which new tissue is continuously produced at the meristem while older tissue is lost at the distal blade ends (Mann, 1973). *L. hyperborea* is a perennial species that has a characteristic seasonal growth pattern. From January to June, the blades grow rapidly, followed by a marked reduction in the rate of growth during the latter months of the year (Kain and Jones, 1976; Pessarrodona, Foggo and Smale, 2019). This slower period of growth produces a narrow band of tissue that forms just above the meristem, creating a "growth collar" that persists on the blade for an entire cycle of blade growth. This collar forms the junction between old and new blade growth until April or May, when the older blade growth detaches (Pessarrodona, Foggo and Smale, 2019). This shedding event, termed May cast, serves as an important source of carbon that is donated to potential receiver habitats (Pessarrodona et al., 2018). Stipe elongation and girth extension also take place during the same months as blade growth. The seasonal variability in the rate of girth extension generates concentric bands within the stipe which are visible when the stipe is cross sectioned and provides a means of age determination (Kain and Jones, 1963). Growth continues for the entirety of an individual's life, which can be over 20 years but is more typically 7 to 12 years, in which time a total length of up to 400 cm can be achieved (Kain and Jones, 1963; Smale et al., 2016; Smith et al., 2022).

Despite the seminal work on UK kelp forest ecology of the 1960's-1970's (Jones and Kain, 1967; Kain, 1971; Kain and Jones, 1963, 1976, 1977), until the mid-2010s there had been little work to further our knowledge and understanding of UK kelp forest ecology. Consequently, the state of knowledge on these ecosystems lagged behind that of other leading scientific nations (Smale et al., 2013). More recent research efforts over the last decade have, however, significantly furthered our understanding of the structure and function of *L. hyperborea* forests in the UK, the assemblages they support and the environmental variables that shape them (Bué et al., 2020; Earp et al., 2024; Gouraguine et al., 2024; Jackson-Bue et al., 2023; King et al., 2021; Smale et al., 2016; Smale et al., 2022; Smith et al., 2022; Teagle et al., 2017, 2018). These works have focussed solely on the northern and western coasts of the UK, leaving a

significant gap in our knowledge on the structure and functioning of kelp forests that occupy the eastern coasts of the UK. These works, however, demonstrate a high degree of variability in *L. hyperborea* structure and function over a range of spatial scales. Over larger scales such that of the latitudinal gradient of the UK, stronger patterns emerge in kelp forest structure that correspond with shifts in environmental variables (Smale et al., 2016; Smale and Moore, 2017). Since *L. hyperborea* is a cold-temperate species, the growth of sporophytes is compromised at temperatures over 20°C and gametophytes cannot persist above 21°C (Bolton and Lüning, 1982; Müller et al., 2009). The cooler, northernmost regions of the UK therefore provide more suitable temperature conditions than warmer southerly areas where temperatures regularly exceed 18°C (Morris et al., 2018). A similar pattern is also observed for light since kelp are autotrophic and rely on light for photosynthesis. Kelps synthesise and store carbohydrates during summer months to be utilised for growth in the following winter growth period (Rinde and Sjøtun, 2005). With summer day lengths in the UK being longer in northern regions, kelp in these regions have lengthier periods of time to produce valuable growth compounds which results in individuals of greater biomass (Rinde and Sjøtun, 2005). Whilst summer day length has a positive effect on *L. hyperborea* performance, irradiance levels also have an influence, and are responsible for driving variations in measures including length, biomass, density and recruitment that have been observed over smaller spatial scales within this species range (Gorman et al., 2013; Bekkby et al., 2019). Wave exposure similarly varies along horizontal gradients, and significantly influences kelp, producing greater densities along with higher biomass and longer individuals at more wave exposed locations (Smale et al., 2016). This is due to greater water velocity enhancing photosynthesis rates and inorganic nutrient uptake that results in elevated growth rates and increased primary productivity (Hurd, 2000; Pedersen et al., 2012). Wave exposure can also have profound influences over smaller spatial scales, with biomass and densities often measured to be several times greater at high wave exposure sites over low exposure sites (Smale et al., 2016). Larger individuals, however, take up more space which results in more northerly regions of the UK having lower densities than the warmer, southerly regions that are occupied by smaller individuals (Pessarrodona et al., 2018; Smale et al., 2016; Smith et al., 2022). The morphology of kelp heavily influences the amount of carbon stored within kelp forests at any one point in time, with larger individuals that have greater biomass containing more carbon (Smale et al., 2016). Therefore, the environmental drivers of kelp forest structure also control the standing stock of carbon, resulting in greater

amount of carbon being stored within kelp forests in the more northerly regions of the UK (Pessarrodona et al., 2018).

1.3 Kelp forest productivity

Since kelp forests store a significant amount of carbon within their tissues, coupled with the growth strategy they exhibit, they form some of the most productive coastal vegetated habitats globally (Duarte et al., 2013). They are not, however, considered to play a primary role in carbon sequestration and cycling. This is due, in part, to the assumption that kelp tissue decomposes too quickly for it to be transported long distances for burial (Howard et al., 2017), but also due to the lack of reliable estimates of carbon fixation, donation, and spatial extent for many species (Reed and Brzezinski, 2009). Not to mention that kelp grow on rocky substrate and are unable to fix carbon in situ into sediment as most other productive vegetated coastal ecosystems do (Hill et al., 2015). A growing body of evidence suggests carbon from macroalgal habitats can be transported long distances from source and to substantial depths (Hobday, 2000). Through video recordings kelp blades have been viewed in fjords at depths of 450 m at an estimated biomass of over 22 g per m^2 (Filbee-Dexter et al., 2018), and analysis of sediment samples of depths down to 262 m shows much of the organic matter to originate from *L. hyperborea* forests (Abdullah, Fredriksen and Christie, 2017). Whilst there's still a lack of information on the pathways of kelp derived organic matter burial, evidence suggests that a large proportion of annual kelp production is deposited into benthic sediments where long-term burial is possible (Abdullah, Fredriksen and Christie, 2017). With the extent of suitable *L. hyperborea* forest habitat around the UK estimated to be 15,984 km^2 (Yesson et al., 2015), the release of considerable quantities of kelp-derived organic matter from these forests likely represents a significant subsidy to surrounding ecosystems and a potential contributor to carbon burial in soft sediment habitats (Pessarrodona et al., 2018).

Not only is the long-distance transportation of kelp derived organic matter potentially very important for carbon storage, but blade material shed from *L. hyperborea* and transported to deep water fjords has been shown to support elevated abundances of deep-water shrimp and amphipods (Ramirez-Llodra et al., 2016). *L. hyperborea* blades also regularly provide food and

habitat to grazing gastropods such as *Patella pellucida* which can be found in considerably elevated abundances (pers. obs.). However, the stipe and holdfast of *L. hyperborea* support significantly greater levels of abundance than the blade. Epiphytic algae covering the stipe of *L. hyperborea* provides habitat for a wide variety of macroinvertebrate fauna, normally dominated by amphipods (King et al., 2021), and holdfasts have root like structures called haptera that create interstitial space for a huge diversity of macroinvertebrate fauna to occupy (Teagle et al., 2018). The number of individuals within a single *L. hyperborea* holdfast can be in the thousands, including over 100 different species (Teagle et al., 2017). Whilst the abundance and diversity that holdfasts support varies with numerous factors such as wave exposure (Norderhaug et al., 2012), turbidity (Moore, 1973) and holdfast size (Teagle et al., 2018), values at the lower end of the published estimates of abundance suggest an individual kelp can support several hundred macroinvertebrates (Sheppard, Bellamy and Sheppard, 1980). In the context of kelp forests with high densities of individual kelp, this is a significant quantity of invertebrates that, along with the assemblages of the general kelp forest understory (Earp et al., 2024), have been shown to support wider diversity through the provision of food (Norderhaug et al., 2005). Additionally, the physical structure of kelp forests provides shelter and refugia to a range of organisms including fish and commercially important crustaceans (Smale et al., 2022; Jackson-Bue et al., 2023). While the diversity associated with kelp forests is well understood, kelp also support a wide range of microorganisms on their surface which are often not considered when discussing associated diversity. Bacteria, fungi, viruses and micro-eukaryotes form the 'microbiome' which acts as the mediator of host functioning and development (Adair and Douglas, 2017). The exact functional roles of the microorganisms that form the microbiome are still not fully understood, however, they are known to influence the hosts resilience to environmental stress and prevent disease, and disruptions in their structure can lead to host mortality and widespread losses (Egan and Gardiner, 2016; Zozaya-Valdés et al., 2017).

1.4 Anthropogenic influences affecting kelp forests

Loss of kelp forests has been documented in many countries globally, including Japan (Tanaka et al., 2012), Australia (Connell et al., 2008; Wernberg, 2021), Canada (Filbee-Dexter, Feehan and Scheibling, 2016) and Norway (Moy and Christie, 2012). The primary reasons for these

losses are 1) an increase in ocean temperature that creates vulnerability through declines in reproduction and growth rates and exceeds physiological tolerance limits (Harley et al., 2012; Wernberg et al., 2013), and 2) changing environmental conditions that influence biotic interactions including epiphytism and herbivory that leads to weakening of individuals and increased fragmentation (Krumhansl, Lee and Scheibling, 2011; Andersen et al., 2011; Schiel, Steinbeck and Foster, 2014). However, since *L. hyperborea* follows an abundant centre hypothesis with the UK central within its range, UK kelp forests are relatively free from the environmental stressors that negatively affect the structure of range edge populations (Smale et al., 2013). Whilst widespread losses have not been documented in the UK, there are examples of localised stressors negatively impacting kelp forest structure and leading to localised loss of habitat. One such example on the Sussex coast was driven by damaging fishing practices and intense storms that resulted in the loss of around 95% of kelp forests along a ~35 km stretch of coastline (Williams and Davies, 2019). Another example, and a focus of the studies within this thesis, was the loss of kelp forests through the disposal of coal mining waste materials onto shores in northeast England.

1.5 Coal mining in the United Kingdom

Coal mining in the UK was an important industry, fuelling the industrial revolution and providing the main source of energy for electricity generation for over 80 years (Palumbo-Roe and Colman, 2010; Durucan, Jozefowicz and Brenkley, 2010). The coalfields of County Durham (hereafter referred to as 'Durham') and Northumberland were some of the most productive in the country, characterised uniquely by coal seams extending into the North Sea (Alderton, 2012; Cooper et al., 2017). Shallow supplies of the coalfields were first exploited, and once exhausted, the deeper seams extending under the sea were extracted (Cooper et al., 2017). Mining took place from the early 1830s until mine closures took place between the 1980s and 1993 due to a combination of safety concerns after a number of catastrophic incidents, as well as miners strikes (Durucan, Jozefowicz and Brenkley, 2010). The close proximity of mines to the coast meant disposal onto adjacent foreshores was the easiest and least logistically challenging solution. This took place by tipping, either by pushing waste directly over the cliff edges, or by 'aerial flights' which consisted of conveyor belt or gondola/bucket loom type mechanisms (Figure 1.1) that extended across the foreshore and deposited waste into the

shallow sublittoral zone (Cooper et al., 2017). The expectation was that waste would be naturally eroded by wave action, tides, storms and weathering (Hydraulics Research Station, 1970), however increased demand for coal resulted in greater exploitation, and after World War II increased mechanisation facilitated this (Cooper et al., 2017). The rate of waste disposal therefore significantly outweighed the rate of erosion and large volumes began to accumulate on the shores (Figure 1.2). Production peaked between the mid-1960s and early 1980s, during which over ten million tonnes of colliery waste were disposed onto shores (Alderton, 2012). The exact volume of waste disposed is unknown, since disposal took place unregulated until 1974 when statutory controls were enforced and the disposal of waste became a licenced activity (Cooper et al., 2017). Estimates suggest over 40 million tonnes of waste were introduced to the shores on just one 12 km stretch of coastline in Durham (www.turning-the-tide.org.uk) where from 1977 disposal was capped at 2.5 million tonnes per year (Eagle et al., 1979), although other estimates suggest this quantity of waste was disposed prior to 1970 (Hydraulics Research Station, 1970).

Figure 1.1. Coal mine waste on the shores of Durham with two different methods of disposal shown. Top image shows Easington (site C2) in 1992. Bottom image shows Blackhall Rocks (year unknown). Credit/Durham Heritage Coast.

Mine wastes are typically solid and liquid materials that are left over after the extraction of valuable target minerals, and they often contain elevated levels of harmful heavy metals. Metals can be divided into two groups regarding their toxicity. Essential metals, mainly chromium (Cr), copper (Cu) and nickel (Ni), are required in low concentrations for organism functioning and the sustenance of life but become toxic when present in concentrations higher than required (Furness and Rainbow, 2018; de Almeida Rodrigues et al., 2022). Non-essential metals such as aluminium (Al), arsenic (As), cadmium (Cd), lead (Pb), mercury (Hg) and silver (Ag), are not required for organism functioning and are toxic when present at any

concentration (Furness and Rainbow, 2018; de Almeida Rodrigues et al., 2022). The disposal of these wastes in Durham and Northumberland had several main effects on coastal habitats. Firstly, it contaminated intertidal and shallow subtidal habitats by introducing vast quantities of pollutants including toxic hydrocarbons and heavy metals (Eagle et al., 1979; Cooper et al., 2017). Secondly, the introduction of the sheer volume of sediment smothered habitats, often under spoil heaps reaching up to 10 m deep (Cooper et al., 2017). Whilst the effects of smothering are largely unrecorded, photographic evidence shows the extent to which coastal habitats were buried (Figure 1.2). The volume of waste introduced to the shore also resulted in significant progradation, shifting the high tide line over 500 m seawards in some locations (Cooper et al., 2017). In Lynemouth Bay, Northumberland, progradation was so severe that a coal-fired power station was built on the newly created 'land'. Waste disposal at this location temporarily ceased in 1994 and the spoil heap rapidly eroded naturally, resulting in the flooding of the power station in winter storms of 1994/95 (Cooper et al., 2017). Similarly in Durham, the sea cliffs became so segregated from the coast that they became heavily vegetated and were considered stabilised (Cooper et al., 2017). Upon the cessation of waste disposal on the Durham coast, which started in 1984 with the final mine closing in 1993, the spoil heaps rapidly eroded at a rate of up to 20 m per year, reducing after 2 to 5 years to 0.5 – 2 m per year as erosion reached older, more compacted spoil (Posford Duvivier, 1993). As well as the direct disposal of sediment-based wastes onto the shoreline, groundwater was continuously pumped out of mines and into the sea in order to keep mines accessible to workers (Figure 1.3). This minewater similarly contained significant quantities of metal pollutants and fine sediment (Younger, 1993) that likely contributed to the negative impacts on surrounding habitats.

Figure 1.2. Blast Beach, County Durham, 1974 (top) and present day (bottom) demonstrating the significant quantity of mine waste deposited. Credit/DM Allen (bottom image). Red arrows indicate the location of sampling at site C1 in Chapters 3-5 of this thesis, which was buried under coal spoil during the mining period.

Between 1997 and 2002 a large-scale remediation initiative took place on the Durham coastline, removing 1.3 million tonnes of waste from a ~12 km stretch of coastline. This £10.5 million operation led to the designation of several parts of the coast between Seaham Beach and Hartlepool as Sites of Special Scientific Interest (SSSI), Special Protected Areas (SPA), Special Areas of Conservation (SAC) and Ramsar sites. Whilst a vast improvement on the condition of the coast was made (Figure 1.2), the effects of its historic industrial past are still clearly visible (Figure 1.4) and waste is still to this day periodically eroded into the sea from coal shelves on both the Durham and Northumberland shores. On top of this, minewater pumping still continues in order to protect neighbouring aquifers that are used for drinking water supply and to stop sewage systems being inundated (Younger, 1993). High density sludge (HDS) treatment plants remove iron (Fe) contamination, however no other contaminants are treated before discharge (Alderton, 2012). Each HDS treatment plant discharges approximately 35 million litres of water into the sea per day, with three treatment plants in Durham discharging around 105 million litres per day (Younger, 1993). Additionally, there are several treatment plants on the Northumberland coast, which all act as sources of potentially large quantities of heavy metal pollutants to the marine environment. Studies investigating the impacts of heavy metal pollutants on kelp have shown various negative impacts including reduced photosynthetic activity, spore development and growth rates (Contreras et al., 2007; Huovinen, Leal and Gmez, 2010; Leal et al., 2018; Contreras-Porcia et al., 2023), however, host response is extremely species specific (Leal et al., 2018) and very few studies have investigated the response of *L. hyperborea*. Furthermore, whilst many studies focus on the negative impacts on reproduction and early life stages, few take into account the subsequent effects on kelp forest structure, ecosystem functioning or productivity. There is, however, evidence of shifts in *L. hyperborea* holdfast associated macroinvertebrate assemblage structure along gradients of pollution (Jones, 1972; Jones, 1973; Sheppard, 1976), although many of these studies attribute the observed negative effects to increased turbidity as a result of the pollutant source, rather than a specific effect of metal toxicity.

Figure 1.3. Minewater discharge at Blackhall Rocks on the County Durham coast, 1974. Credit/Catherine Smith.

Previous research has quantified some of the effects of coal mining operations in the northeast of England on marine habitats including intertidal rocky and sandy habitats, and subtidal soft sediment habitats. Hyslop et al. (1997) investigation on the effects of colliery waste on littoral communities in Durham and Northumberland demonstrated detrimental effects on the species richness and diversity of sandy and rocky shore communities. On sandy shores, a maximum of two macroinvertebrate species were recorded per shore height – a reduction of 75% over nearby unaffected shores. On rocky shores, macroalgae species richness was reduced by up to 47% at sites affected by colliery spoil over those unaffected (Hyslop et al., 1997). Shifts in benthic soft sediment communities were observed in subtidal areas where the benthos was severely depleted, and crab and lobster habitats were completely smothered resulting in a large reduction in the productivity of commercial potting (Eagle et al., 1979). Studies including Sheppard, Bellamy and Sheppard (1980) and Jones (1972) reported shifts in *L. hyperborea* holdfast associated macroinvertebrate communities corresponding with the severity of pollution, but also suggest the effects could be a result of increased turbidity. For example, larger numbers of suspension feeders are found in association with increased organic matter and suspended load, which may come about as a result of colliery waste disposal (Jones, 1972; Sheppard et al., 1980). Whilst recovery of habitats shortly after the cessation of mining was spatially variable yet broadly limited (Johnson and Frid, 1995), very little attention

has been focussed upon developing an understanding on the current state of habitats in these affected areas, and in particular, kelp forest habitat. Since the majority of studies on the effects of colliery waste disposal took place during mining activity, no studies have characterised marine habitats at locations that were directly under large volumes of mine spoil for decades due to their inaccessibility at the time.

Figure 1.4. The 'coal shelf' at Blast Beach (Site C1), County Durham, showing present day evidence of historic coal mining waste disposal.

Although the kelp forests that were once buried under meters of coal spoil have regrown, the extent of their recovery and the health and functioning of the habitat they create is unknown. Additionally, the structure and function of kelp forests along the wider geographic area of UKs North Sea coast is greatly understudied. Very few studies in the last 50 years have focussed on kelp forest habitats in this geographic region, and in that time, it is very likely that changes to the coastline have taken place, particularly in the case of the Durham and Northumberland coasts as they recover from the effects of industrialisation.

1.6 Aims and hypotheses

This thesis, therefore, aims to fill the knowledge gaps on the structure of kelp forests on the UKs North Sea coast, adding to the breadth of knowledge that previous studies over the last decade have gained on the structure of kelp forests on the western coast of the UK. This will be achieved through kelp forest surveys at a range of sites and depths carried out in Chapter 2. Additionally, I aim to determine if historic coal mining operations that ceased over 30 years ago have a negative impact on the structure, productivity and biodiversity of kelp forests today. To achieve this, comparative surveys of multiple aspects of kelp forest structure and function will be carried out between polluted and non-polluted areas. Sites characterised as 'polluted' in these comparative studies are proxies of pollution that represent historically affected areas where kelp forests were buried under spoil heaps for extended periods of time (possibly up to tens of years). Conversely, 'non-polluted' sites are located away from mining activity. Following this structure, Chapter 3 will investigate the structure and productivity of kelp forest habitats, Chapter 4 will focus on the diversity associated with kelp holdfasts and stipes, and finally, Chapter 5 will analyse the structure of the kelp surface bacterial microbiome on a variety of kelp tissues. The lack of previous studies conducted on aspects of kelp structure and functioning in this geographic area make it difficult to determine evidence-based hypotheses. However, based on the responses of other kelp species to environmental perturbations it is likely that the significant quantities of waste that were disposed of, the quantity of heavy metals introduced to the marine environment, and the present day impact of minewater discharges will have had negative impacts on the structure and function of these habitats. The results from these studies will form a baseline of kelp forest structure on the North Sea coastline of the UK and will provide a foundation for future research in this understudied region. This baseline will not only allow for comparisons with other kelp-dominated ecosystems but will also facilitate monitoring of potential changes in response to ongoing environmental pressures, such as climate change and coastal pollution.

I hypothesise that kelp forests in areas historically affected by coal mining waste will exhibit lower productivity, negatively impacted structure, and diminished biodiversity compared to unaffected areas, due to the long-term impacts of heavy metal pollution, sedimentation, and habitat degradation. Furthermore, it is anticipated that differences in the bacterial

microbiome, particularly reduced diversity and shifts in assemblage structure, may correlate with observed variations in kelp forest structure and associated fauna due to their influence on host health. These hypotheses will direct the thesis and aim to improve our understanding on how historical anthropogenic impacts have shaped, and may continue to influence, the resilience and ecological function of these important coastal habitats.

1.7 Author Declaration

Chapters 2, 3, 4 and 5 have been prepared as independent units and are in the final stages of being prepared for submission to scientific journals for publication. As a result, therefore, there are elements of repetition within the introductions and certain sections of the discussions. This repetition accounts for no more than 5% of the entire thesis and, as such, does not attempt to fulfil any substantive requirements or contribute artificially to the overall content of the thesis.

Chapter 2. Regional-scale variability in the structure and carbon standing stock of *Laminaria hyperborea* forests across gradients of depth in the North Sea.

2.1 Introduction

Kelp, large brown macroalgae primarily of the Order Laminariales, are distributed on temperate and sub-polar reefs along ~36% of global coastlines (Jayathilake and Costello, 2021). Here, they form extensive, highly productive and diverse forests that provide a range of valuable ecosystem goods and services for human society (Beaumont et al., 2008; Smale et al., 2013). As foundation species, kelp create biogenic habitat and support diverse associated assemblages and food webs through high primary productivity (Mann, 1973; Dayton, 1985; Rassweiler et al., 2018), alongside playing an important role in coastal processes such as wave attenuation (Pinsky, Guannel and Arkema, 2013), nearshore sedimentation (Connell, 2005), nutrient cycling (Pfister, Altabet and Weigel, 2019) and carbon storage (Pessarrodona et al., 2018).

Although kelp forests can play an important role in these processes, the degree to which they do so is generally governed by their structure and spatial extent (Morris et al., 2020). The structure and distribution of kelp forests is controlled by an array of interacting physical processes including temperature (Wernberg et al., 2015; Smith et al., 2022), light availability (Desmond, Pritchard and Hepburn, 2015; Smith et al., 2022) and wave exposure (Harrold, Watanabe and Lisin, 1988; Norderhaug et al., 2012), as well as ecological processes such as competition (Arkema, Reed and Schroeter, 2009) and herbivory (Watanabe and Harrold, 1991). However, in many regions the structure and functioning of kelp forests is impacted by rapidly changing environmental conditions and increasing pressure from anthropogenic influences (Ling et al., 2009; Arnold et al., 2016; Provost et al., 2017; Wernberg et al., 2024). Climate change is an underlying cause for major changes in kelp forest structure through warming-driven shifts in species' distributions (Smale et al., 2020), and marine heatwaves, which are driving the alteration and collapse of kelp forest habitats across multiple continents (Tyler-Walters, 2007; Arafeh-Dalmau et al., 2019; Smale et al., 2019). Processes operating across the

land-sea interface, such as coastal development and agricultural practices leading to decreased coastal water quality, have also contributed to the degradation and disappearance of kelp forests in many regions (Krumhansl et al., 2016). The impacts of these anthropogenic stressors are only likely to intensify in the future. It is therefore imperative to have robust understanding of the structure of these important habitats to manage and protect them, and to have a baseline to restore the system to, should they be negatively impacted in the future.

Kelp forest structure is also a key determinant of the quantity of carbon stored within the respective forest. 'Carbon standing stock' is a measure of the quantity of carbon stored within kelp tissues at a specific point in time (Hill et al., 2015) and is primarily determined by the morphology and density of individuals of a specific kelp species, with larger individuals and higher density forests typically storing greater quantities of carbon (Smale and Moore, 2017). Given the potential spatial extent of kelp species both globally (~36% of coastlines; Jayathilake and Costello, 2021) and within the current study area of the United Kingdom (UK; 15,984 km^2; Yesson et al., 2015), there is likely to be a significant amount of carbon stored within the habitats they underpin, with estimates suggesting carbon standing stock to be 1-2 orders of magnitude greater than other vegetated temperate marine habitats such as seagrass beds or saltmarshes (Garrard and Beaumont, 2014). Kelp also act as 'carbon donors', as the vast majority of primary productivity is exported from the source habitat (Krumhansl and Scheibling, 2012; Smale et al., 2022) and is often transported to carbon storage habitats where it contributes to the allochthonous organic matter that they sequester (Trevathan-Tackett et al., 2015; Queirós et al., 2023; Filbee-Dexter et al., 2024).

Along the rocky wave-exposed coastline of the United Kingdom, kelp forests are generally dominated by the stipitate kelp *Laminaria hyperborea* (Gunnerus) Foslie 1884*,* whose range extends from northern Portugal to northern Norway (Sjøtun et al., 1993; Pinho et al., 2016), reaching depths of >40 m in clear waters (Hiscock, 1992; Tyler-Walters, 2007), although generally 15 to 20 m around much of the UK coastline (Smith et al., 2022). In favourable conditions *L. hyperborea* forms extensive, dense forests that create habitat both directly (Teagle et al., 2018) and indirectly (Sjøtun, Christie and Fosså, 2006; Bué et al., 2020; Earp et al., 2024) that in turn support inshore fisheries and coastal biodiversity (Johnson and Hart,

2001; Norderhaug, Fredriksen and Nygaard, 2003; Burrows, 2012; Smale et al., 2022). Around a decade ago our understanding of the ecology of kelp forests along the extensive and complex coastline of the UK lagged behind other leading scientific nations (Smale et al., 2013), but recent research efforts have characterised the structure and function of *L. hyperborea* forests and their associated assemblages in the UK, with a particular focus on the northern and western coasts (Gouraguine et al., 2024; Smale et al., 2016; Smale and Moore, 2017; Smith et al., 2022; Teagle et al., 2018). Whilst these previous studies show a large degree of variability in kelp forest structure and function across the latitudinal range of the UK, they also show these regions to have some of the most dense and productive kelp habitats within this species range, with individuals reaching over 2.5 m in length and found in densities of up to 60 individuals per m^{-2}.

Although these previous studies have significantly added to our knowledge of the structure, function and ecosystem services provided by UK kelp forests, they have not included kelp forest ecosystems found along the eastern coast of the UK, despite historical work conducted on the UK coastline of the North Sea indicating the presence of extensive *L. hyperborea* forests (Whittock, 1969). Here, we address this knowledge gap by investigating the structure of *L. hyperborea* forests along a gradient of depth (2-10 m below chart datum) at six survey sites within two regions on the North Sea coastline of the eastern UK. We also examine estimates of carbon standing stock for *L. hyperborea* forests at a further four regions, representing a latitudinal gradient of 9° and spanning a range of environmental conditions. This study allows for comparisons between kelp forests throughout this species range and provides one of the first comprehensive insights into the structure of kelp forests on the North Sea coastline of the UK.

2.2 Methods

2.2.1 Kelp forest structure and depth distribution

In June 2021, kelp forests dominated by *L. hyperborea* were surveyed in two regions along the North Sea coastline of eastern UK: NE England (A) and SE Scotland (B) (Figure 2.1). Within each

region, three sites were selected based on the following criteria: 1) sites included sufficient areas of rocky subtidal reef at depths of 5 m (below chart datum, BCD; all depths hereafter relate to BCD), with two of the three chosen sites in each region characterised by a sloping gradient from 2 to 10 m depth (or the deepest extent of kelp forest); 2) sites were representative of the wider region in terms of coastal geomorphology and not obviously influenced by localized anthropogenic activities (e.g. sewage outfalls) and; 3) sites were "open coast" and moderately to fully exposed to wave action. Regions were separated by a distance of 45 km, while sites were separated by between 0.3 km and 3.5 km.

To investigate the structure of *L. hyperborea* forests, SCUBA divers placed five to eight replicate 1 m^2 quadrats haphazardly within the main kelp forest habitat, estimated the percent cover of the kelp canopy and counted the number of canopy and sub-canopy individuals. Canopy plants were defined as mature sporophytes forming part of the main canopy, while sub-canopy plants included mature sporophytes as well as juveniles with digitate blades and a well-developed stipe found beneath the main canopy. First year recruits with undivided blades were counted but were excluded from the analyses due to uncertainty in their identification and considerable spatial patchiness. The density of sea urchins (exclusively *Echinus esculentus*) within quadrats was also recorded (Table 2.1). The morphology and biomass of canopy forming plants was investigated by collecting ten haphazardly selected individuals per sampling depth, per site. Whole plants were collected by dislodging holdfasts from the substratum and returning them to the surface where morphological characteristics including stipe length (cm), total length (cm), stipe biomass (g fresh weight; FW), and total biomass (g FW) were recorded. Individuals were also aged by counting annual growth rings on cross-sections of the stipe sampled close to the stipe-holdfast junction (as described by Kain and Jones, 1963). All data and sample collection was conducted at 5 m depth at each of the three chosen sites in each region, with additional sampling taking place at 2 and 10 m depth (or the deepest extent of kelp forest if shallower than 10m) at two of the three chosen sites in each region (A2, A3, B2 and B3). At these sites, the maximum depth of kelp forest was also recorded.

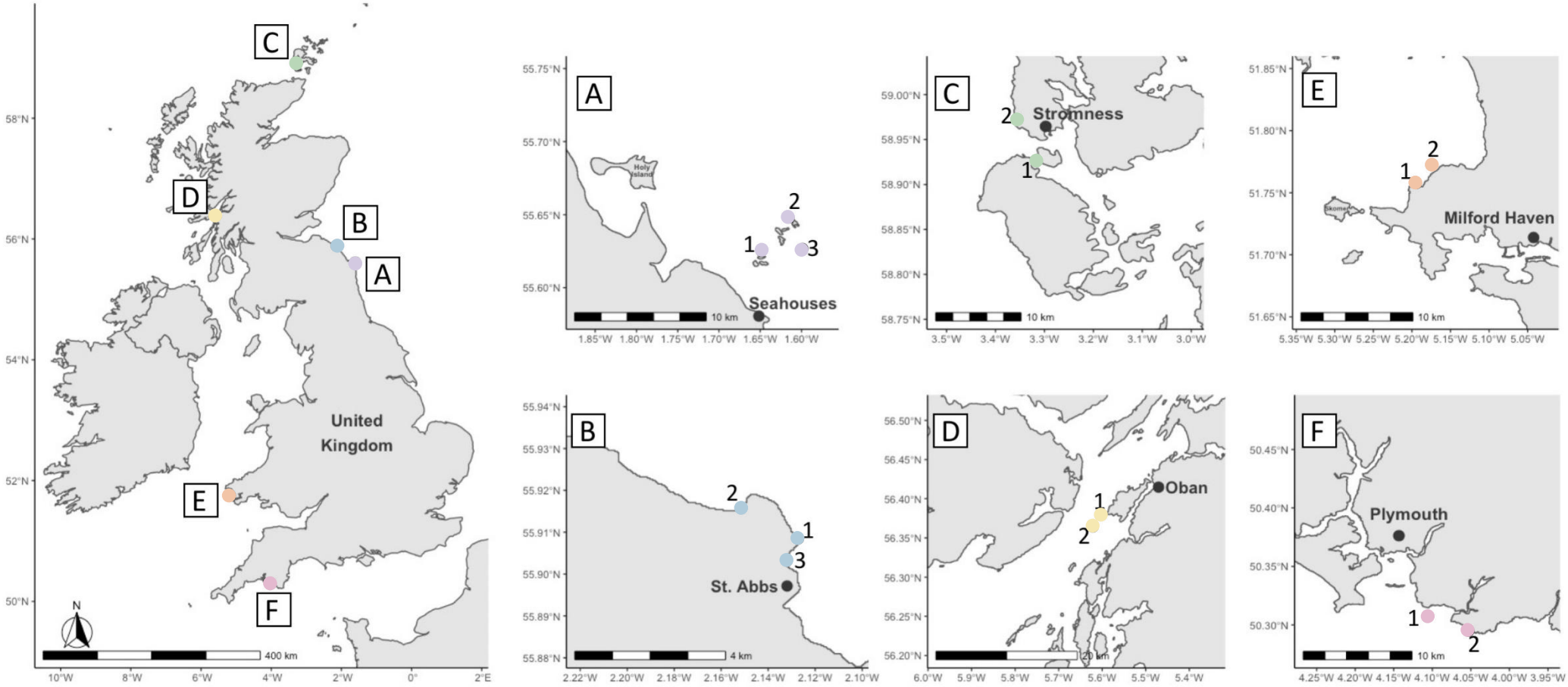

Figure 2.1. Study regions across the United Kingdom: (A) NE England, (B) SE Scotland, (C) N Scotland, (D) W Scotland, (E) SW Wales, (F) SW England. Small maps indicate locations of study sites within each region. Regions A and B are new survey regions sampled in the present study. Data for the previously sampled regions of C-F are from Smith et al. (2022).

2.2.2 Carbon standing stock

Additional data on the morphology of *L. hyperborea* in the UK, spanning a further four regions and a latitudinal gradient of almost 9°, were sourced from Smith et al. (2022). Carbon standing stock was estimated following the methods of Smale et al. (2016) in which the relationship between fresh weight (FW) and dry weight (DW) of basal blade, distal blade and stipe tissue were calculated from 47 kelp plants collected from regions C, D, E and F (N Scotland, W Scotland, SW Wales and SW England, respectively; Fig 1). Study wide averages calculated in Smale et al. (2016) showed the DW:FW ratio varied between different regions of the kelp plant, with mean values of 0.29, 0.17 and 0.21 for basal blade, distal blade and stipe, respectively (Smale et al., 2016). Here, we averaged these values for basal and distal blade DW:FW to obtain a value for the whole kelp blade of 0.23 and for the stipe of 0.21. These values were then used to convert our measurements of whole plant fresh weight from NE England and SE Scotland to whole plant dry weight. Site averages of DW for canopy forming *L. hyperborea* were multiplied by the average density of canopy forming individuals recorded in the 1 m^2 quadrats at each site, giving an estimated biomass (DW) per 1 m^2. Finally, the conversion of DW per m^2 to carbon standing stock was based on previous research on a range of kelp species that indicates approximately 30% of DW is carbon (Smale et al., 2016; Pessarrodona et al., 2018).

2.2.3 Environmental data

Data for various environmental variables known to influence kelp forest structure (Smale et al, 2016) were extracted. Wave exposure was determined from log_{10} wave fetch values extracted from Burrows (2020), with all study sites categorised as 'exposed', with values greater than 3.5 log_{10} (Burrows, 2012) (Table 2.1). Sea surface temperature (SST), pH and chlorophyll *a* concentration (proxy for turbidity) for the period between 2000 and 2014 were extracted from Bio-ORACLE (Assis et al., 2018) using the 'sdmpredictors' package in RStudio v. 4.2.1 (R Core Team, 2022). However, due to the proximity of the sites to one another and the resolution of the environmental data, most data were only available on the regional scale and therefore only wave fetch data was used in further analyses.

2.2.4 Statistical analysis

Patterns of spatial variability in *L. hyperborea* forest structure (i.e. canopy density, total density and total canopy biomass), individual-level metrics (i.e. canopy former biomass, stipe length, total length and age) and carbon standing stock were analysed using univariate permutational analyses of variance (PERMANOVA) (Anderson, 2001). Variation in kelp forest metrics between all sites in NE England (A) and SE Scotland (B) at 5 m depth, was determined using two-way PERMANOVA with Region (fixed, 2 levels) and Site (random, 3 levels and nested within Region) as factors. Variation in kelp forest metrics between two sites in NE England (A) and SE Scotland (B) and across depths was determined using three-way PERMANOVA with Region (fixed, 2 levels), Site (random, 2 levels and nested within Region), Depth (fixed, 3 levels) and their interactions as factors. The distributions of morphological and density data were checked and conformity to normal distribution confirmed. Variation in carbon standing stock between sites at the six study regions (A-F; Figure 2.1) at 5 m depth was determined using a two-way PERMANOVA with Region (fixed, 6 levels) and Site (random, 2 levels and nested within Region) as factors. For each analysis, permutations (9,999 under a reduced model) were based on Euclidean distance similarity matrices constructed from untransformed data. Where the number of permutations was low (i.e. <100), p values derived from Monte Carlo simulations were used. Pairwise post hoc comparisons were performed where significant differences ($p<0.05$) were detected.

Relationships between $\log_{10}$ values of wave fetch and kelp forest structure (i.e. canopy density, total density and total canopy biomass) and individual-level metrics (i.e. canopy former biomass, stipe length, total length and age) at a depth of 5 m were examined using distance based linear models (DISTLM). The relationship between urchin density and the maximum kelp forest depth were also tested using DISTLM. All DISTLM models were based on Euclidian distance similarity matrices and run using 9,999 permutations. Statistical analyses were conducted using PRIMER 7 software (Clarke and Gorley, 2015) with the PERMANOVA add-on (Anderson, 2008). Model assumptions were checked, and all figures were made in RStudio v. 4.2.1 (R Core Team, 2022) using the packages “car” (Fox, Weisberg and Price, 2001), “ggplot2” (Wickham, 2016), “ggpubr” (Kassambara, 2016) and “rstatix” (Kassambara, 2019).

2.3 Results

2.3.1 Spatial variability in the structure of *L. hyperborea* forests

At 5 m depth, *L. hyperborea* dominated at all sites in NE England and SE Scotland (100% of canopy forming individuals recorded in quadrats), although the kelp species *Alaria esculenta* and *Saccharina latissima* were observed in very low abundances at some sites. The mean (± 1 SE) density of canopy forming *L. hyperborea* individuals ranged from 7.3 ± 0.5 to 12.3 ± 0.5 ind.m^{-2} (B2 and B1 respectively), while the total density of individuals (canopy and subcanopy) ranged from 16.8 ± 2.6 to 32.0 ± 5.1 ind.m^{-2} (B2 and A2 respectively; Figure 2.2a-b). Both canopy density and total density varied across small spatial scales, with significant variation between sites nested within regions, but not between regions (Table 2.2; Figure 2.2a-b). Stipe length and total length of canopy forming individuals showed significant small-scale variation between sites nested in regions, with total length additionally varying significantly between regions. Indeed, the total length of canopy forming individuals was significantly greater in NE England (272.8 ± 8.5 cm) compared to SE Scotland (196.5 ± 6.6 cm; Figure 2.2d; Table 2.2). The stipe length of canopy forming individuals ranged from 83.6 ± 8.3 to 170.0 ± 2.5 cm (B2 and A1 respectively).

The biomass of canopy forming individuals was significantly greater in NE England (1869.2 ± 118.9 g FW ind^{-1}) compared to SW Scotland (1105.7 ± 88.6 g FW ind^{-1}), whereas the total canopy biomass ranged from 6.6 ± 0.6 to 19.6 ± 0.8 kg FW m^{-2} (B2 and A3 respectively) and exhibited significant variation between sites nested in regions, but not between regions (Table 2.2; Figure 2.2e-f). The age of canopy-forming individuals ranged from 6.0 ± 0.4 to 6.9 ± 0.5 years (B3 and A2 respectively) and did not vary significantly across sites or regions (Table 2.2; Figure 2.2g).

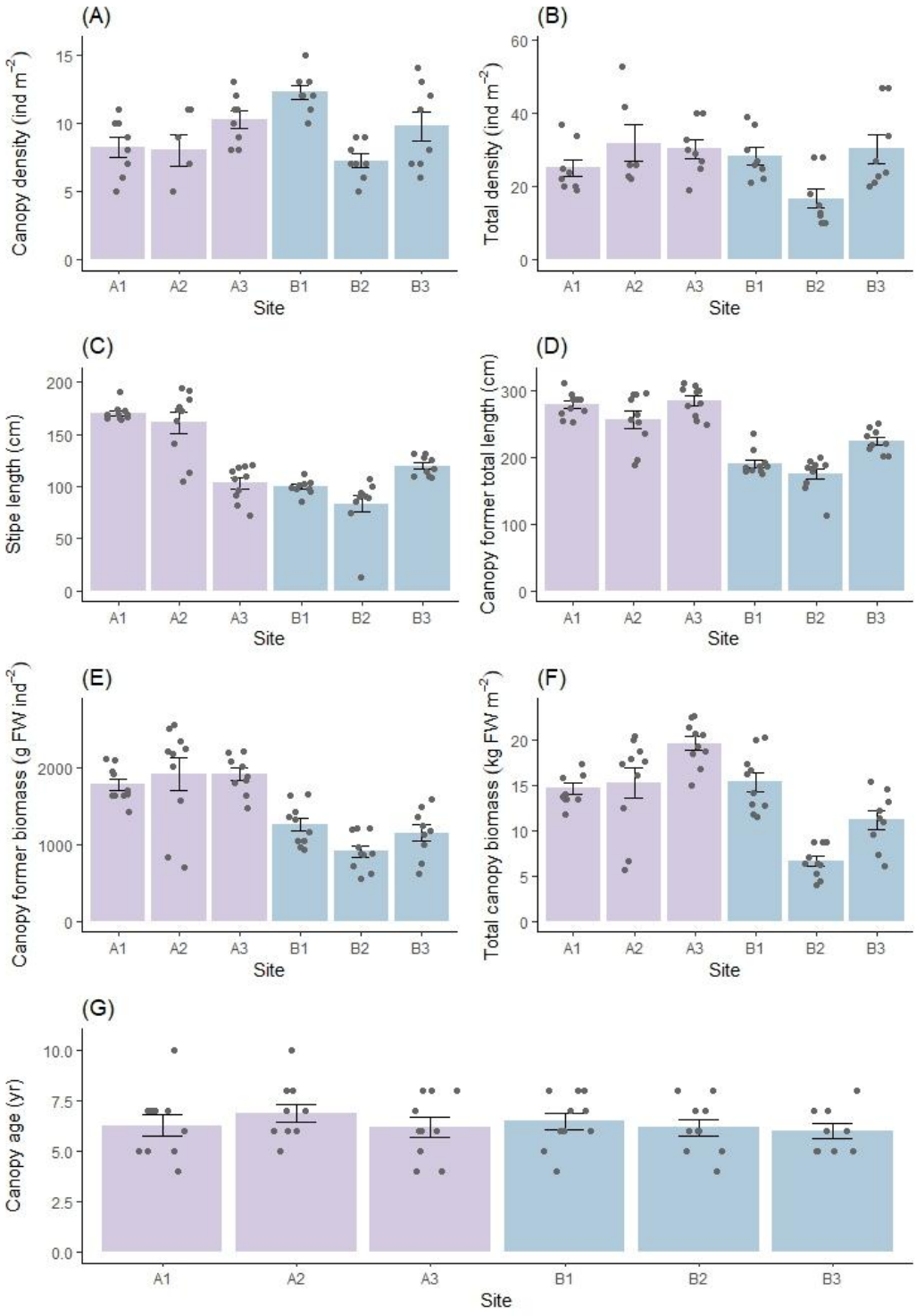

Figure 2.2. Structure of *Laminaria hyperborea* populations at sites within regions A (NE England) and B (SE Scotland) at a depth of 5 m BCD. Bars represent mean values ± SE. Points represent raw data values. (n ≥ 6 for quadrat-level variables: A, B & F; n ≥ 9 for plant-level variables: C, D, E & G). FW: Fresh Weight. Ind.: Individual. See Figure 2.1 for study site locations.

Table 2.1. Environmental drivers of kelp forest structure at six study sites within two regions of NE England and SE Scotland. Mean annual sea surface temperature (SST) and chlorophyll *a* values were extracted from Bio-ORACLE *(Assis et al., 2018)* for the years 2000 to 2014. Wave fetch values are extracted from Burrows (2020). Urchin density is the average number of Echinus esculentus recorded in 5-8 replicate 1 m^2 quadrats at a range of sampling depths at each site. Site locations can be seen in Figure 2.1.

Region	Site Code	Site Name	Latitude	Longitude	Wave Fetch (log10 of 3-cell mean)	Mean SST (°C)	Chlorophyll *a* Concentration (ml/m^3)	Urchin Density (ind./m^2)	
								Sampling Depth (m)	Density (±SE)
NE England	A1	Knoxes Reef	55.62336	-1.64840	4.427	9.904	3.765	**5**	1.375±0.263
								2	0.625±0.263
	A2	Northern Hares	55.64674	-1.61241	4.417			**5**	1.000±0.365
								10	1.000±0.365
								2	0.200±0.200
	A3	Crumstone	55.62673	-1.59781	4.478			**5**	1.125±0.295
								10	1.200±0.735
SE Scotland	B1	Woody Rocks	55.90663	-2.12850	4.307	10.186	3.499	**5**	4.125±1.156
								2	1.000±0.516
	B2	Pettico Wick	55.91567	-2.15102	4.068			**5**	1.700±0.796
								7	2.500±0.764
								2	0.300±0.211
	B3	White Heugh	55.90466	-2.13161	4.191			**5**	1.625±0.498
								10	0.625±0.263

Table 2.2. Univariate permutational ANOVAs to test for variability in population and individual level kelp metrics between regions and sites at a depth of 5 m BCD. Significant values ($p < 0.05$) are indicated in **bold**. Significance values followed by a '+' are derived from Monte Carlo simulations. Variables per m^2 and per canopy-forming individual tested between two study regions (A and B), carbon standing stock tested between all six regions (A-F: Figure 2.1).

Response Variable	Region			Site(Region)			Res df
	df	*F*	p	df	*F*	p	
Per m^2							
Canopy density	1	0.31	0.5982+	4	6.48	**0.0007**	40
Total density	1	0.69	0.4433+	4	3.48	**0.0156**	40
Total canopy biomass	1	3.33	0.1438+	4	13.11	**0.0001**	53
Per canopy-forming individual							
Stipe length	1	3.49	0.1342+	4	22.46	**0.0001**	53
Total length	1	21.05	**0.0104+**	4	6.48	**0.0001**	53
Canopy plant biomass	1	45.97	**0.0033+**	4	1.44	0.2318	53
Age	1	0.79	0.4233+	4	0.73	0.7300	53
Carbon standing stock							
Canopy carbon	5	9.37	**0.0092**	6	4.59	**0.0002**	99

2.3.2 Environmental drivers

All sites were considered "exposed" to wave action, however sites in NE England had greater wave fetch values compared to those in SE Scotland, with the most exposed site being A3 (4.478) and least exposed B2 (4.068) (Table 2.1). Whilst data was only available on the regional scale for other proposed environmental drivers (and not used in formal analysis), mean SST was ~0.3°C greater and chlorophyll *a* concentration roughly 0.3 ml/m^3 lower in SE Scotland than in NE England. When testing the relationship between wave fetch and measures of kelp forest structure, DISTLM tests found significant relationships between wave fetch and total density, as well as all measures of morphology (stipe and total length and canopy plant biomass) (Table S2.1) with sites characterised by greater wave exposure supporting greater densities, longer lengths and overall greater canopy plant biomasses.

2.3.3 Depth distribution of kelp forests in NE England and SE Scotland

At the four sites where kelp forests were studied across a depth gradient, *L. hyperborea* was dominant at all depth increments. Kelp forest structure was again highly variable over small spatial scales, with significant variation in most individual and population level metrics between sites nested within regions and depths (Table 2.3; Figure 2.3). The density of canopy-formers and the total density of *L. hyperborea* tended to decrease with increasing depth at all sites (Figure 2.3a-b). Although there was significant variability between sites nested in region and depths (Table 2.3; Figure 2.3a-b), which was driven by non-significant declines in density between 2 and 5 m depth at a limited number of sites, as well as variability in kelp density at 2 m for some sites. In terms of *L. hyperborea* canopy percent cover, there was a significant region by depth interaction (Table 2.3), with cover at 10 m being lower in SE Scotland compared to NE England (Figure 2.3c). In contrast, at all other depths canopy cover was similar across sites and regions with values often reaching 100% (Figure 2.3c). For sub-canopy plants there was a significant interaction between sites nested within regions and depths (Table 2.3). In general, percent cover of sub-canopy individuals decreased with depth at all sites, although the rate of decline varied between sites (Figure 2.3d). Total canopy biomass also varied between sites nested within regions and depths (Table 2.3). At all sites total canopy biomass was lowest at 10 m, but there was significant variation between sites and regions, while the

greatest total canopy biomass occurred at 2 m at all sites except A3 where it occurred at 5 m (Figure 2.3h).

Stipe length, total length, and canopy plant biomass varied significantly between sites nested in regions and depths (Table 2.3; Figure 2.3c,e-f). As with *L. hyperborea* density, there was a tendency for all these factors to decrease with depth, with the exception of site A3 and B3 where these metrics increased from 2-5 m and then decreased again down to 10 m depth (Figure 2.3e-g). Stipe length and total length were generally greater at site A2 compared to site A3 across all depth ranges, with the exception of total length at 5 m which was greater at site A3. The age of canopy forming *L. hyperborea* plants did not vary with depth but did vary across sites nested within regions, with A3 (5.7 ± 0.5 yr) and B3 (4.8 ± 0.3 yr) supporting younger canopy forming plants compared to A2 (6.3 ± 0.3 yr) and B2 (5.7 ± 0.3 yr) (Table 2.3; Figure 2.3i).

Kelp forest maximum depth extent was deepest in NE England at site A2 where it reached 13 m, whereas at site A3 it reached only 11 m. Maximum kelp forest depth in SE Scotland was considerably lower than in NE England, reaching just 7 m at site B2 and 10 m at site B3 (Table S2.2). Although there was no significant relationship between the density of urchins and the maximum depth penetration of kelp forests (Table S2.3), the relationship did approach significance ($p=0.07$), with the highest urchin density being recorded at the site with the shallowest kelp forest depth penetration (7 m at site B2). No trend was observed across the other three sites.

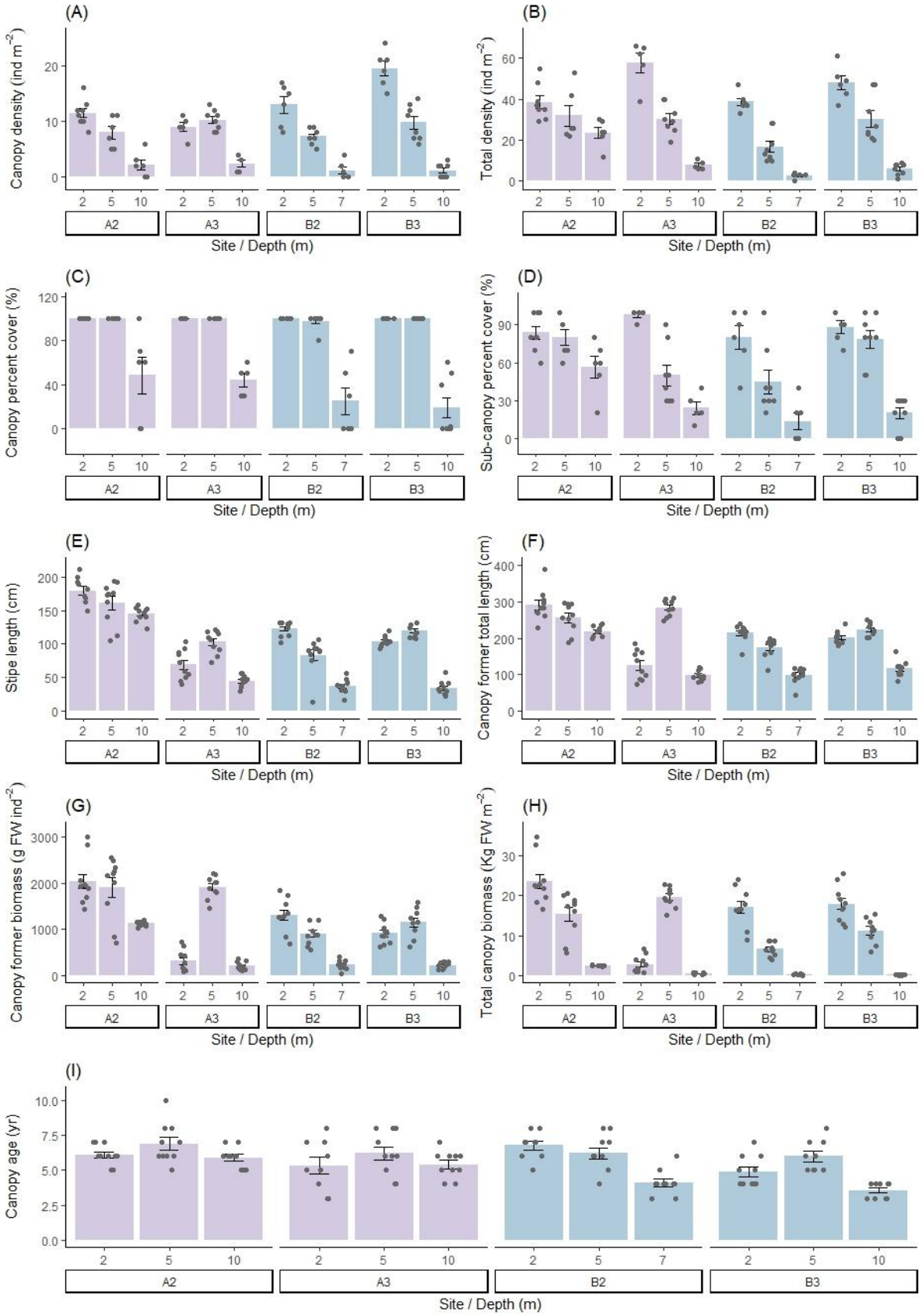

Figure 2.3. Structure of Laminaria hyperborea populations at sites within regions A (NE England) and B (SE Scotland) at depths of 2 m, 5 m and 7-10 m BCD. Bars represent mean values ± SE. Points represent raw data values. (n ≥ 6 for quadrat-level variables: A, B & F; n ≥ 9 for plant-level variables: C, D, E & G). FW: Fresh Weight. Ind.: Individual. See Figure 2.1 for study site locations.

Table 2.3. Univariate permutational ANOVAs to test for variability in population and individual level kelp metrics between regions, sites and depths for two regions in the UK (A and B; Figure 2.1). Significant values ($p < 0.05$) are indicated in **bold**. Significance values followed by a '†' are derived from Monte Carlo simulations.

Response	Region			Depth			Site(Region)			Region x Depth			Site(Region) x Depth			Res df
Variable	df	*F*	p	df	*F*	p	df	*F*	p	df	*F*	p	df	*F*	p	
Per m²																
Canopy density	1	0.85	0.4514†	2	8.34	0.1134†	2	8.34	**0.0006**	2	3.75	0.1115	4	4.81	**0.0022**	79
Total density	1	3.11	0.2175†	2	118.02	**0.0082**†	2	6.39	**0.0022**	2	0.13	0.8737	4	8.19	**0.0001**	79
Total canopy biomass	1	0.33	0.6235†	2	5.91	0.1538†	2	28.73	**0.0001**	2	0.94	0.4762	4	41.38	**0.0001**	118
Canopy percent cover	1	79.84	**0.0095**†	2	31.13	**0.0319**†	2	0.06	0.9365	2	25.92	**0.0059**	4	0.16	0.9614	79
Sub-canopy percent cover	1	0.95	0.4275†	2	27.80	**0.0326**†	2	7.6	**0.0008**	2	0.52	0.6132	4	4.44	**0.0036**	79
Per canopy-forming individual																
Stipe length	1	0.56	0.5303†	2	6.28	0.1355†	2	204.26	**0.0001**	2	1.53	0.315	4	12.92	**0.0001**	118
Total length	1	0.86	0.4532†	2	8.39	0.1423†	2	77.4	**0.0001**	2	0.48	0.6533	4	37.53	**0.0001**	118
Canopy plant biomass	1	1.10	0.4023†	2	6.51	0.13†	2	59.9	**0.0001**	2	0.79	0.5223	4	21.64	**0.0001**	118
Age	1	1.99	0.2669†	2	2.65	0.2484†	2	6.02	**0.0041**	2	3.93	0.0847	4	1.80	0.1451	118

2.3.4 Carbon standing stock

Average carbon standing stock held within *L. hyperborea* canopies across the 6 study regions was 858 ± 79 g C m^{-2}. The standing stock of carbon varied significantly between sites nested within regions (Table 2.2) and was greatest at site C1 (N Scotland; 1578 ± 94 g C m^{-2}) and lowest at site E1 (SW Wales, 303 ± 38 g C m^{-2}) (Figure 2.4). Variability among sites within a region was most pronounced in SE Scotland (B) where standing stock varied by ~51% between sites, and was least pronounced in SW England (F) where variation was just ~11% (Figure 2.4). While there were clear differences between most sites nested within regions there were also some clear regional effects (Table 2.2). With the exception of SE Scotland, cooler regions in the north of the UK tended to have greater carbon standing stocks compared to warmer southern regions. These differences were significant between N Scotland compared to SW Wales and SW England, and NE England compared to SW Wales (Figure 2.4).

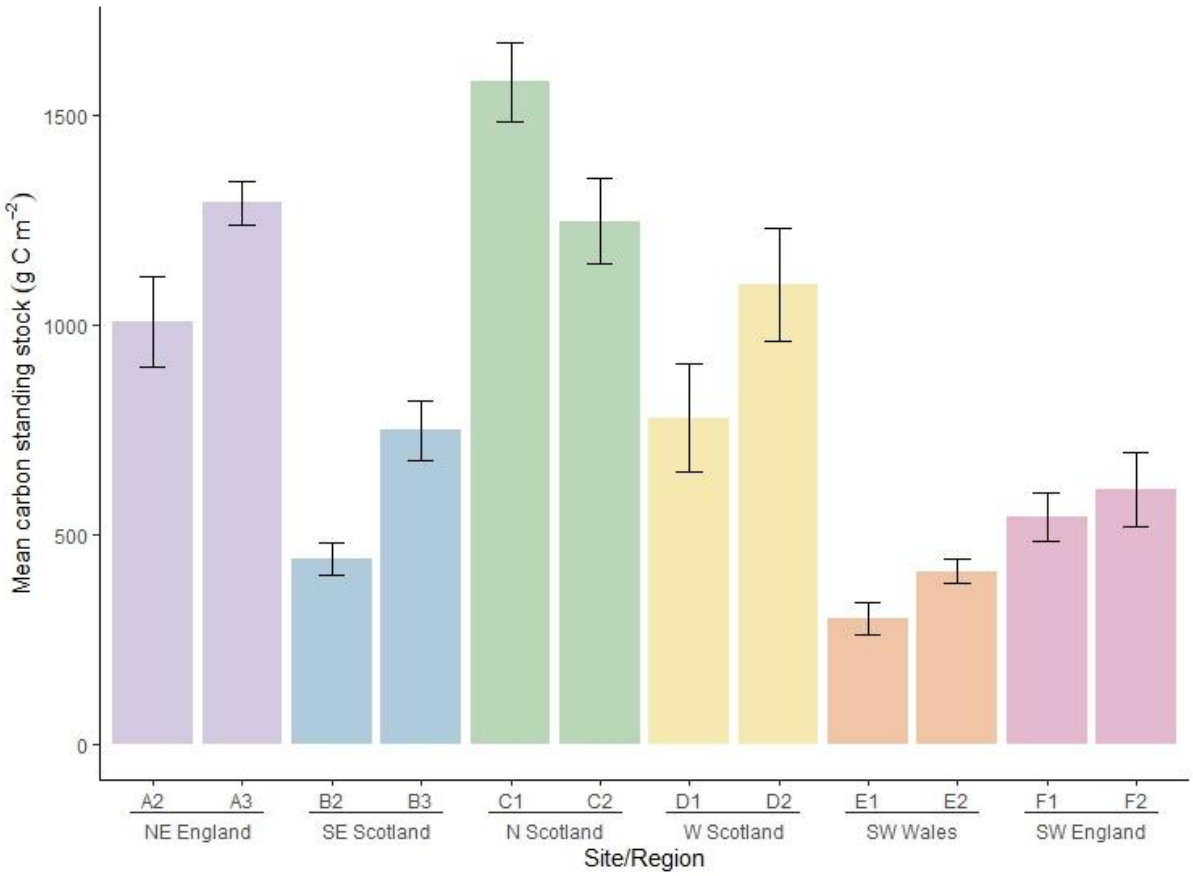

Figure 2.4. Estimated *Laminaria hyperborea* canopy carbon standing stock (g C m^{-2}) at study sites around the United Kingdom. Bars represent mean values ± SE, n = 8-10. See Figure 2.1 for study site locations.

2.4 Discussion

The structure of *Laminaria hyperborea* forests in NE England and SE Scotland varied across a range of spatial scales. At 5 m depth, the total length and biomass of canopy forming individuals were markedly different between regions, with individuals in NE England significantly greater in length and biomass than those in SE Scotland. At this depth, all other measures of density, biomass, and morphology varied over smaller spatial scales with significant site within region level effects. For example, both the greatest and lowest values of canopy density were measured at sites in SE Scotland, and total canopy biomass varied almost threefold between sites within the region. *L. hyperborea* forests also varied along a depth gradient extending from 2 to 10 m. Canopy and total *L. hyperborea* density generally decreased with depth, but there was also significant variation between sites nested within regions and depth. The percent cover of *L. hyperborea* canopy was generally 100% at 2 m and 5 m depth but reduced considerably at 10 m, and at this depth, cover was significantly lower in SE Scotland than NE England. Sub-canopy percent cover also declined with depth, but the rate of decline varied between sites. At 10 m depth, the biomass of canopy forming individuals, as well as stipe length and total length were lower than those of individuals at shallower depths. In half of our study sites, these measures peaked at 2 m, and the other half at 5 m. The total biomass of canopy forming individuals was greatest at 5 m in all but one study site. Age varied across sites nested in region and depth but did not vary across depths. At sites across the UK, carbon standing stock varied significantly between sites within the six study regions, as well as across regions. With the exception of SE Scotland, standing stock was generally greatest, albeit more variable across sites in cooler northern areas of the UK.

The range of values recorded for stipe length in NE England and SE Scotland were comparable in magnitude to other previously studied regions of the UK (Smale et al., 2016; Smale and Moore, 2017; Smith et al., 2022) and Norway (Rinde and Sjøtun, 2005; Pedersen et al., 2012; Bekkby et al., 2019; Gundersen et al., 2021). Stipe length varies along latitudinal gradients in both the UK and Norway, likely as a result of cooler sea surface temperatures and increased light levels promoting enhanced growth (Smale et al., 2016). In the UK, where *L. hyperborea* populations are located towards the centre of its range, stipe length generally increases with latitude (Smale et al., 2016). In Norway which includes the poleward range edge of this species,

stipe length increases from low to mid latitudes before decreasing at higher latitudes towards its range edge (Gundersen et al., 2021). These patterns suggest that *L. hyperborea* follows an abundant centre model (Sagarin, Gaines and Gaylord, 2006) in terms of its population structure. Stipe lengths recorded on the North Sea coast of the UK align with this pattern, with sizes comparable to those found in more northern regions of the UK, including N and W Scotland, as well as mid-latitude regions of Norway; regions in which some of the greatest *L. hyperborea* stipe lengths have been recorded. While not as strong as for stipe length, total length is generally greater in more northern regions of the UK (Smale et al., 2016; Smith et al., 2022). Here, we found that total length was generally comparable to, if not greater than, other UK and Norwegian regions at both similar and higher latitudes, suggesting that NE England and SE Scotland are optimum habitats for kelp growth.

While there are no significant latitudinal effects in terms of kelp density, in the UK, *L. hyperborea* density typically increases towards the south coast, possibly due to kelp forests being characterised by smaller individuals with lower biomass that occupy less space, allowing a greater number of individuals to persist in a given area (Smale et al., 2016; Pessarrodona et al., 2018). Similar patterns have been observed in Norway, where the greatest densities are typically found towards the northern and southern latitudes of the countries coast, corresponding with areas where individuals are generally shorter and have lower biomass (Gundersen et al., 2021). *L. hyperborea* densities in SE Scotland and NE England were generally comparable to, or greater than, other regions of similar latitude within the UK, but were considerably lower than mid-latitude Norway where densities are typically at their lowest (Pedersen et al., 2012; Smale et al., 2016; Gundersen et al., 2021).

Smaller *L. hyperborea* generally have a reduced biomass, and therefore trends in stipe length and biomass are often similar. In the UK, the biomass of canopy forming individuals varies along a latitudinal gradient, with individuals of greater biomass found in more northern regions (Smale et al., 2016). Our results conform with this trend, with values of canopy-forming plant biomass in SE Scotland comparable to other regions of the UK at similar latitudes, although measures for NE England were among some of the greatest ever recorded for *L. hyperborea* in the literature, from even the highest UK latitudes (Smale et al., 2016; Smith et

al., 2022) as well as Norway's mid latitudes (Gundersen et al., 2021). Estimates of standing biomass, however, were considerably lower than Norwegian kelp forests (Gundersen et al., 2021) yet still comparable to estimates from northern regions of the UK (Smale et al., 2016; Smith et al., 2022).

While there are clear latitudinal patterns in kelp forest structure, our results, and those of previous studies (Smale et al., 2016; Smith et al., 2022), show high levels of small-scale variability (i.e. between sites within a region). Changes in environmental conditions over large latitudinal gradients are responsible for some of the patterns we see in kelp forest structure, however, environmental conditions also vary over smaller scales and are likely to be responsible for driving the variability measured between sites within a region here. Several studies have highlighted numerous key interacting variables that influence kelp forest structure over small scales (Pedersen et al., 2012; Smale et al., 2016; Smale and Moore, 2017; Gundersen et al., 2021; Smith et al., 2022). Notably, wave exposure is consistently identified as a primary driver of variation in kelp forest structure (Sjøtun, Fredriksen and Rueness, 1998; Pedersen et al., 2012; Bekkby et al., 2014; Smale et al., 2016), with our findings showing that increased wave exposure is associated with higher measures of kelp biomass, density, and length. These effects are evident not only at the site level but also between regions, where the greater wave exposure observed in NE England results in significantly greater individual lengths and biomasses compared to SE Scotland. The biology and morphology of *Laminaria hyperborea* are known to vary with wave exposure, which is positively correlated with the species' presence (Bekkby et al., 2009). Higher water velocity, driven by wave exposure, enhances rates of photosynthesis and inorganic nutrient uptake (Hurd, 2000), leading to increased growth rates and primary productivity (Pedersen et al., 2012). Consequently, we observe greater performance of *L. hyperborea* in more wave-exposed areas, particularly in the form of increased biomass, density, and length (Pedersen et al., 2012; Smale et al., 2016; Gundersen et al., 2021). The impact of wave exposure on kelp forests can be profound, with biomass and density seen to quadruple between low and high exposure sites within a single region (Smale et al., 2016). Increases in density are often driven by an increase in the number of sub-canopy individuals, while the number of canopy-forming individuals remains unchanged. Although these sub-canopy individuals contribute little to the overall biomass, they form a critical reserve that can be utilised to replace lost canopy individuals (Pedersen et

al., 2012). Here, we found a significant effect of wave fetch on the total density but not on the density of canopy-formers, suggesting that wave fetch may be driving important processes in terms of recruitment or competition within the kelp forest sub-canopy.

Being a cold-temperate species, *L. hyperborea* gametophytes cannot persist in sea water temperatures over 21°C and sporophytes are compromised at temperatures over 20°C (Bolton and Lüning, 1982; Müller et al., 2009). Within the UK, the cooler northernmost regions, including the present study area, are therefore likely to provide more suitable conditions to favour populations of *L. hyperborea* than the warmer southern regions, where maximum seawater temperatures regularly exceed 18°C in summer months (Morris et al., 2018; Smale et al., 2016). Summer months in the UK are also characterised by longer day lengths. Kelp, being autotrophic, require light for photosynthesis, and since day length during the summer – the period of time when kelp synthesise and store carbohydrates to utilise for growth in the following growth season – is greater in higher latitudes, populations in the north of the UK benefit from an extended photoperiod in which greater biomass individuals can be produced (Rinde and Sjøtun, 2005; Smale et al., 2016). Indeed, day length may be more important than actual irradiance levels in driving large scale variability (Drew, 1983), however even across small spatial scales, light availability is a key factor in controlling the recruitment, biomass, size, density and growth of this species (Gorman et al., 2013; Bekkby et al., 2019) and may be responsible for driving some of the small spatial-scale variation measured in this study.

As photosynthetic organisms, kelp similarly show variability across depth gradients as they do with horizontal gradients. Given that light availability decreases with depth, kelp productivity also decreases with depth, meaning smaller individuals and reduced densities are often observed in deeper waters (Sjøtun, Fredriksen and Rueness, 1998; Bekkby et al., 2019). In addition to light availability, sedimentation rates can also be a determining factor in the structure of macroalgal habitats (Smale and Moore, 2017; Otero-Ferrer et al., 2020), however, with our sites being characterised by a sloping gradient, along with being fully exposed to wave energy, we did not see any evidence of sediment deposition during sampling. It is likely, however, that at shallow depths, greater turbulence relative to deeper areas could have an impact on kelp productivity through increased motion of individuals. This would lead to

elevated rates of nutrient transfer, greater availability of light to kelp blades, and increased rates of plant dislodgement that alleviates intraspecific competition – all factors that may lead to greater biomass accumulation and growth rates compared with deeper populations that experience less motion (Hurd, 2000; Pedersen et al., 2012; Bekkby et al., 2019).

Light availability also influences the depth to which kelp forests may extend, with kelp around the UK reported at depths of up to 48 m in areas of high water clarity, but absent / limited to ~2 m in areas with more turbid waters (e.g. Liverpool Bay and the Severn Estuary; Birkett et al., 1998). While *L. hyperborea* in NE England and SE Scotland were of a comparable size at similar depths to those observed in colder, more northerly regions of the UK and southern Norway, it is interesting to note that kelp forests in SE Scotland did not extend beyond 10 m (7 m at site B2), whereas in N and W Scotland kelp forests extend to 13 m and 24 m respectively (Smith et al., 2022). The lower depth distributions of forests in NE England were slightly deeper, at 11 m and 13 m, however the majority of the sites we surveyed along the North Sea coast had more comparable depth penetrations to southern regions of the UK (e.g. 9 m SW Wales, 10 m SW England; Smith et al., 2022). Differences in water clarity/turbidity on a local scale have impacted kelp forest depth penetration in regions around the world. For example, locally, Loch Linnhe in W Scotland experiences high sedimentation rates (Overnell and Young, 1995) that limit kelp depth to ~6.5 m (Tsiamis et al., 2020). Further afield, land use that subsequently impacts water clarity has been shown to limit kelp depth in New Zealand (Desmond, Pritchard and Hepburn, 2015), and in the South Shetland Islands, increased volumes of sediment run-off due to ice melt have reduced the lower depth distribution of several macroalgal species (Deregibus et al., 2023). Since turbidity is proven to limit kelp forest depth penetration globally, it is possible that elevated turbidity relative to previously surveyed sites at similar latitudes in the UK could be responsible for the patterns of depth penetration observed here in SE Scotland, and to a lesser extent in NE England.

Aside from light availability, the lower depth distribution of *L. hyperborea* is thought to be somewhat controlled by grazing pressure from the sea urchin *Echinus esculentus* in the UK (Jones and Kain, 1967) and *Strongylocentrotus droebachiensis,* in Iceland (Hjorleifsson, Kassa and Gunnarsson, 1995). Here, the effect of urchin density on kelp forest depth distribution

approached significance, however, whilst not significant, the greatest average urchin density was recorded at the site with the shallowest kelp forest depth extent. Whilst this could be an effect of other aforementioned abiotic processes, it could also suggest that elevated urchin densities may have a limiting effect on the depth penetration of kelp forests, however the scarcity of data collected here does not allow inferences to be made and this requires further investigation at a wider range of sites. Despite this, the density of urchins recorded here (albeit very variable between sites) was elevated in comparison to other regions of the UK, reaching a maximum density of 4.125 ind. m^{-2} at 5 m depth (site B1), whereas elsewhere in the UK urchin densities are rarely recorded to exceed 1 ind. m^{-2} (Smale et al., 2016; Smith et al., 2022). Currently, the influence of urchins on kelp forest structure in the UK is thought to be weak in contrast with other abiotic drivers. The green urchin (*S. droebachiensis)* tends to be present in high densities at depths much below that of the lower depth distribution of kelp (Scheibling and Hatcher, 2013) and densities of *E. esculentus* are generally low enough to avoid exerting significant pressure on kelp forests, as well as being more abundant at depths greater than the lower kelp distribution in many parts of the UK (Comely and Ansell, 1988; Burton et al., 2019). However, there are some local exceptions to this, for example high urchin densities of around 3 per m^2 at a depth of 4.5 m off the Isle of Man caused significant reductions in the standing crop of *L. hyperborea* and prevented its depth penetration below approximately 5 m (Jones and Kain, 1967; Kain and Jones, 1977).

Despite some localised examples of higher urchin densities, there is currently no evidence to suggest that sea urchin grazing - known to cause overgrazing and shifts to barren areas in other regions within this species range (Hagen, 1983) - has impacted the structure or abundance of UK kelp forests. Additionally, along the UK coastline, grazing by small herbivores such as gastropod molluscs does not appear to exert significant pressure on kelp forests (Hargrave et al., 2017). This indicates that biological factors are unlikely to play a major role in influencing the structure or carbon standing stock within UK *L. hyperborea* forests. Carbon storage in kelp forests is variable throughout this species range and is driven primarily by interacting environmental and biological interactions that determine the amount of carbon stored at any given time (Smale et al., 2016). However, environmental factors, particularly temperature stress, can significantly affect macroalgal productivity and, consequently, the carbon storage potential of these forests. Populations at the warmer edge of their geographic range, where

they frequently experience heat stress, often exhibit reduced productivity and carbon storage capacity (Allen, Breshears and McDowell, 2015). Our findings align with previous studies that have shown southern populations along the UK's latitudinal gradient have lower carbon standing stock compared to cooler, northern populations (Smale et al., 2016; Pessarrodona et al., 2018). Previous research attributes this pattern to variations in summer light levels and maximum sea temperatures across the latitudinal gradient (Smale et al., 2016). Additionally, factors such as wave fetch and tidal water motion, which vary over smaller spatial scales, are also thought to influence carbon standing stock and may explain the significant variation observed between sites within the same region (Smale et al., 2016).

The highest average value of carbon standing stock within this study (1578 g C m^{-2}; site C1 in N Scotland) was comparable to previous estimates, however, with the inclusion of an additional two northern sites over previous estimates of standing stock in the UK, our study wide average of 858 g C m^{-2} (including both southern and northern populations) is greater than previous values for the UK and (Smale et al., 2016; Pessarrodona et al., 2018) represent the first estimates of carbon standing stock for kelp forests on the North Sea coast of the UK. Although there was significant variation in carbon standing stock between sites in NE England and SE Scotland, as well as a large differences between sites nested within regions, the results suggest that NE England, in particular, stores a large quantity of carbon within its *L. hyperborea* forests, and that this standing stock is greater than most published data (with the exception of N Scotland; Table 4). The total amount of carbon stored within kelp forest habitats in NE England and SE Scotland, however, is dependent on the spatial extent of kelp forest habitat, and further work is required to accurately map kelp forest extent along North Sea coastlines.

In conclusion, the findings of this study establish an initial baseline of the structure of *L. hyperborea* forests in NE England and SE Scotland and provide a comparison of forests in these regions to those in other areas of the UK and elsewhere across this species range. Comparing across the UK and Norway, our results suggest that kelp forests in NE England and SE Scotland are amongst some of the tallest and represent some of the greatest carbon standing stock values reported for this species, suggesting optimal growth conditions in these areas. However, without data on the spatial extent of this species along North Sea coastlines, we are unable to

make inferences on the total amount of carbon stored within these habitats. Further research to understand the extent of kelp forest habitats is needed to fully comprehend their carbon storage capacity. While we discuss the effect of multiple environmental factors on the structure and carbon standing stock of kelp forests, we were only able to capture the specific effect of wave fetch in this study. In-situ measurements would be an optimum tool for understanding the effects of other environmental drivers and the impact small changes in these can have over the small spatial scales sampled here.

Although the presented data are representative of only a single point in time, previous research conducted since 2014 suggests that UK populations are stable throughout time (Pessarrodona et al., 2018; Smale et al., 2020), with historical surveys suggesting this stability could span nearly 50 years (Jupp and Drew, 1974). The present study therefore provides an important baseline for kelp forests of the UK's North Sea coastline. Evidence suggests that they are structured and function similarly to other *L. hyperborea* forests of the UK, and the baseline this study adds to provides support for the protection and management of these important ecosystems.

Chapter 3. Growth and productivity of kelp forests along a historically industrialised coastline

3.1 Introduction

Anthropogenic influences have become equally as influential as natural factors in shaping marine environments over the past 5,000 years (Bell and Walker, 2014). Human activities have altered biological communities on a global scale through processes such as the introduction of non-native species, exploitation of natural habitats for resources, and the modification of environmental factors that shape species distributions. Consequently, many habitats no longer resemble their natural, historical state (Hobbs, Higgs and Harris, 2009). While the exploitation of fossil fuels has increased greenhouses gasses globally (Malik, Lan and Lenzen, 2016), creating widespread negative impacts (Harfoot et al., 2018), it has also produced localised environmental challenges. Mining fossil fuels, such as coal, generates waste materials that significantly affect natural habitats in many regions through the introduction of pollutants (Leblanc et al., 2000; Li et al., 2014; Liu et al., 2021). These mining byproducts often contain elevated concentrations of naturally occurring elements that are toxic to life in high concentrations, especially aquatic life where such elements are naturally present in minimal amounts (de Almeida Rodrigues et al., 2022). Rising fossil fuel demand in the 20th century resulting in increased mining activity has exacerbated these issues, leading to significant waste management problems in many regions worldwide (Mudd, 2007).

In the UK, coal mining was an incredibly important industry, fuelling the industrial revolution and serving as the primary energy source for electricity generation for decades (Durucan, Jozefowicz and Brenkley, 2010). In some regions, however, waste management presented a logistical challenge, and disposal into coastal habitats was the primary chosen solution due to its ease and low cost (Hydraulics Research Station, 1970; Alderton, 2012). Coal mines in northeast England were some of the most productive in the country, exploiting coal seams extending into the North Sea (Alderton, 2012; Cooper et al., 2017). The proximity of these mines to the coast made this method of waste disposal very convenient. The approach relied on natural erosion processes from tidal and storm action to remove disposed waste from

shores and disperse it throughout marine environments at the mercy of currents (Eagle et al., 1979). This was considered to be a successful mode of waste removal for many decades, however, over time, increased demand for coal drove a major rise in waste outputs, with some mines depositing up to 2.5 million tonnes of waste annually onto shores (Eagle et al., 1979; Cooper et al., 2017) of which natural erosion processes could not keep up with. This practice led to the accumulation of extensive waste deposits on beaches, which smothered entire habitats and introduced significant quantities of heavy metals into coastal ecosystems (Eagle et al., 1979; Alderton, 2012), including copper, iron, lead, cadmium and many others that are toxic to marine life (de Almeida Rodrigues et al., 2022). This had negative effects on coastal ecosystems, including sandy and rocky intertidal habitats (Eagle et al., 1979; Hyslop et al., 1997; Alderton, 2012), and subtidal kelp forests (Jones, 1972; Jones, 1973; Sheppard, 1976; Sheppard, Bellamy and Sheppard, 1980). Areas of intertidal habitat were completely smothered by coal waste (Figure 1.2), and although undocumented, would likely have led to their complete demise. Surviving neighbouring habitats experienced huge reductions in the abundance and diversity of taxa (Hyslop et al., 1997), as well as the absence of organisms normally characteristic to the habitat (Eagle et al., 1979).

Temperate and sub-polar subtidal areas of rocky reef across the world are occupied by large canopy forming seaweeds that function as foundation species. Belonging to the order Laminariales, kelp form highly productive and ecologically important habitats. These kelp forests play an important role in structuring marine habitats, underpinning marine food webs (Dayton, 1985; Rassweiler et al., 2018) and supporting high levels of biodiversity (Johnson and Hart, 2001; Christie et al., 2003; Norderhaug et al., 2005; Teagle et al., 2018; Smale et al., 2022; King et al., 2022). Their physical structure provides direct ecological impacts through the modification of water flow (Connell, 2005; Pinsky, Guannel and Arkema, 2013) and the provision of refugia and feeding grounds for a wide range of organisms including macroinvertebrates and fish, some of which are commercially important (Earp et al., 2024; Jackson-Bue et al., 2023; King et al., 2021; Smale et al., 2022; Teagle et al., 2018). Kelp forests are also among some of the most productive coastal habitat types globally (Duarte et al., 2013), acting as important carbon donors by transporting macroalgae derived carbon to sedimentary receiver habitats both nearby (Hill et al., 2015) as well as several hundreds of kilometres away (Hobday, 2000). Additionally, kelp forests also store a significant quantity of

carbon within their tissue at any one point in time (Hill et al., 2015). The quantity, however, is governed by the structure and spatial extent of forests, with larger, heavier individuals typically containing greater quantities of carbon (Smale and Moore, 2017).

Along the wave exposed rocky coastline of the United Kingdom (UK) kelp forests are dominated by *Laminaria hyperborea* (Gunnerus) Foslie 1884, a stipitate kelp whose range extends from northern Portugal to northern Norway (Sjøtun et al., 1993; Pinho et al., 2016), forming dense stands at depths down to, typically, 15 to 20 m around much of the UK (Smith et al., 2022). Pioneering works by Kain and Jones (Kain and Jones, 1963; Kain, 1971; Kain and Jones, 1976) gave insights into the growth, reproduction and biology of *L. hyperborea* in the UK, although until around a decade ago our knowledge and understanding of the structure and function of kelp forest ecosystems lagged behind other leading scientific nations (Smale et al., 2013). Recent research has made a concerted effort to characterise the structure and function of *L. hyperborea* forests in the UK (Smale et al., 2016; Smale and Moore, 2017; Teagle et al., 2018; Bué et al., 2020; Smith et al., 2022; Smale et al., 2022; Jackson-Bue et al., 2023; Gouraguine et al., 2024; Earp et al., 2024), as well as to understand the effects of anthropogenic influences upon them (Smale et al., 2015; Smale and Vance, 2016; Arnold et al., 2016; Hargrave et al., 2017; Pessarrodona et al., 2018; Pessarrodona, Foggo and Smale, 2019; Smale, 2020; Earp et al., 2024), however the effects of pollutants are still not well understood. Indeed, various studies have investigated the effects of pollutants on kelp (Contreras et al., 2007; Scherner, Bonomi Barufi and Horta, 2012; Leal et al., 2018; Oyarzo-Miranda et al., 2020; Jara-Yáñez et al., 2021), however, very few of these have looked at the impacts on the structure and function of kelp forests (Oyarzo-Miranda et al., 2020), let alone the effects on that of *Laminaria hyperborea* forests. This study investigates the impact of historic coal mining waste disposal on the structure, growth and productivity of *L. hyperborea* forests. By drawing comparisons between sites impacted by mine waste disposal that were buried under spoil for multiple decades, and those that were unaffected, I intend to assess whether the legacy of coal mining waste continues to affect the structure and function of kelp forest habitats that contribute to wider ecosystem functioning in this region. Previous research has highlighted the negative impacts of the coal mining operations on marine habitats in this area, however, there has been little focus on the structure or functioning of kelp forest

habitats. This represents a significant gap in our knowledge of how this species responds to both historic and lingering present day environmental perturbations.

3.2 Methods

3.2.1 Study design and location

To investigate the effect of historic mining pollution on kelp forest structure, growth and productivity, sampling was undertaken at 2 sites within each of 3 locations (Figure 3.1) along the northeast England coastline between October 2021 and August 2022. Locations were selected based on presence or absence of historic coal mining waste disposal, whereby locations A and C were heavily impacted throughout the active mining period between the 1900s and 1990s and were buried under spoil for much of this period, and location B represented an area where no mining activity took place. All locations were fully exposed to wave action and had a dominance and abundance of *L. hyperborea.* An asymmetrical design was employed (with two impacted locations separated by one unimpacted location) as there were no locations both unaffected by historic mine waste disposal and with kelp present along the north Durham coastline. Sites within each location were separated by a distance of between 1 km and 3 km, and locations were separated by between 20 km and 50 km.

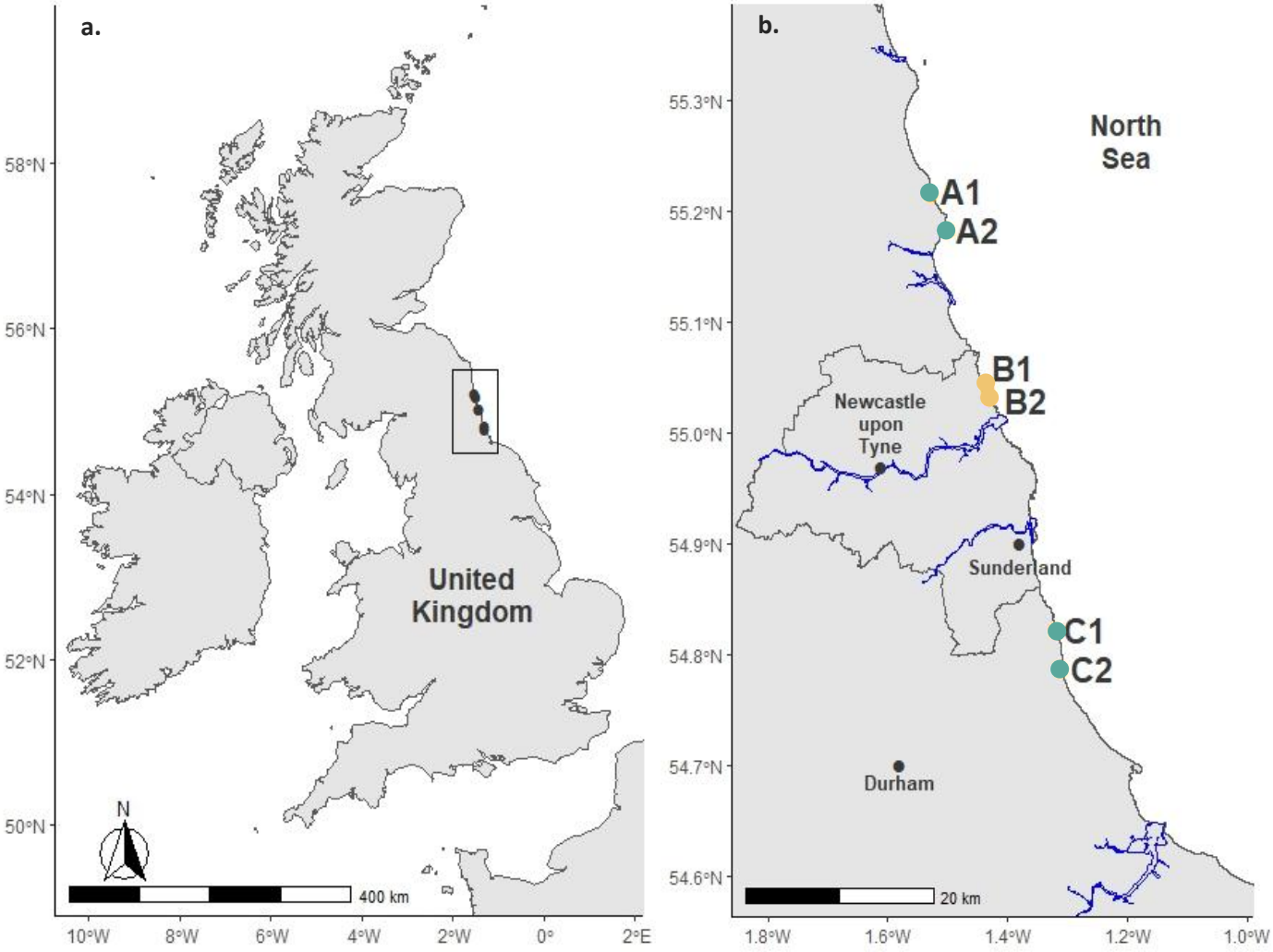

Figure 3.1. Study area (a) showing the position of the two sites (1 and 2) within each of three sampling locations (A, B and C) (b). Sampling locations A and C represent areas impacted by mining waste, while B was unaffected.

3.2.2 Kelp forest structure

To investigate the structure of the kelp forest at each site, sampling took place during spring low tides at two time intervals: October 2021 (T1) and August 2022 (T2). During each sampling effort, ten replicate $1m^2$ quadrats were haphazardly placed within the kelp forest at between 0 and 0.3 m below chart datum (BCD) and the density of canopy forming individuals was recorded. Ten replicate individuals from within the kelp forest were also haphazardly selected for the measurements of morphology and biomass. Whole individuals were collected by dislodging holdfasts from the substratum for the measurement of the following characteristics:

stipe length (cm), blade length (cm), total length (cm) and total biomass (g fresh weight (FW)). Additionally, at T2 individuals had stipe biomass (g FW) and blade biomass (g FW) measured separately by cutting individuals at the blade/stipe junction. Individuals were also aged by counting annual growth rings on cross-sections of the stipe, as described by Kain and Jones (1976).

Values of carbon standing stock were calculated following the methods of Smale et al. (2016). The relationship of fresh weight (FW) to dry weight (DW) of distal blade, basal blade and stipes was first calculated. The relationship between fresh weight (FW) and dry weight (DW) was investigated separately for basal blade, distal blade and stipe segments, since the relationship varies between segments and anatomical regions (Smale et al., 2016). For distal and basal blade FW:DW relationships, 10 blade samples were collected from mature canopy forming individuals each month from October 2021 to August 2022. Basal and distal segments of a single blade digit from each individual were weighed (FW), dried at 60°C for 48hrs, and reweighed (DW). The relationship between FW and DW at each site and month was then calculated using linear regressions. Given the impact of poor weather conditions on the regularity of sampling, FW:DW data was averaged for each site from samples collected in only May, June and August when sites were visited more consistently (Table S3.1). Average FW:DW values for distal and basal blade at each site were then averaged to give a FW:DW value for whole blades. For stipes, additional samples were collected in August 2024 from sites in location B (Figure 3.1) and were dried using the same method as described for blades. These values of whole blade and stipe FW:DW were then used to transform stipe and blade FW biomasses measured during T2 at each study site into DW values for whole plants. Whole plant DW values were then converted to carbon content based on previous research that suggests the carbon content of DW *Laminaria hyperborea* tissue to be approximately 30% (Smale et al., 2016; Pessarrodona et al., 2018). Whole plant carbon content was then multiplied by the respective site density to give an estimate of carbon content per m^{-2} of kelp forest.

3.2.3 Biomass accumulation and loss

The accumulation and loss of biomass in 10 haphazardly selected mature canopy forming kelp was measured monthly (or as close to monthly as possible taking into account accessibility – see table S3.1 for details) using a modified hole-punch method (Pessarradona et al. 2019). Using this method, selected kelp were individually tagged using a labelled cable tie covered in surgical tubing and a series of holes were punched into the blade at 5 cm (H1) and 10 cm (H2) from the meristematic junction, with an additional hole punched in an outer digit at 10 cm (H3) above the meristematic junction. H2 and H3 account for differences in growth rates between digits of an individual kelp (Kain and Jones, 1976). At the same time as hole-punching, the length of hole-punched digits were measured. After approximately 1 month, tagged individuals were retrieved and returned to the laboratory. The final length of hole-punched central (L1) and outer (L3) digits and the position of previously punched holes on central and outer digits were recorded. On average, 26 individuals were retrieved across all sites on each sampling occasion (Table S3.1).

Elongation and erosion (cm) rates were initially calculated before conversion to biomass (g) gain and loss. For the conversion from cm to g, additional data was collected from sites in location B (Figure 3.1) during August 2024. In total, 20 individuals were collected from two sites (B1 and B2) and the entire width of the blades were sectioned into three 5 cm long segments from both distal and basal parts of the blade. Segments were cleaned of epiphytes, weighed, and the middle section of the 3 segments from both the distal and basal ends were dried at 60°C for 48hr. The relationship between dry weight (DW) and fresh weight (FW) was investigated using linear regression separately for basal and distal segments, since the relationship varies between segments (Smale et al., 2016). Relationships were all very strong, with R^2 values of over 0.92 (Figure S3.1). The weights of the remaining two distal and basal segments from each individual were then estimated using the calculated relationship. The estimated and measured values of dry biomass were then averaged between the three segments and divided by their length (5 cm) to give a value for the dry biomass per unit length (g/cm) for each of the basal and distal areas of the kelp blade (B_{basal} and B_{distal}, respectively). Elongation and erosion rates (cm) of blade tissue could then be converted to accumulation and loss of biomass (g DW).

Biomass accumulation (BA) for each individual was calculated as:

$$BA = E \times B_{basal} / d$$

In which d is the number of days between tagging and retrieval, and E is the average blade elongation from the central and outer digits, calculated using the distance between the initial hole punch position and the final hole punch position, as follows:

$$E = 0.5 \times [(H1_{final} - 5) + (H2_{final} - 10)] + (H3_{final} - 10)$$

Biomass loss (BL) for each individual was calculated as:

$$BL = M \times B_{distal} / d$$

In which M is the average blade loss calculated using the difference between the initial length and final length of central (L1) and outer (L3) digits, taking into account respective digit elongation (e), as follows:

$$M = 0.5 \times [(L1_{initial} + e) - L1_{final}] + [(L3_{initial} + e) - L3_{final})]$$

Additionally, biomass loss from kelp forests through whole plant dislodgement was quantified over the course of the study. At each study site, three replicate plots were established with 10 canopy forming kelp in each plot. Each individual was tagged using a cable tie covered in surgical tubing. Plots were revisited after 11 months and tagged individuals were recounted. In order to calculate the biomass lost through dislodgement of whole plants (D) at each site, the following equation was used:

$$D = (Dis \times Den \times DW) / T$$

In which T is the number of tagged kelps in each plot (10), Dis is the number of dislodged individuals recorded, Den is the average density of the *L. hyperborea* forest surrounding the established dislodgement plots at each site, and DW is the average dry weight of individuals

at each site during the months of May, June and August (as used previously in the calculation of carbon standing stock).

3.2.4 Statistical analysis

Patterns of spatial variability in *L. hyperborea* forest structure (i.e. density and canopy biomass) and individual-level metrics (i.e. canopy former biomass, stipe length, blade length, total length and age) were analysed using univariate permutational analysis of variance (PERMANOVA) (Anderson, 2001). Three-way PERMANOVAs were used with the factors of pollution (fixed, 2 levels), site (random, 2 levels nested in non-polluted, 4 levels nested in polluted), time point (fixed, 2 levels) and their interactions. The distributions of morphological and density data were checked and conformity to normal distribution confirmed. Similarly, to analyse variation in biomass accumulation and loss through blade erosion a three-way univariate PERMANOVA was used with the levels of pollution (fixed, 2 levels), sites (random, 2 levels nested in non-polluted, 4 levels nested in polluted), months (fixed, 9 levels) and their interactions as factors. Variation in carbon standing stock and biomass loss through whole plant dislodgement were analysed using two-way univariate PERMANOVAs, testing for differences between factors of pollution (fixed, two levels) and site (random, 2 levels nested in non-polluted, 4 levels nested in polluted). For each analysis, permutations (9,999 under a reduced model) were based on Euclidean distance similarity matrices. Where permutations were low (i.e. <100) p values derived from Monte Carlo simulations were used. PERMANOVAs are typically more robust to heterogeneous variations and non-normal distributions than traditional ANOVAs, however variation in dispersion between treatments can have an influence (Anderson, Gorley and Clarke, 2008). Therefore, investigations to determine whether within-group dispersion varied between levels of factors was carried out using permutational dispersion (PERMDISP) tests. Where significant variation was found, the significance threshold for PERMANOVA tests was reduced to $p<0.01$ (Earp et al., 2024; Leclerc et al., 2023), rather than $p<0.05$ which was used as the level of significance elsewhere. All statistical analyses were conducted, and model assumptions checked, in PRIMER 7 software (Clarke and Gorley, 2015) with the PERMANOVA add-on (Anderson, 2008). All figures were made in RStudio v 4.2.1 (R Core Team, 2022) using the package “ggplot2” (Wickham, 2016).

3.3 Results

3.3.1 Kelp forest structure

All study sites were dominated by *Laminaria hyperborea* with no other kelp species recorded in quadrats. Mean (± 1 SE) kelp length was highly variable between sites at T1 ranging from 105 ± 5 cm (site B2) to 169 ± 10 cm (site A2). However, at T2 values were considerably more similar, ranging from 147 ± 7 cm (site B2) to 162 ± 6 cm (site A2) (Figure 3.2a). A similar pattern of less variation between sites at T2 was observed in both mean stipe and blade lengths (Figure 3.2a). Stipe length ranged from 54 ± 4 (site B2) to 94 ± 9 cm (site C2) at T1 and from 72 ± 5 (site C2) to 89 ± 6 cm (site A2) at T2, and blade length ranged from 51 ± 2 (site B2) to 75 ± 3 (site A2) at T1 and from 69 ± 3 (site A1) to 77 ± 3 cm (site C2) at T2 (Figure 3.2a).

Both mean (± 1 SE) individual kelp biomass and canopy biomass (per m^{-2}) were also much more variable between sites at T1 than at T2 (Figure 3.2b-c). Individual biomass ranged from 619 ± 90 (site B2) to 1093 ± 122 g ind^{-1}. (site A2) at T1 and 686 ± 54 (site C2) to 1267 ± 68 g ind^{-1}. (site C1) at T2, whilst canopy biomass ranged from 7.3 ± 1.1 (site B2) to 27.3 ± 1.6 kg m^{-2} (site B1) at T1 and from 13.1 ± 1.5 (site A1) to 17.2 ± 0.9 kg m^{-2} (site C1) at T2 (Figure 3.2b-c). Again, less variation between sites was measured in mean (± 1 SE) density at T2 than at T1, which ranged from 11.8 ± 1.1 (site B2) to 25.5 ± 2.1 ind. m^{-2} (site B1) at T1 and 13.6 ± 1.2 (site C1) to 24.5 ± 2.5 (site C2) at T2 (Figure 3.2d). Mean age (± 1 SE) was expectedly greater across all sites at T2 than at T1 (Figure 3.2e). Site C2 consistently had the youngest kelp at 3.6 ± 0.2 years at T1 and 4.7 ± 0.2 years at T2, and had considerably less within-site variability at both T1 and T2 compared to other sites. The oldest recorded individual was 9 years old (site A2).

Whilst morphological measures were generally more variable at T1, values at T2 showed a general level of homogeneity across sites and levels of pollution. This was similarly observed in carbon standing stock values, which only varied by 341 g C m^{-2} between the greatest and lowest site averages (Figure 3.3). Sites in polluted location C both displayed greater values of mean standing stock than other sites, with 1,321 ± 71 (C1) and 1,241 ± 99 g C m^{-2} (C2), although polluted site A2 had a similar value to site C2 of 1,225 ± 115 g C m^{-2}. Among the non-

polluted sites, site B2 had the greatest value of carbon standing stock at 1,167 ± 112 g C m^{-2}. Site B1 showed the lowest value across the study of 980 ± 118 g C m^{-2}, however this was not dissimilar to polluted site A1 which had 1,030 ± 121 g C m^{-2} (Figure 3.3).

Except for blade length, all measures varied significantly between sites nested in pollution by time (Table 3.1). Blade length, like all other measures, varied significantly between sites nested in pollution, however it was also significantly greater at T2 than at T1 (Table 3.1). Although significant differences over spatial and temporal scales were observed, there were no consistent patterns across sites, times or levels of pollution. Carbon standing stock (measured only at T2) did not vary significantly over any scales measured (Table 3.1).

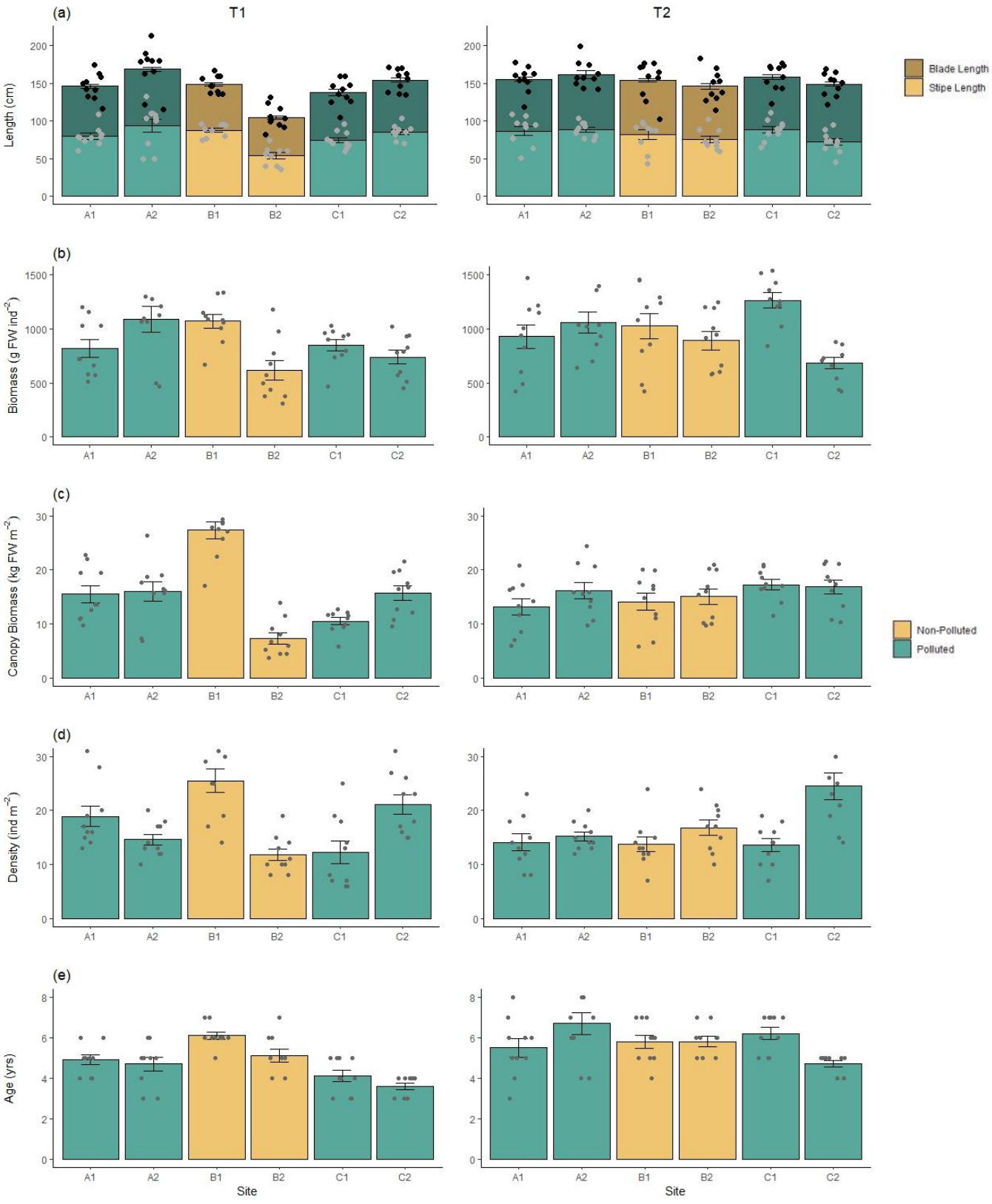

Figure 3.2. Structure of *Laminaria hyperborea* forests at sites affected (locations A & C) and unaffected (location B) by historic coal mine waste disposal in northeast England. Bars represent mean values ± SE (n=10). Points represent raw data values. FW: Fresh Weight. Ind.: Individual. Site and locations can be seen in Figure 3.1.

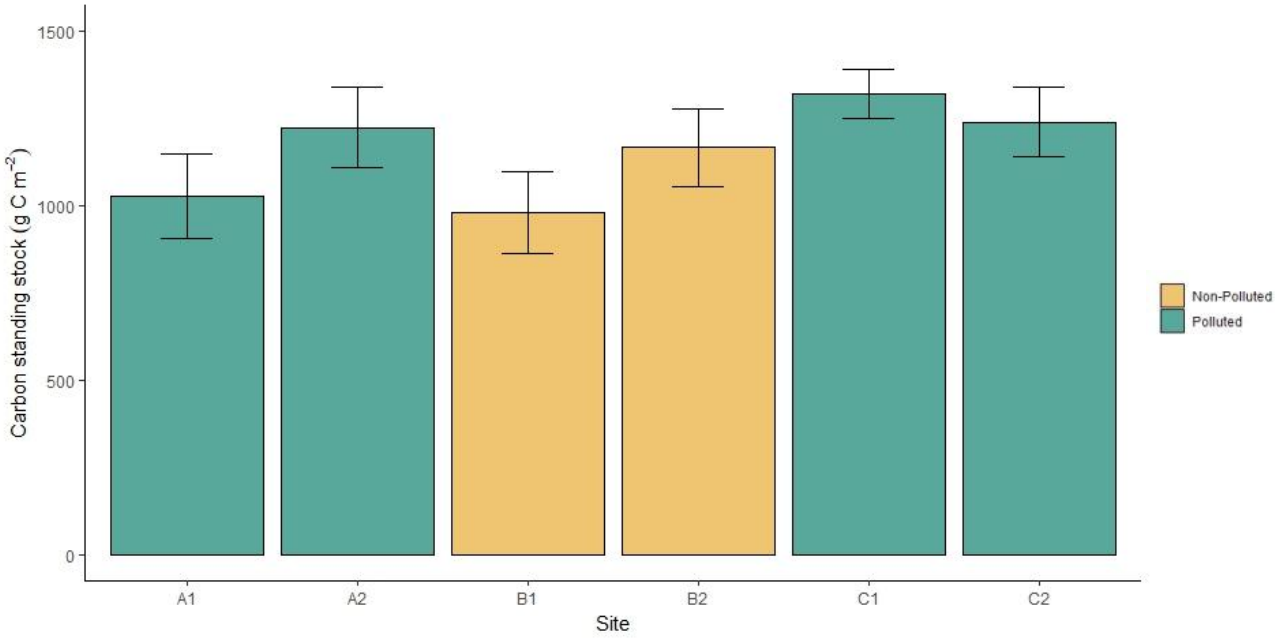

Figure 3.3. Carbon standing stock of *Laminaria hyperborea* forests at sites in northeast England affected (locations A and C) and unaffected (location B) by historic coal mine waste disposal. Bars represent mean values ± SE. Ind.: Individual. Sites and locations can be seen in Figure 3.1.

3.3.2 Biomass accumulation and loss

Rates of biomass accumulation and loss varied significantly over temporal and spatial scales, with a site nested in pollution by month interaction for both variables (Table 3.2). Across all sites, rates of biomass accumulation followed a general seasonal trend, with rates increasing steadily from October, and peaking between May and June before declining (Figure 3.4a). Among the polluted sites, A1 exhibited the highest rate of biomass accumulation, peaking at 2.16 ± 0.16 g DW day^{-1} in May. This was almost double all other polluted sites (A2, C1 and C2) which had more modest peak values ranging between 1.00 ± 0.12 (C1, May) and 1.20 ± 0.17 g DW day^{-1} (A2, May). Generally, rates of biomass accumulation were lower at all sampled months in non-polluted sites than polluted sites, however this trend was not statistically significant. Whilst polluted sites showed higher peak biomass accumulation rates than non-polluted sites, accumulation rates returned to similar levels post-peak, therefore, exhibiting much greater declines in biomass accumulation rates at polluted sites over non-polluted. By August, all sampled sites had returned to low rates of accumulation of between 0.25 ± 0.03

and 0.10 ± 0.01 g DW day^{-1}, aside from site C1 which remained relatively high at 0.67 ± 0.03 g DW day^{-1} (Figure 3.4a).

Rates of biomass loss through erosion were generally more variable than rates of biomass accumulation (Figure 3.4a-b). Where sampled, rates of loss were generally low during the months of February and March, with most sampled sites increasing the rate of loss through April and June, before decreasing again between June and December (Figure 3.4b). Among the polluted sites, A1 showed the highest rate of biomass loss, peaking at 0.81 ± 0.04 g DW day^{-1} in May (Figure 3.4b). This was substantially higher than other polluted sites, where peak values were lower and ranged from at 0.51 ± 0.09 (C1, May) to 0.35 ± 0.04 g DW day^{-1} (C2, May). Among non-polluted sites, the rate of biomass loss peaked at 0.37 ± 0.13 g DW day^{-1} in June at site B2, with similar values also measured at site B1. Peak biomass loss rates were observed between the months of April and June for all sites, coinciding with May cast, during which the growth collar containing old blade growth is shed.

Values of annual biomass loss from whole plant dislodgement did not vary between sites or levels of pollution, although differences between sites nested in pollution did approach significance ($p=0.054$; Table 3.2). Whilst non-significant, there were some differences seen between sites. Among the polluted sites, A2 showed the highest value of biomass loss through dislodgement at 1959 ± 226 g C m^{-2} yr^{-1} (Figure 3.4c). This was considerably higher than other polluted sites, where values ranged from 1191 ± 229 (site C2) to 1409 ± 141 g C m^{-2} yr^{-1} at site C1. Non-polluted sites showed more modest values of biomass loss from dislodgement compared to polluted sites (Figure 3.4c). Site B2 lost 1369 ± 124 g C m^{-2} yr^{-1}, which was similar to some of the higher values seen in polluted sites, while site B1 demonstrated the lowest overall loss from dislodgement of 941 ± 181 g C m^{-2} yr^{-1}.

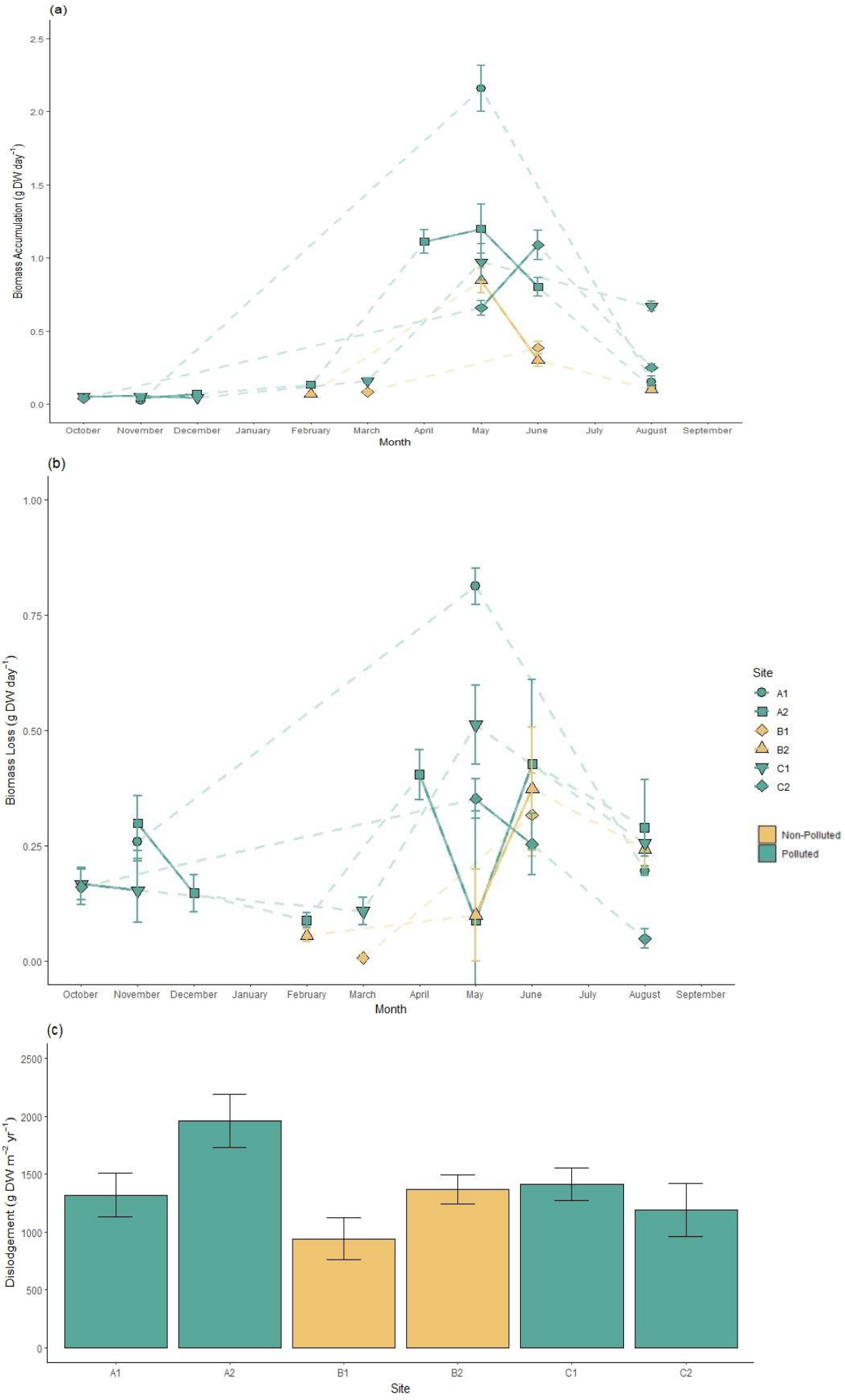

Figure 3.4. Annual pattern of biomass accumulation (a), biomass loss through erosion (b) and biomass loss through whole plant dislodgement (c) occurring in *Laminaria hyperborea* forests at sites in northeast England affected (locations A and C) and unaffected (location B) by historic coal mine waste disposal. Points represent mean values ± SE. Dashed lines between points where data was not collected in consecutive months. Ind.: Individual. Sites and locations can be seen in Figure 3.1.

Table 3.1. Univariate permutational ANOVAs to test for variability in population and individual level kelp metrics between time points, levels of pollution and sites (nested in pollution). Models were run using 9,999 permutations based on similarity matrices derived from Euclidian distances, with 'Time' (where applicable) as a fixed factor, 'Pollution' as a fixed factor and 'Site' as a random factor nested within 'Pollution'. Significant values ($p < 0.05$) are indicated in **bold**. Significance values followed by a '†' are derived from Monte Carlo Simulations due to the low number of unique permutations. p-values underlined indicate a significant result of PERMDISP tests and therefore a significance threshold reduction to $p < 0.01$. '-' indicates the term was not included in the statistical model.

Response	Time			Pollution			Site(Pollution)			Time x Pollution			Site(Pollution) x Time			Res df
Variable	df	*F*	p	df	*F*	p	df	*F*	p	df	*F*	p	df	*F*	p	
Per m²																
Canopy density	1	0.32	0.5949	1	0.002	0.9682†	4	12.71	**0.0001**	1	0.37	0.5776	4	8.23	**0.0001**	108
Total canopy biomass	1	0.03	0.8556	1	0.07	0.7945†	4	12.93	**0.0001**	1	0.35	0.5854	4	17.13	**0.0001**	108
Carbon standing stock	-	-	-	1	1.43	0.2988†	4	1.37	0.2524	-	-	-	-	-	-	54
Per canopy-forming individual																
Stipe length	1	0.45	0.5327	1	1.39	0.2992†	4	6.38	**0.0001**	1	0.36	0.5726	4	4.34	**0.0024**	108
Blade length	1	22.44	**0.0123**	1	4.22	0.1041†	4	2.91	**0.0273**	1	8.41	0.0524	4	1.17	0.3221	108
Total length	1	3.68	0.1268	1	2.52	0.1875†	4	7.20	**0.0001**	1	1.77	0.2572	4	4.03	**0.0043**	108
Total plant biomass	1	1.40	0.2905	1	0.03	0.8679†	4	8.70	**0.0001**	1	0.001	0.9718	4	3.20	**0.0164**	108
Age	1	7.01	0.0589	1	1.62	0.2721†	4	7.11	**0.0001**	1	4.03	0.1187	4	2.65	**0.0356**	108

Table 3.2. Univariate permutational ANOVAs to test for variability in biomass accumulation, biomass loss through erosion and biomass loss through whole plant dislodgement between months (where applicable), levels of pollution and sites (nested in pollution). Models were run using 9,999 permutations based on similarity matrices derived from Euclidian distances, with 'Month' as a fixed factor, 'Pollution' as a fixed factor and 'Site' as a random factor nested within 'Pollution'. Significant values ($p < 0.05$) are indicated in **bold**. Significance values followed by a '†' are derived from Monte Carlo Simulations due to the low number of unique permutations, and p-values underlined indicate a significant result of PERMDISP tests and therefore a significance threshold reduction to $p < 0.01$. '-' indicates the term was not included in the statistical model.

Response	Month			Pollution			Site(Pollution)			Month x Pollution			Month x Site(Pollution)			Res df
Variable	df	*F*	p	df	*F*	p	df	*F*	p	df	*F*	p	df	*F*	p	
Biomass Accumulation	8	4.29	0.0304	1	4.65	0.086†	4	10.75	**0.0001**	4	0.36	0.7885	8	21.06	**0.0001**	205
Biomass Loss	8	0.98	0.5298	1	2.07	0.2017†	4	3.21	0.0164	4	0.72	0.6003	7	4.45	**0.0003**	201
Dislodgement	4	-	-	1	1.21	0.3323†	4	3.14	0.0536	-	-	-	-	-	-	12

3.4 Discussion

Kelp forests play an important role in habitat creation, biodiversity support and coastal carbon cycling, and have received increasing attention to understand their structure and function over the last two decades (Bekkby et al., 2014; de Bettignies et al., 2013; Earp et al., 2024; Harrold et al., 1988; Hill et al., 2015; Jackson-Bue et al., 2023; Krause-Jensen and Duarte, 2016; Krumhansl and Scheibling, 2012; Pérez-matus et al., 2007; Pinho et al., 2016; Smith et al., 2022; Zahn et al., 2016). While kelps importance is becoming ever more understood, the impact of anthropogenic stressors such as marine pollution are still understudied, particularly on the study species, *Laminaria hyperborea*. The results of this study show that while there were differences between sites, there was no evidence for the continued impact of historic coal waste disposal on kelp forest structure or functioning, suggesting these systems are relatively resilient, despite the major environmental perturbations these habitats experienced for nearly 100 years.

Chapter 2 gave the first up to date overview of the typical structure of kelp forests in this geographic region, showing that kelps typically reach lengths of around 235 cm, weigh approximately 1400 g per individual, and form dense stands of around 10 individuals per m^2. Here, the structure of kelp forests was different, with kelp typically being shorter, younger and having lower biomass. Since individuals were smaller, this allows a greater number of individuals to occupy a given area and therefore densities measured here were greater than in the wider region (Chapter 2) as well as previous studies at similar latitudes (Smale et al., 2016; Smith et al., 2022). While direct comparisons to the wider region show differences in kelp forest structure, comparisons made between polluted and non-polluted areas showed no consistent patterns or differences. Although no historic kelp forest surveys exist prior to, or during, the active disposal period (1899 to 1993), it is likely that the volume of waste disposed onto the coast would have caused significant habitat destruction (Figure 1.2). Studies conducted in habitats near to waste disposal locations provide evidence of habitat degradation, showing large reductions in species abundance and diversity in a range of habitats including rocky and sandy intertidal shores and subtidal soft sediment habitats (Eagle et al., 1979; Hyslop et al., 1997). Given the lack of significant variation between polluted and non-polluted locations studied here, these findings suggest that historic coal mining pollutants

have had limited long-term effects on the kelp themselves. Additionally, the similarities in kelp forest structure between these locations suggests substantial recovery has occurred since the cessation of mine waste disposal in 1993, or since the remediation work commencing in 1997 on the Durham coast (location C) that removed much of the remaining mine waste.

A similar lack of differences between polluted and non-polluted locations was found in measures of kelp productivity. Rates of biomass accumulation, loss and dislodgment varied significantly between sites, but this was likely natural variation driven by local scale differences in environmental conditions. In comparison to previous studies, rates of biomass accumulation observed here were broadly similar; however, natural variation across sites meant that some of the higher rates exceeded those recorded elsewhere (Pessarrodona, Foggo and Smale, 2019). Rates of biomass loss, however, while generally lower than those demonstrated in previous studies, were elevated for a longer duration. Pessarrodona, Foggo and Smale (2019) showed loss rates to increase over the months of March and April before returning to almost zero in May, whereas findings here showed an increase in loss rates to last several months, increasing from April through June, with rates still elevated in August. In contrast to the comparatively lower rates of biomass loss, dislodgement was considerably greater here than measured previously (Pessarrodona et al., 2018). The biomass lost through the dislodgment of whole kelp individuals was on average twice as large as previous findings, with peak values over three times greater (Pessarrodona et al., 2018). This may be a consequence of the more open coast nature of this study compared to the previous work. Whilst biomass accumulation measures growth, biomass loss and dislodgement measure the quantity of biomass released from kelp forest habitats that can be transported to potential receiver habitats that act as carbon sinks (Duarte et al., 2013; Smale et al., 2022). These processes, along with the annual phenomenon of ‘May cast’ whereby old growth kelp blades are shed, are important pathways of potential carbon sequestration (Pessarrodona et al., 2018). Kelp tissues accumulate in deep coastal or offshore areas and have the potential to be locked away in sediments for long periods of time (Pedersen et al., 2020; Filbee-Dexter et al., 2024). However, the difficulties in monitoring these pathways make the quantification of carbon sequestration a difficult task.

Whilst there were differences in both kelp forest structure and productivity between the results here and those previously published, it is important to note that sampling took place at considerably shallower depths here than most previous studies. King et al. (2020) demonstrated productivity of the morphologically similar kelp species *Laminaria digitata* to be considerably greater than recorded both here and in previous studies of *L. hyperborea*. Whilst this could be inter-species variability, it could also be a function of the location each species occupies. Being an intertidal species, *L. digitata* occupies a higher energy environment than the subtidal *L. hyperborea*. Since previous studies on *L. hyperborea* productivity have focussed on kelp occupying depths of several metres (Smale et al., 2020), or those in more sheltered locations (Pessarrodona, Foggo and Smale, 2019), it is likely that the populations surveyed here experience a higher energy environment that may drive the observed differences in productivity. Likewise, studies focussing on *L. hyperborea* forest structure generally survey populations at depths greater than 2 metres, and therefore the differences observed between the findings here and previous studies could also be a function of the difference in depth.

Although minimal effect of pollution were detected across this study, there were noteworthy differences observed at site C2. This site experienced one of the highest volumes of waste disposal into the coastal environment along this coastline, with over 2.5 million tonnes of waste per year being disposed at the mines peak output (Eagle et al., 1979). Although most morphological measurements at site C2 were consistent with those of the wider study, kelp here were consistently younger and exhibited greater densities than other sites. The age of kelp was also considerably less variable than at other sites, and the maximum age of kelp was lower than that of all other sites. These patterns suggest that, as described by Vásquez et al. (2000), increased pollution levels may reduce survivability and lead to younger populations.

The metal pollutants driving the negative impacts described by Vásquez et al. (2000) have also been identified in high concentrations in mine wastes from this area (Eagle et al., 1979; Alderton, 2012). In particular, elevated levels of iron (Fe) which have been identified in macroalgae and molluscs from location C (Alderton, 2012), and extremely high levels of copper (Cu) that have been found in sediments at the same location (Eagle et al., 1979). *L. hyperborea*

is known to bioaccumulate metals (Schiener et al., 2015), and some kelp species accumulate pollutants in specific tissues, especially perennial species (Burger et al., 2007). While it is known that kelps can absorb these pollutants, their effect on kelp forest structure and functioning are not fully understood. Evidence suggests that harmful metals, such as Cu and Fe, can negatively impact habitat structure. For instance, in Chile, *Lessonia trebaculata,* exhibited a marked decline in abundance near pollution outflows, with increased reproduction, survival, and forest density observed at greater distances from pollution sources (Vásquez et al., 2000). Although the exact mechanism of this negative influence remains unclear, metal pollutants appear to impact early life stages more than adult individuals. Contreras et al. (2007) showed that Cu exposure significantly reduced spore release and spore settlement, and even low concentrations of Cu completely inhibited the formation of male and female gametophytes, completely disrupting development (Contreras et al., 2007), with potentially devastating effects on natural populations. Moreover, Cu can exacerbate other stressors such as ocean acidification and warming, making it a potentially serious threat to kelp forest structure and therefore negatively impact wider ecosystem functioning (Leal et al., 2018). However, the impact of metal pollutants is likely species-specific (Huovinen, Leal and Gmez, 2010), and research on their effects on *Laminaria hyperborea* remains limited, highlighting an area that warrants further investigation.

While species in the study area are known to accumulate high concentrations of potentially toxic metal pollutants, we lack knowledge on the bioavailability of these metals at the study sites. In addition to historical waste disposal, abandoned mines continue to pump groundwater, carrying excessive concentrations of various metal pollutants (Younger, 1993; Cooper et al., 2017). However, high concentrations may not cause negative effects if the pollutants are not in a bioavailable, or labile, form (Contreras et al., 2007). Additionally, some research suggests that the presence of nitrates can mitigate the rate of bioaccumulation and subsequent negative effects of metals including Cu (Huovinen, Leal and Gmez, 2010). Although pollutants are still being introduced into the environment today, their influx may be intermittent or varied, for example, greater volumes of groundwater would be pumped into coastal habitats during periods of heavier rainfall. Negative consequences may therefore only occur if pollutant releases coincide with critical periods, such as spore release or early developmental stages (Contreras et al., 2007; Huovinen, Leal and Gmez, 2010; Leal et al.,

2018). Additionally, pollutants may disperse quickly in the marine environment, meaning significant impacts might only be measurable very close to the groundwater outflows, depending on the sensitivity of the species in question.

In conclusion, this study provides valuable insights into the resilience of *L. hyperborea* forests along a historically industrialised coastline where coal mine waste disposal has, at least in the past, significantly shaped the marine environment. Despite the potential for long-term impacts from metal pollutants, the structural and functional integrity of kelp forests appears to have largely recovered to a level where they are comparable to nearby unaffected sites. Differences between polluted and non-polluted sites were minimal, with the exception of site C2, where altered morphological measures suggest the possibility of some lingering local stress. However, overall, the robustness of kelp in response to past pollution highlights their capacity to persist under the presence of some environmental stressors. Further research is required to understand the bioavailability of remaining pollutants at these polluted sites and their potential impacts on this species at different life stages. It is additionally important to understand their interactions with other stressors, such as warming and acidification. This will be crucial in assessing future risks to these important ecosystems as environmental pressures continue to evolve.

Chapter 4. Variability in macroinvertebrate assemblages associated with *Laminaria hyperborea* stipes and holdfasts along a historically industrialised coastline.

4.1 Introduction

Kelps are large canopy forming macroalgae that form highly productive and ecologically important marine ecosystems. Comprised of species within the order Laminariales, kelps are foundation species that are found along approximately 36% of global coastlines (Jayathilake and Costello, 2021). Kelp forests not only play an important role in structuring marine habitats, but they underpin food webs (Duarte and Cebrián, 1996; Elliott Smith and Fox, 2022) and support high levels of biodiversity (Leliaert et al., 2000; Steneck et al., 2002; Pérez-matus et al., 2007; Zahn et al., 2016; Bué et al., 2020; King et al., 2021; Smale et al., 2022; Jackson-Bue et al., 2023; Gouraguine et al., 2024). Whilst kelp forests also alter the ecological environment indirectly, through the attenuation of light, modifying water flow, and influencing nutrient cycling, kelp individuals themselves have a direct role in supporting diverse biological communities (Smith, 1996b; Anderson et al., 2005; Teagle et al., 2018; Bué et al., 2020). The physical structure of kelp serves as a refuge and provides substrate and feeding grounds for wide range of marine organisms, specifically, a diverse assemblage of macroinvertebrates that inhabit the holdfasts and, in some species, stipes of kelp individuals (Teagle et al., 2018; King et al., 2021). One species in particular, *Laminaria hyperborea,* has morphological features that strongly contribute to its ability to sustain diverse macroinvertebrate assemblages consisting of a large, structurally complex holdfast and a stipe covered in dense epiphytic algae (Teagle et al., 2018; King et al., 2021).

L. hyperborea is a large stipitate kelp that is distributed across the northeast Atlantic, extending from northern Portugal to northern Norway, with its range reaching the Barents Sea and northwest Russia (Sjøtun et al., 1993; Schoschina, 1997; Müller et al., 2009). This species has a large, perennial holdfast which consists of numerous haptera (root-like structures) that act as an attachment structure, anchoring the kelp to the substrate, as well as providing a complex habitat for a range of species (Teagle et al., 2017). The holdfast itself can support more than

100 species and thousands of individuals (Christie et al., 2003), mostly consisting of macroinvertebrates such as annelids, crustaceans and echinoderms. Additionally, the epiphytes attached to the stipe add structural complexity and provides shelter and food for a high diversity and abundance of macroinvertebrates (King et al., 2021).

Despite their ecological importance, the threats to kelp forests from a range of ecological stressors are increasing. Rising sea surface temperature (SST) has led to declines in kelp populations globally and are driving shifts in species distributions (Smale, 2020), with potentially cascading effects for the wider ecosystem through an alteration of kelp forest food webs (Smale et al., 2022). Within the range of *L. hyperborea*, a shift in species composition at the trailing range edge has been observed, with an increase in the relative abundance of the warm-water species *L. ochroleuca* (Smale et al., 2015). In other regions of the world rising SST has resulted in a transition from dense kelp forest to areas dominated by turf-forming algae (Krumhansl et al., 2016; Filbee-Dexter and Wernberg, 2018). In both cases, significantly lower biodiversity is supported and large shifts in the species composition of associated fauna have been recorded. Whilst these pressures are ever increasing and likely to worsen under future climate scenarios, there is still need for recognition of the lingering impacts of historical anthropogenic impacts, which may still be affecting kelp forest ecosystems many decades after the original impacts have ceased.

One such example is the impact of historic coal mining in the United Kingdom (UK). During the industrial revolution and for most of the 20th century, coal mining was an important industry in the UK, providing a large proportion of the energy used in electricity generation (Durucan, Jozefowicz and Brenkley, 2010). In northeast England, coal seams extending to the North Sea coastline were heavily exploited, however, along with extremely large quantities of valuable coal were great volumes of waste material (Alderton, 2012). This waste provided a logistical challenge in terms of disposal, and since many mines were situated close to the coastline, it was deemed practical, at the time, for this waste to be disposed into coastal environments – a practice which continued at industrial scales for almost a century (Hydraulics Research Station, 1970). The waste consisted mostly of coal spoil, which originated from mine washeries (where coal was separated from waste material through washing) and was made up of mostly 2-300

mm clasts of sediment-based waste material (Eagle et al., 1979) including materials with high concentrations of trace metals and toxic hydrocarbons (Alderton, 2012). The disposal of this waste had direct and severe negative effects on intertidal and subtidal communities (Edwards, 1975; Johnson and Frid, 1995), smothering vast expanses of habitat and resulting in a maximum of only two species per shore height on intertidal rocky shores on the Durham coast (Hyslop et al., 1997). It was thought that natural erosion by the sea would remove the waste from the coastline, and that this process would be adequate to keep up with the rate of disposal. However, along just one stretch of coastline (~12 km) in Durham, UK, over 40 million tonnes of waste was tipped onto the shore from just four mines (Gutt et al., 1974; Cooper et al., 2017). The volume of waste generated and disposed onto shores rose with increased demand for coal and natural processes were unable to keep up with the rate of deposition. This resulted in waste material accumulating, resulting in severe progradation whereby the high tide line retreated seaward by up to 256 m in some areas of Durham (Hydraulics Research Station, 1970; Cooper et al., 2017), and a staggering 515 m in Northumberland where coal spoil was 10 m deep on some shores (Cooper et al., 2017). Upon the closure of mines and the cessation of waste tipping, accumulated waste was quickly eroded, and shorelines retreated at a rate of up to 20 m per year (Posford Duvivier, 1993). Throughout the nearly 100 year operating period of these mines, pollutant rich sediments were eroded from spoil heaps on the shores and dispersed throughout nearby coastal environments.

While the physical impact of mine waste dumping on the northeast coastline of the UK was vast only a small number of studies have investigated its impact on marine species and habitats. For example, Sheppard, Bellamy and Sheppard (1980) demonstrated reduced faunal abundance and diversity as well as a shift in faunal composition in *L. hyperborea* holdfasts along gradients of heavy metal pollution on the Durham coast. Eagle et al. (1979) reported severe depletion of species in subtidal areas affected by waste disposal and the accumulation of waste but noted a small amount of recovery in areas where disposal had ceased many years prior and waste material had started to naturally disperse. In the intertidal, Hyslop et al. (1997) described severe negative impacts of mining waste on the abundance and diversity of macroinvertebrates and a reduction in the diversity of macroalgae. Six months post closure of the last operating mine on the Durham coast in 1993, subtidal infaunal communities showed some level of recovery, however sites surveyed further south where mines closed several years

earlier showed no recovery (Johnson and Frid, 1995). In summary, prior studies show negative effects on several marine habitats, however, since the closure of mines very few studies have been conducted to understand the current state of these marine habitats, and none have investigated the recovery of the directly impacted marine habitats following the shorelines being cleared up as part of the Turning the Tides Project. The aim of this study was, therefore, to investigate whether historic coal mining waste disposal still negatively impacts macroinvertebrate assemblages associated with *L. hyperborea* holdfasts and stipes 30 years since the cessation of mining by comparing kelp forest habitats at sites directly affected by historic mine waste disposal and those that were not.

4.2 Methods

4.2.1 Study design

Collection of *Laminaria hyperborea* holdfasts and stipes took place at 2 sites in each of 3 locations (Figure 4.1) along the northeast United Kingdom coastline during October 2021. Sites were chosen based on the presence of the dominant canopy forming kelp, *Laminaria hyperborea,* and by being areas either directly affected by coal mining waste disposal (locations A and C), where disposal occurred between the late 1890s and early 1990s and habitats were buried for decades, or sites unaffected by waste disposal (location B). Although the total volumes of waste disposed in each location are unavailable, rates of historic waste disposal in location A reached around 1.8 million tonnes per year, and in location B around 2.5 million tonnes per year (Eagle et al., 1979). Sites within a location were separated by a distance of 1 to 3 km, and locations were separated by a distance of 20 to 50 km.

At each site, five replicate holdfast and stipe samples were collected during spring low tides. Mature, canopy forming *L. hyperborea* individuals were haphazardly selected from the main kelp forest habitat at a depth of between 0 and 0.3 m below chart datum (BCD). The stipe of each individual was cut at 30 cm above the stipe holdfast junction. The remaining attached stipe was then immediately covered with a large cotton sample bag to stop mobile fauna escaping. The stipe was then cut at the stipe holdfast junction and the sample bag sealed. The

holdfast was then covered with another large cotton sample bag before prising the holdfast off the rock substrate and sealing the bag. Only individuals that had distinct holdfasts (i.e. none fused with other individuals) and were > 2 m from an already sampled individual were collected. Samples were placed in 70% industrial methylated spirit (IMS) until processing.

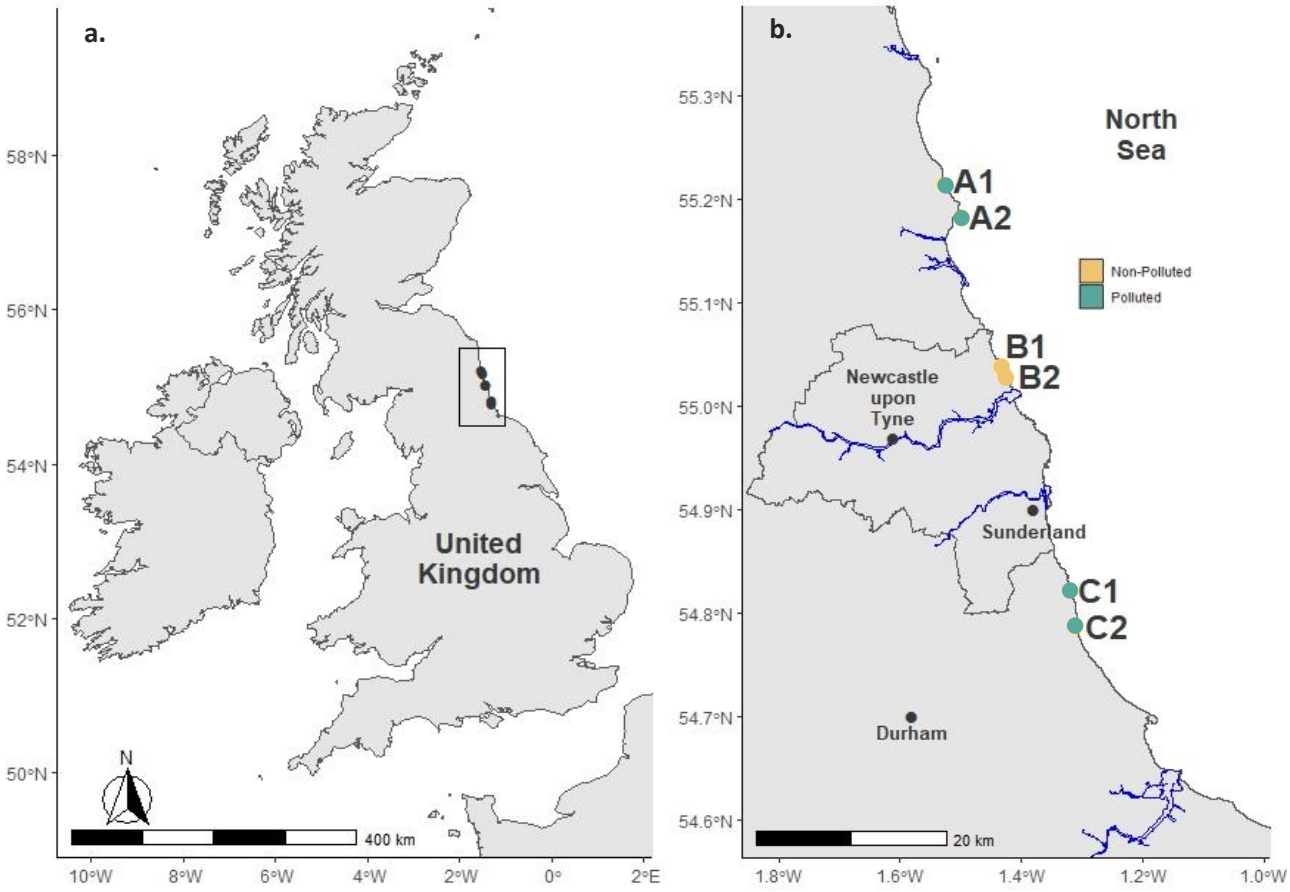

Figure 4.1. Study area (a) showing the position of the two sites (1 and 2) within each of three sampling locations (A, B and C) (b). With locations A and C (green points) representing sites impacted by mining waste and location B (yellow points) not affected by mining waste.

To process, each individual holdfast was placed into a 1 mm sieve and rinsed in freshwater to remove any loose macroinvertebrates. The holdfast volume was then quantified via displacement; entire holdfasts were wrapped in plastic cling film, submerged in water, and the volume of water displaced was recorded. Holdfasts were then returned to the 1 mm sieve and haptera were removed, opening up the holdfast to remove all macroinvertebrate fauna from within. The cleaned holdfast structure was then resubmerged in water and its displacement volume recorded. Each measure of volume was repeated 3 times per holdfast and the average

value was used in further analyses. The volume of haptera was then subtracted from the total holdfast volume to give the volume of habitable space within each holdfast. Stipe samples were processed separately and were washed with freshwater in a 1 mm sieve to remove all macroinvertebrates. All macroinvertebrates from both holdfast and stipe samples were stored separately in 70% IMS and later identified to the highest possible taxonomic resolution (68% to species level) and enumerated.

4.2.2 Statistical analysis

Metrics of species richness, abundance, Shannon-Weiner diversity H' index and Pielou's evenness index J' were calculated and their patterns of variation analysed using univariate permutational analysis of variance (PERMANOVA). A 2-factor design was employed with pollution (fixed factor, 2 levels: polluted, non-polluted) and site (random factor, 4 levels nested in polluted, 2 levels nested in non-polluted). Permutations (9,999 under a reduced model) were based on Euclidian distances generated from untransformed data. Where significant differences among individual factors were detected ($p<0.05$), pair-wise tests were conducted. Variation in the volume of holdfasts was also tested with the same design.

Variability in assemblage structure was analysed using multivariate permutational analysis of variance (PERMANOVA). The same model design was used as for univariate tests, however permutations (9,999 under a reduced model) were based on a modified Gower similarity index (Anderson, Ellingsen and McArdle, 2006) constructed from square root transformed abundance data. Where significant differences among individual factors were detected ($p<0.05$), pair-wise tests were conducted. Where significant differences between groups within a factor were observed, a similarity of percentage procedure (SIMPER) was carried out to investigate which taxa contributed most to the observed dissimilarity. Patterns in multivariate assemblage structure of holdfast associated fauna were visualised using non-metric multidimensional scaling (nMDS) plots.

Holdfast volume influences assemblage structure (Sheppard, Bellamy and Sheppard, 1980; Ojeda and Santelices, 1984; Smith, 1996a), since not only do larger holdfasts have a greater colonisable area, but they are also more structurally complex due to a greater number of haptera (Orland et al., 2016). For this reason, total holdfast volume, as well as the volume of habitable space, were considered as covariates in both uni- and multivariate analyses of holdfast associated fauna data. Due to high covariance between these factors (Figure S4.1), the total holdfast volume was chosen for analysis, as it is more comparable to previous studies (Christie et al., 2003; Teagle et al., 2018) and the method of measurement is less likely to introduce error.

Prior to all PERMANOVA analysis, differences in within group dispersion for all model terms was analysed using the PERMDISP routine, and where significant differences were observed, the threshold of significance was reduced to a more conservative $p<0.01$ (Earp et al., 2024; Leclerc et al., 2023). All assumption checking, statistical analysis, and MDS figure creation was conducted using PRIMER 7 software (Clarke and Gorley, 2015) with the PERMANOVA+ add on (Anderson, 2008). All other figures were made in RStudio v 4.2.1 (R Core Team, 2022) using the "ggplot2" package (Wickham, 2016).

4.3 Results

In total, 7,594 individuals belonging to 125 taxa were identified. Holdfasts harboured a much greater number of individuals than stipes, with a total of 7,094 individuals found within holdfasts and 500 on stipes. Within holdfasts, the phylum Mollusca represented the most abundant group, with 2,868 individuals across 51 taxa, followed by Arthropoda (2,072 individuals across 28 taxa, though over 85% of these individuals were from 2 taxa: *Balanus crenatus* and *Verruca stroemia*), and Annelida (1,573 individuals across 31 taxa). Annelida had a greater proportional abundance at non-polluted sites compared to polluted ones, whilst the opposite pattern was observed for Arthropoda (Figure 4.2a). The filter feeding Arthropoda *Balanus crenatus* and *Verruca stroemia* made up a minimum of 90% of Arthropoda abundance at polluted sites, yet a maximum of 57% at non-polluted sites (Figure 4.2a). On stipes, Mollusca

also represented the most abundant phylum (Figure 4.2b) (429 individuals across 8 taxa), followed by Arthropoda (66 individuals across 6 taxa).

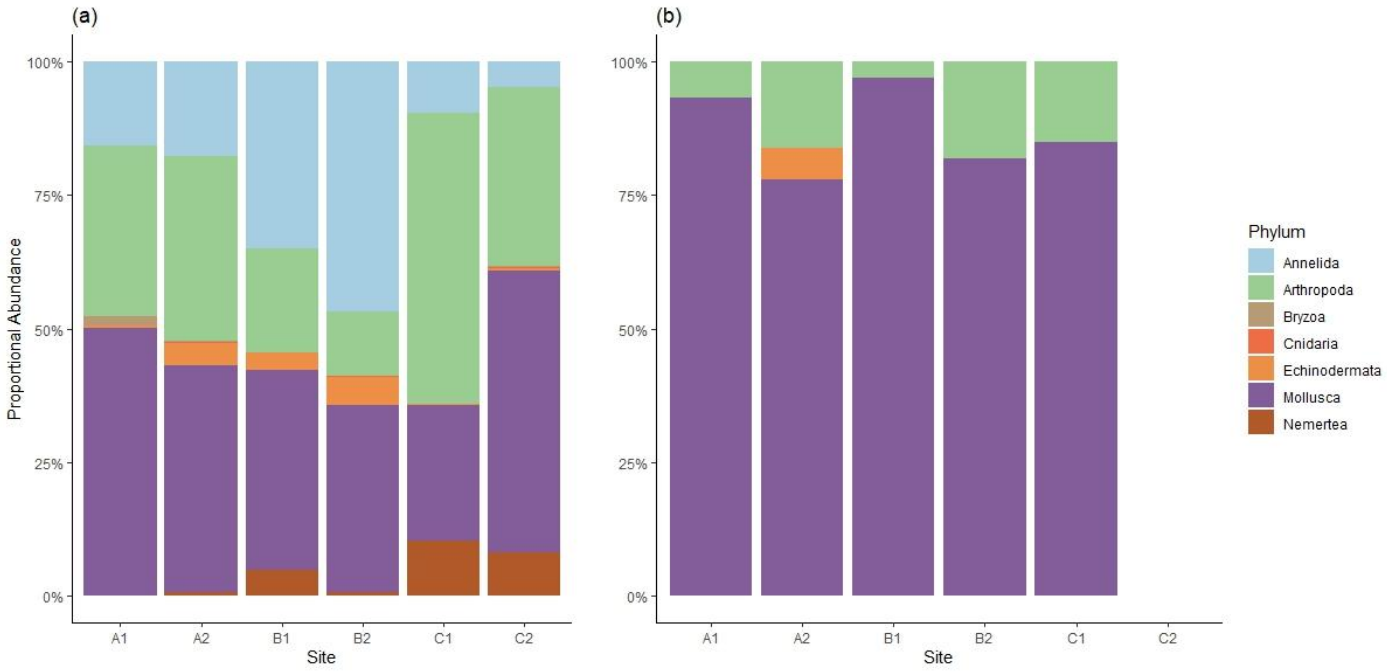

Figure 4.2. Proportion of macroinvertebrate phyla associated with *Laminaria hyperborea* (a) holdfasts and (b) stipes. Sites and locations can be seen in Figure 4.1. Lack of data for stipe fauna at site C2 was due to no organisms being present on stipes.

Abundance and diversity varied significantly across small scales, with significant site nested in pollution effects detected for nearly all measures in both stipes and holdfasts, while evenness only varied between sites nested in pollution in holdfasts (Table 4.1). Species richness in holdfasts also varied significantly amongst levels of pollution (Table 4.1), whereby non-polluted sites showed much greater richness than polluted sites (Figure 4.3a). Although holdfast Shannon-Weiner diversity (H') was greater at non-polluted sites (Figure 4.3c), and abundance was also higher with the exception of one polluted site (Figure 4.3b), these differences were not statistically significant (Table 4.1). Pielou's evenness (J') was only different between sites nested in location and this was only significant at location A (Figure 4.3d). In other locations, evenness was very similar between sites, with location C demonstrating the least even distribution of species abundances within holdfasts (Figure 4.3d). Holdfast volume was a significant covariate for both species richness and Shannon-Weiner diversity (H'), indicating a strong influence of habitat size on these measures (Table 4.1). Patterns of stipe

associated abundance and diversity were considerably more variable than for holdfast fauna (Figure 4.4a-d). Additionally, aside from having a more even distribution of species abundances (Figure 4.4d), other measures of stipe associated diversity and abundance were generally much lower than those for holdfast fauna (Figure 4.4a-c). While no significant effect of pollution was found on any measures of abundance or diversity of stipe associated fauna (Table 4.1), polluted sites generally had greater stipe associated abundance and diversity than non-polluted sites. Conversely to this pattern, there was a complete absence of stipe-associated macroinvertebrates at polluted site C2 (Figure 4.2). This corresponded with an observation of a total lack of epiphytic stipe algae, which provides habitat for macroinvertebrates (Christie et al., 2003).

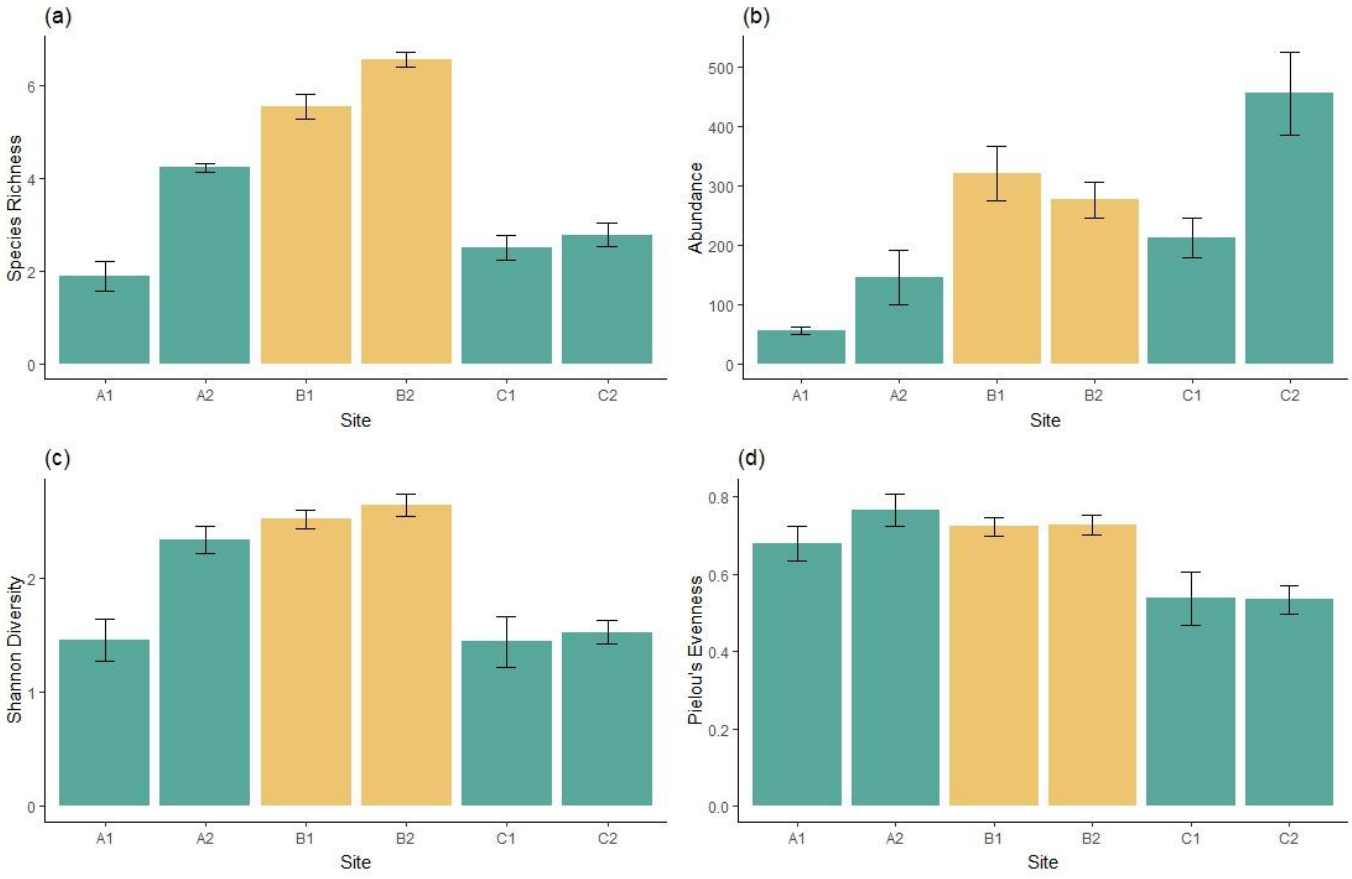

Figure 4.3. Univariate metrics of holdfast associated macroinvertebrate assemblages: (a) species richness, (b) abundance, (c) Shannon-Weiner diversity (H') and (d) Pielou's evenness (J'). Values represent means ± 1 SE. n=5. Sites and locations can be seen in Figure 4.1.

Multivariate analysis revealed that the assemblage structure of both holdfast and stipe-associated fauna varied significantly across small scales, with significant site nested in pollution

effects detected (Table 4.2). Non-metric MDS ordinations showed no clear patterns in stipe associated assemblage structure between sites or levels of pollution (Figure 4.6). In contrast, some partitioning of holdfast associated assemblage structure was observed between levels of pollution, and a clear pattern of greater holdfast volumes in non-polluted sites was demonstrated (Figure 4.5; Table S4.1; Figure S4.1, S4.2). Although PERMANOVA found no significant effect of pollution on assemblage structure for either stipes or holdfasts, holdfast volume had a significant effect on holdfast-associated assemblages (Table 4.2). These results suggest that whilst assemblage structure may not be directly affected by pollution, it may be indirectly influenced through reduced habitat size in polluted areas. On average, holdfast volumes were twice as large at non-polluted sites compared to polluted sites (Figure S4.2).

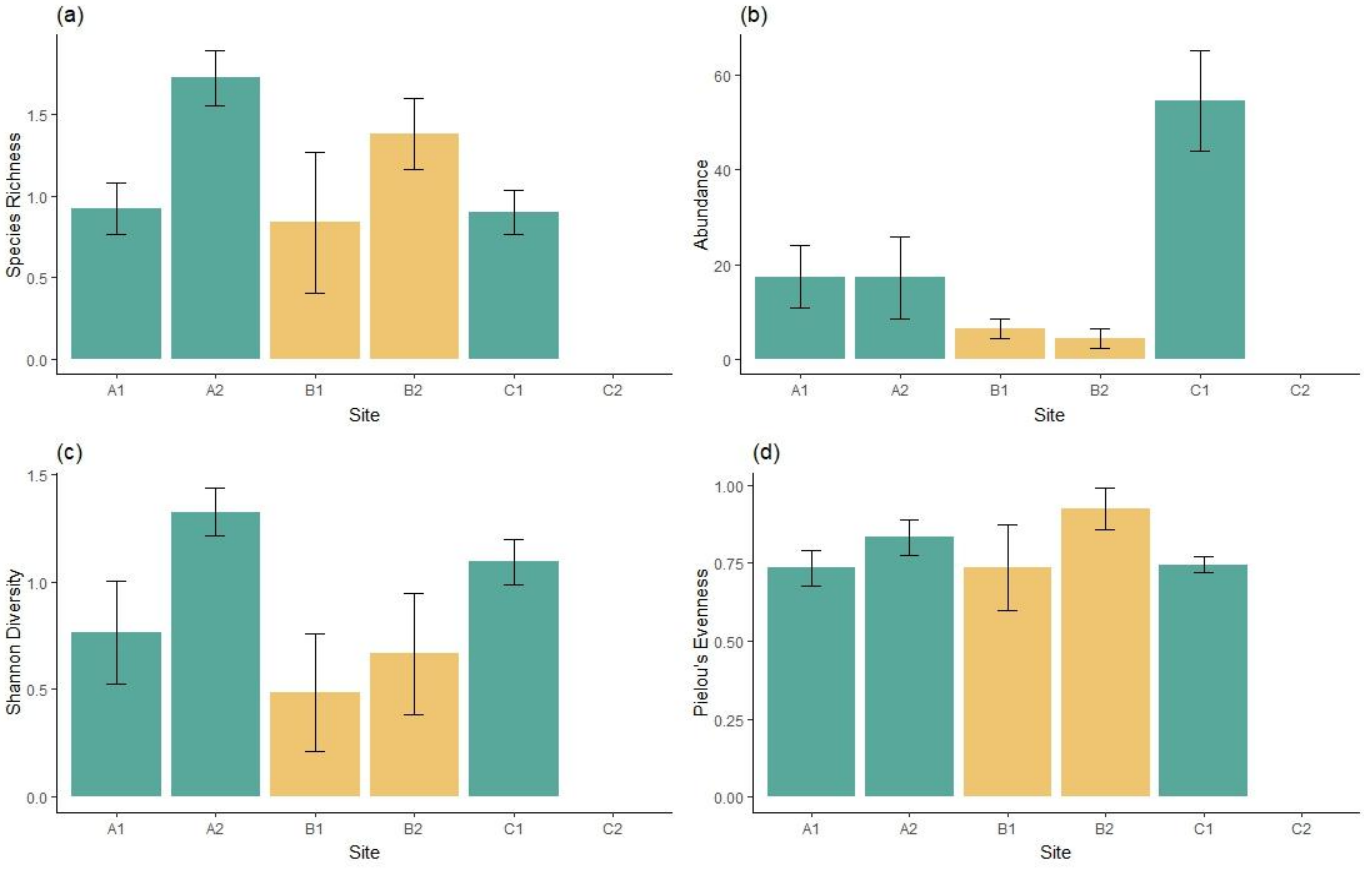

Figure 4.4. Univariate metrics of stipe associated macroinvertebrate assemblages: (a) species richness, (b) abundance, (c) Shannon-Weiner diversity (H') and (d) Pielou's evenness (J'). Values represent means ± 1 SE. n=5. Sites and locations can be seen in Figure 4.1.

SIMPER analysis indicated that the observed differences in holdfast associated assemblage structure between sites were driven primarily by variations in the abundance of species including the sessile arthropod *Verruca stroemia* and the mollusc *Modiolus modiolus* (Figure 4.7; Table S4.2). Non-polluted sites B1 and B2, though significantly different from each other, had a lower average dissimilarity than between polluted sites, with smaller contributions from the 5 taxa that contributed the most to the observed differences (Table S4.2). For stipe faunal assemblages, the mollusc *Lacuna vincta* was responsible for large contributions to the observed dissimilarity between most sites, with the mollusc *Patella pellucida* consistently the second largest contributor (Figure 4.8; Table S4.3).

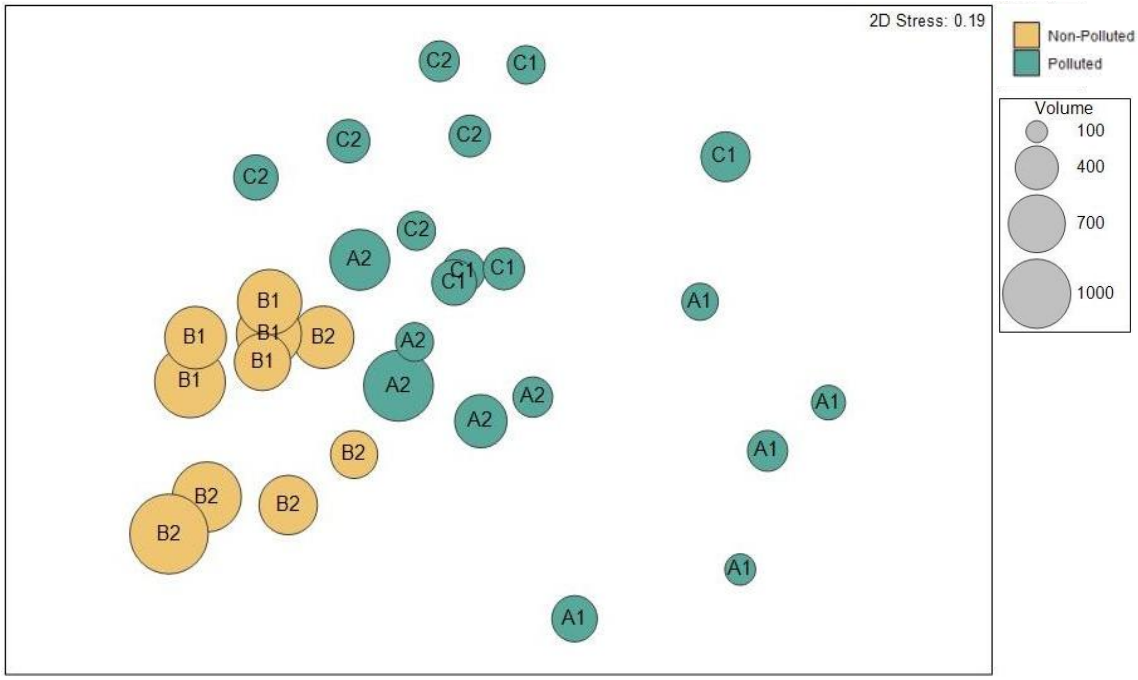

Figure 4.5. Non-metric MDS plot of holdfast associated macroinvertebrate assemblage structure of *Laminaria hyperborea* individuals at sites subjected to coal waste dispersal (Locations A & C) and sites not directly exposed to such pollution (Location B). Sites and locations can be seen in Figure 4.1. Point size indicates holdfast volume (ml). Data based on modified Gower similarity derived from square root transformed abundance data. Each point represents a single holdfast.

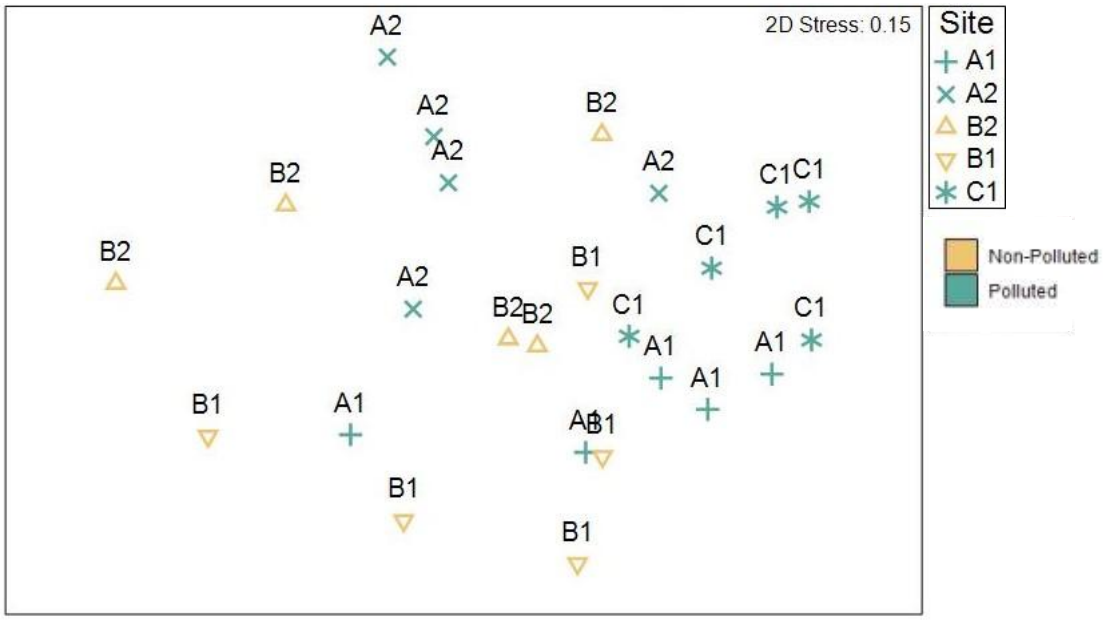

Figure 4.6. Non-metric MDS plot of stipe associated macroinvertebrate assemblage structure of *Laminaria hyperborea* individuals at sites subjected to coal waste dispersal (Locations A & C) and sites not directly exposed to such pollution (Location B). Sites and locations can be seen in Figure 4.1. Data based on modified Gower similarity derived from square root transformed abundance data. Each point represents a single stipe.

Table 4.1. Univariate PERMANOVA testing variation in holdfast and stipe associated macroinvertebrate faunal abundance and diversity metrics between levels of pollution and sites (nested in pollution). Holdfast volume was used as a covariate in tests of holdfast abundance and diversity metrics. Results indicated with 'ŧ' are derived from Monte-Carlo simulations due to a low number of unique permutations. Significant results are indicated in **bold**.

	Species Richness			Abundance			Shannon H'			Pielou's Evenness J'		
Response Variable	df	*F*	p	df	*F*	p	df	*F*	p	df	*F*	p
Holdfast												
Holdfast Volume	1	20.79	**0.0005**	1	0.55	0.4804	1	12.93	**0.0035**	1	2.24	0.1929
Pollution	1	8.29	**0.0190**	1	0.09	0.8437	1	2.47	0.2190	1	0.18	0.6852
Site(Pollution)	4	12.02	**0.0001**	4	12.99	**0.0001**ŧ	4	5.03	**0.0030**	4	4.60	**0.0064**
Res df	23			23			23			23		
Stipe												
Pollution	1	0.25	0.6069	1	2.30	0.2963	1	4.85	0.1156	1	1.55	0.3972ŧ
Site(Pollution)	3	4.50	**0.0379**	3	6.44	**0.0040**	3	1.24	0.3267	3	1.95	0.2369
Res df	20			20			20			20		

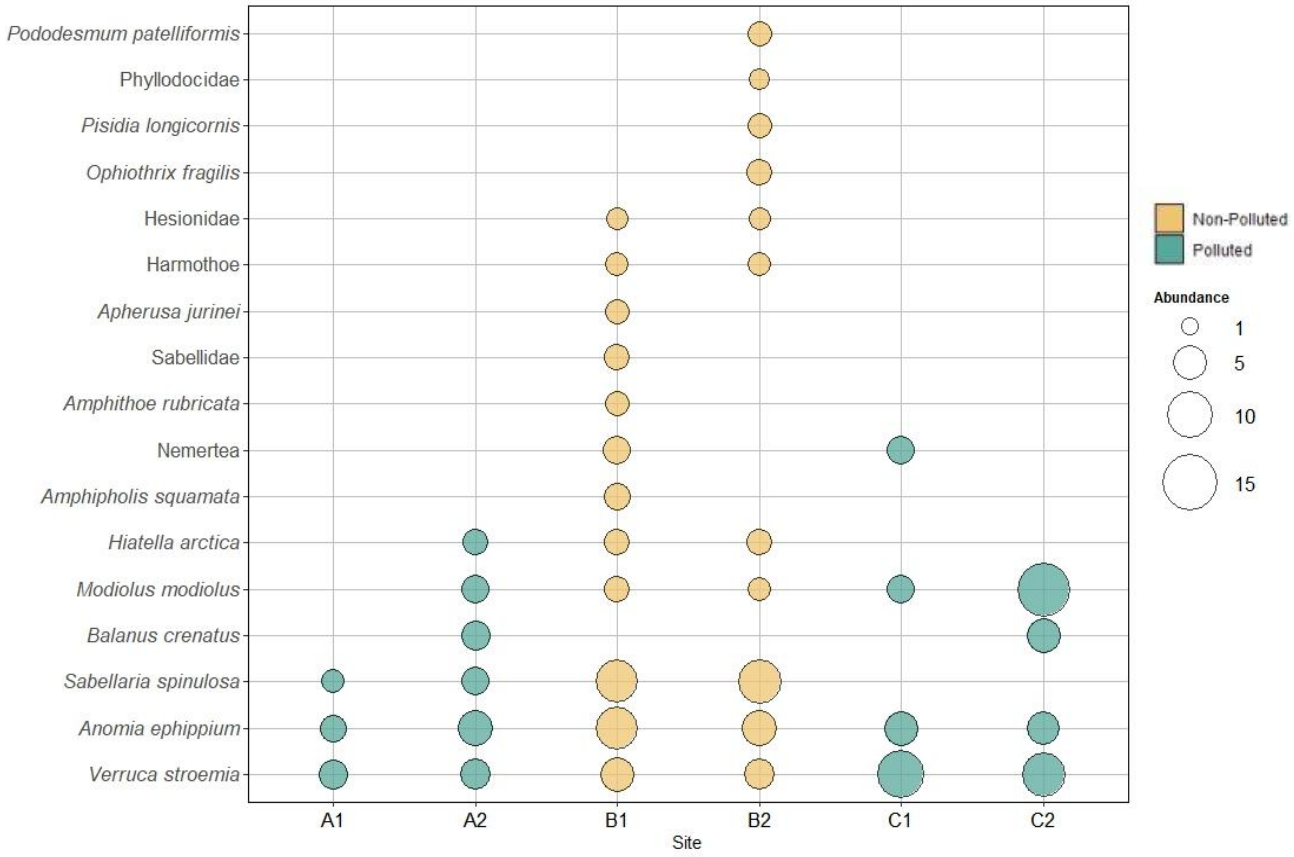

Figure 4.7. Taxa contributing to the average dissimilarity between holdfast associated macroinvertebrate assemblages at sites subjected to coal waste dispersal (Locations A & C) and sites not directly exposed to such pollution (Location B) as determined by SIMPER analysis performed on square root transformed data. Bubble size indicates relative abundance of taxa at each site after standardisation by holdfast volume. Site locations can be seen in Figure 4.1. See Table S4.2 for full SIMPER tables.

Table 4.2. Multivariate PERMANOVA testing variation in holdfast and stipe associated macroinvertebrate assemblage structure between levels of pollution and sites (nested in pollution). Holdfast volume was used as a covariate for comparisons of holdfast assemblage structure. Results indicated with 'ɬ' are derived from Monte-Carlo simulations due to a low number of unique permutations. Significant results are indicated in **bold**.

	Holdfast Community Structure			Stipe Community Structure		
	df	*F*	*p*	df	*F*	*p*
Holdfast Volume	1	2.42	**0.0001**	-	-	-
Pollution	1	1.03	0.4396	1	0.92	0.5001ɬ
Site(Pollution)	4	2.23	**0.0001**	**3**	3.39	**0.0001**
Residual	23			20		

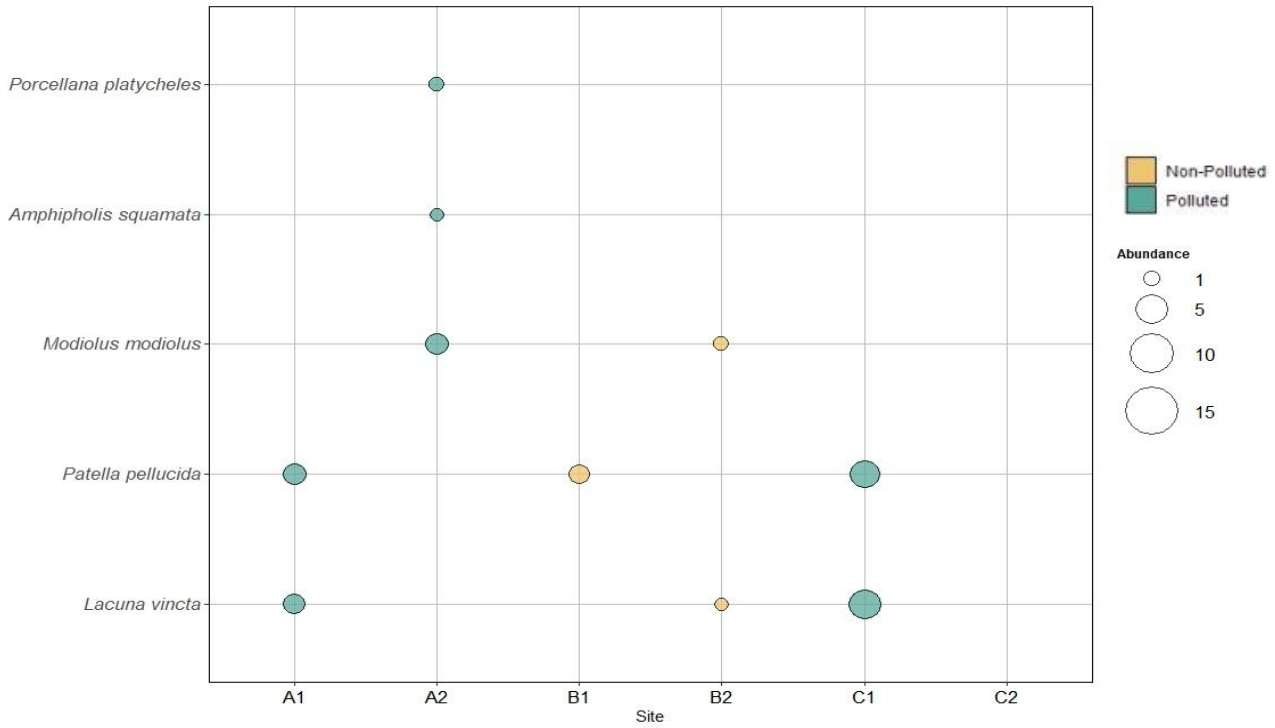

Figure 4.8. Taxa contributing to the average dissimilarity between stipe associated macroinvertebrate assemblages at sites subjected to coal waste dispersal (Locations A & C) and sites not directly exposed to such pollution (Location B) as determined by SIMPER analysis performed on square root transformed data. Bubble size indicates relative abundance of taxa at each site. No taxa were recorded at site C2. Sites and locations can be seen in Figure 4.1. See Table S4.3 for full SIMPER tables.

4.4 Discussion

Kelp forests support high levels of biodiversity, with their stipes and holdfasts providing habitat for a diverse array of macroinvertebrate fauna (Teagle et al., 2017). The assemblages sampled in this study were, in some cases, diverse and highly abundant, representing typical *Laminaria hyperborea* habitats that have been described in previous research (Bué et al., 2020; Earp et al., 2024; Edwards, 1980; King et al., 2021; Leclerc et al., 2015; Sheppard, 1976; Sheppard et al., 1980; Teagle et al., 2018). This study identified individuals belonging to 125 distinct taxa. Holdfasts harboured considerably greater diversity and abundance than stipes, with an average of 22 taxa per holdfast and 3 per stipe. Although these values are lower than those observed in previous studies, the average number of taxa recorded per holdfast at non-polluted sites (~35) is much more comparable to previous observations from both *L.*

hyperborea (Sheppard, Bellamy and Sheppard, 1980; Christie et al., 2003; Teagle et al., 2018) and other kelp species globally (*Macrocystis pyrifera:* Ojeda and Santelices, 1984*; Ecklonia radiata*: Smith, 1996b).

The study wide average of 3 taxa per stipe, however, was considerably lower than previous studies on this species, where on average 10-15 taxa have been observed (Norderhaug et al., 2012; King et al., 2021). A key feature of *L. hyperborea* stipes is a dense covering of epiphytic algae which is known to provide habitat and food for a range of macroinvertebrates. Indeed, the abundance of macroinvertebrates is positively correlated with epiphytic biomass (Christie et al., 2003). Across all sites, stipe epiphyte load was generally low. This in part, could be a function of high levels of turbidity in nearshore habitats along this stretch of coastline, but also sampling depth. Most previous studies on *L. hyperborea* associated fauna investigate kelp sampled at several metres below chart datum (BCD), whereas samples here were collected much shallower at 0-0.3 m BCD, making comparisons difficult. Other studies have, however, shown that red algal epiphytes are less diverse and abundant in shallower waters and on younger kelp (Whittick, 1983), likely a result of increased desiccation stress in kelp exposed to air at low water, as was the case in this study. Due to the direct provision of habitat structure by algal epiphytes (Christie et al., 2003), this is likely to have negative effects on the abundance and diversity of macroinvertebrate taxa found on stipes and could be responsible for the lower numbers recorded here. It is also noteworthy that no macroinvertebrate fauna were found on the stipes of kelps sampled at site C2, likely because of the complete absence of epiphytes. This site was where Easington Colliery mine waste was disposed and is one of the most heavily impacted sites in this geographical area in terms of the volume of mine waste tipped onto the coast and the duration of active disposal (Alderton, 2012). The absence of kelp associated epiphytic algae in areas of high pollution has been documented previously (Jara-Yáñez et al., 2021). Many brown algae species, including kelp, have developed mechanisms to tolerate heavy metal contamination. One such mechanism involves the production of mucilage to chelate and expel metals from their tissues (Huovinen, Leal and Gmez, 2010). This process results in high pollutant concentrations on the tissue surfaces, and on kelp stipes this can inhibit the settlement of epiphytic algae (Contreras et al., 2007; Oyarzo-Miranda et al., 2020).

Whilst there was significant between-site variability in the assemblage structure, diversity and abundance of both stipe and holdfast associated fauna, the predicted anthropogenic driven difference in these measures between polluted and non-polluted areas was not observed in stipe associated fauna. In holdfasts, however, pollution had a significant negative effect on species richness and there was a tendency towards reduced diversity and abundance. There was also some partitioning of assemblages with pollution, although this was not significant. This partitioning was driven by a clear difference in holdfast volume, where holdfasts were larger at non-polluted sites. Whilst the effect of holdfast volume has been shown numerous times in previous studies for *L. hyperborea* (Sheppard, Bellamy and Sheppard, 1980; Christie et al., 2003), the pattern of smaller holdfasts in polluted areas has not been previously reported for this species.

In general, larger holdfasts support greater levels of biodiversity (Sheppard, Bellamy and Sheppard, 1980; Smith, 1996a; Christie et al., 2003; Anderson et al., 2005; Teagle et al., 2018), although this relationship may vary in certain situations, such as in very old, large holdfasts where encrusting species can be highly abundant and take up space for other organisms to occupy (Anderson et al., 2005). This relationship is not only attributed to the ability of larger holdfasts to harbour more individuals due to greater habitat size, but also to the increased structural complexity they offer (Orland et al., 2016). The greater number of haptera creates more interstices and niches for a wider range of macroinvertebrate fauna to inhabit. Although it's not fully understood what drives holdfast size, aside from age, kelp morphology is strongly influenced by hydrodynamic forces (Harrold, Watanabe and Lisin, 1988; Sjøtun, Fredriksen and Rueness, 1998; Pedersen et al., 2012; Bekkby et al., 2014) and these forces may also play a role in generating larger (and possibly stronger) attachment structures. Consequently, we would expect to see larger holdfasts with greater volumes in areas that are more exposed to wave action (Sjøtun and Fredriksen, 1995). This is unlikely to be the case here, since sites in this study are situated along a stretch of open coastline and are likely to experience very similar levels of wave exposure. Therefore, it is probable that other factors are driving the observed differences in holdfast volumes between polluted and non-polluted areas.

A potential driver of the patterns observed could be a result of the large quantities of toxic heavy metals released into the environment, alongside the high volumes of sediment. These heavy metals included copper, zinc and lead that can be highly toxic to many aquatic organisms (de Almeida Rodrigues et al., 2022) with these chemicals known to bioaccumulate in kelp (Burger et al., 2007; Evans and Edwards, 2011). The impacts of these pollutants on kelp growth and development have been investigated with varying results (Hopkin and Kain, 1978; Contreras et al., 2007; Jara-Yáñez et al., 2021). However, studies rarely incorporate the effect of pollutants on holdfast size, weight or volume. Where they do, studies have shown short term exposure of the early life stages of *Macrocystis pyrifera* to heavy metal pollutants resulted in negative effects on the growth of holdfasts throughout their lifetime, even when returned to normal environmental conditions (Jara-Yáñez et al., 2021). While this has not been tested in *L. hyperborea*, it could provide a potential mechanism for the observations made here.

As well as the negative effects of heavy metal pollutants, it is likely that the volumes of sediment-based waste disposed into these areas had negative impacts through increased turbidity (Moore, 1972). It was noted that sites previously affected by mine waste were much more turbid than those that were unaffected (pers. obs.). This observation was most obvious during summer months when suspended matter is generally at its lowest (Wilson and Heath, 2019), yet at affected sites turbidity remained high. Mine waste at polluted sites is continually eroding from the shoreline (Figure 1.4) likely contributing to the turbidity patterns observed. Previous research has highlighted shifts in faunal assemblages from less turbid to more turbid areas, where higher proportions of filter and deposit feeding amphipods such as *Monocorophium sextonae* and *Tritaeta gibbosa* were found at more turbid sites (Moore, 1973; Teagle et al., 2018) likely a result of increased levels of suspended organic matter. One study along the North Sea coastline of the UK reported a reduction in species richness and diversity with an increase in turbidity, along with a subsequent increase in the proportion of suspension feeders (Sheppard, Bellamy and Sheppard, 1980). Similarly, we observed a significant increase in species richness in holdfasts from polluted to unpolluted sites, as well as greater diversity at all sites and greater abundance at all but one site. We also observed considerably greater abundances of filter feeding Arthropods including *Verruca stroemia* and *Balanus crenatus* at polluted sites, aligning with the findings of previous studies (Moore, 1973; Sheppard, Bellamy

and Sheppard, 1980; Teagle et al., 2018). Holdfasts also act as sediment traps, with more structurally complex holdfasts, with a greater number of haptera, trapping larger volumes of sediment (Moore, 1973). Whilst this can be beneficial to some taxa through food provision (Smith, 1996b), high sediment loads can also lead to smothering and scouring of holdfasts. While it is possible that differences in turbidity between sites played a part in the variability of holdfast associated assemblages, it is difficult to attribute the observed differences to this without in-situ measurements of turbidity or holdfast sediment content. Given that anthropogenic influences such as historical mining or present-day dredging activities can influence sedimentation rates and turbidity, which can both have negative effects on kelp forest macroinvertebrate communities, these factors should be considered important and warrant inclusion in future investigations.

This study showed that although there is natural variation occurring across small scales, there is still evidence of the impact of historical coal mine waste disposal. Although the effects of pollution were not consistently observed across stipes and holdfasts, or for all of the response variables measured, there was a clear pattern of increased holdfast size at non-polluted sites which corresponded with increased macrofaunal richness and abundance. These results are novel and warrant further study to determine the mechanisms underpinning this observation. While there was no effect of historic mine waste on stipe associated fauna it is worth noting that at the most impacted site that kelp associated epiphytes were absent suggesting that extreme pollution or sediment loading may completely disrupt stipe-associated habitats, though further investigation is required to confirm this.

In terms of faunal abundance, over 590 macroinvertebrate individuals were recorded on one kelp, however, values were more typically in the range of 200-300 individuals per kelp. Given that kelp densities at these sites average 15 individuals per square meter (Chapter 3), scaling these macroinvertebrate abundances would suggest the presence of several thousand individuals per square meter of kelp forest. With kelp forest habitat along the UK coastline predicted to cover an area of approximately 15,984 km² (Yesson et al., 2015), this underscores their significant contribution to biodiversity. Furthermore, it suggests that the fauna associated

with kelp holdfasts and stipes are likely to play an important role in trophic processes and contribute significantly to ecosystem functioning.

In conclusion, the findings underscore the complex interactions between natural variability and anthropogenic impacts that act as drivers in structuring kelp forest ecosystems. The observation of smaller holdfasts in polluted areas highlights a potential pathway through which pollution may alter kelp-associated biodiversity, particularly in heavily impacted coastal regions. This study contributes to a growing body of literature that emphasizes the importance of habitat structure in supporting marine biodiversity. Future research should explore how pollution, especially from heavy metals and sedimentation, interacts with other environmental factors to shape kelp forest communities over broader spatial and temporal scales. Understanding these dynamics is essential for the conservation and management of kelp forests, which are critical to sustaining the biodiversity and functioning of coastal ecosystems worldwide.

Chapter 5. Patterns in *Laminaria hyperborea* bacterial microbiome community structure across a range of spatial scales along a historically industrialised coastline.

5.1 Introduction

Kelps are a group of large, canopy forming macroalgae belonging to the order Laminariales. They are foundation species distributed along ~36% of global coastlines (Jayathilake and Costello, 2021) and are ecologically and commercially important (Krumhansl et al., 2016). As dense stands on rocky coasts they form forests that provide habitats for diverse communities including invertebrates (Zahn et al., 2016; King et al., 2021), algae (Leliaert et al., 2000), fish (Pérez-matus et al., 2007; Jackson-Bue et al., 2023) and mammals (Steneck et al., 2002). They also provide a critical source of energy to marine and terrestrial food webs (Duarte and Cebrián, 1996; Elliott Smith and Fox, 2022) and provide a range of ecosystem services including food provision, nutrient cycling and coastal defence (Connell, 2005; Pinsky, Guannel and Arkema, 2013; Pfister, Altabet and Weigel, 2019). They are, however, impacted by stressors over a range of spatial scales leading to regional-scale losses in some parts of the world (Krumhansl et al., 2016). For example, global stressors, such as climate change have negatively affected kelp forests from individuals to communities (Smale, 2020), while local to regional stressors such as eutrophication, pollution, over-grazing and invasive species have resulted in a decline in kelp forest extent and in many cases a shift towards systems dominated by turf-forming algae (Filbee-Dexter and Wernberg, 2018).

In the UK, kelp forests are considered to be in a good ecological state. They are generally located at the centre of their distributional range where they are least affected by environmental stressors (Smale et al., 2013), and are largely unaffected by anthropogenic pressures. For these reasons, there is no evidence of large-scale losses of UK kelp forests (Wilding et al., 2023). There are, however, some small-scale examples of kelp forest decline. For example, on the Durham coastline coal mining waste disposal practices led to the loss of intertidal and subtidal biodiversity, (Eagle et al., 1979; Johnson and Frid, 1995; Hyslop et al., 1997), including some areas of kelp forest through the smothering of these habitats by coal

spoil. Historically in the UK, coal mining was an important industry, fuelling the industrial revolution and acting as the primary source of the worlds energy until the late 1960s (Durucan, Jozefowicz and Brenkley, 2010). In the northeast of England, intense exploitation of coal seams that ran into the North Sea led to the logistical issue of where to dispose of coal mining waste (Alderton, 2012). The easiest and cheapest solution for the disposal of waste material was directly onto shores near mining sites. This practice took place for almost 100 years, during which time approximately 5 million tonnes of coal spoil was tipped onto the Durham coastline per year (Gutt et al., 1974), including 2.5 million tonnes tipped in just one year from a single mine during the 1980s (Eagle et al., 1979; Cooper et al., 2017). It is estimated that a total in excess of 40 million tonnes was deposited along this coastline by 1970 (Hydraulics Research Station, 1970). This resulted in coastal habitats being smothered by waste containing considerable quantities of harmful trace metals and toxic hydrocarbons (Johnson and Frid, 1995; Alderton, 2012). Waste material from terrestrial spoil tips in the same geographic area have been found to contain elevated levels of metals including iron, copper, lead, zinc, cadmium and mercury, as well as other environmentally harmful minerals and compounds (Palumbo-Roe and Colman, 2010). Although unrecorded, it is very likely that coal spoil deposited in coastal areas contained similarly harmful materials that would have leached out into the surrounding marine environment. This in turn had negative impacts on the surrounding habitats, leading to the elimination of many species (Jones and Ellis, 1976; Ellis and Hoover, 1990), destabilisation of sediments resulting in a loss of infaunal assemblages (Ellis and Hoover, 1990; Hyslop et al., 1997), and a reduction of macroalgal richness by approximately 48% on rocky intertidal shores (Hyslop et al., 1997). Some of the worst affected areas were remediated between 1997 and 2003 as part of the 'Turning The Tide' (www.turning-the-tide.org.uk) project which removed 1.3 million tonnes of waste from the coast, the process of which has led to the designation of parts of the coastal stretch from Seaham Beach to Hartlepool as a Site of Special Scientific Interest (SSSI), a Special Protected Area (SPA), a Special Area of Conservation (SAC) and a Ramsar site. While these sites are barely recognisable, following the removal of mine waste (Figure 5.1; Figure 1.2), the evidence of their industrial past is still very much evident (Figure 1.4). Although there has been extensive ecological recovery along this coastline, it is unclear whether these coastal systems have fully recovered compared to areas that were not directly affected by colliery waste.

Figure 5.1. Before (1992) (A) and after (2010) (B) the 'Turning The Tide' project undertook remediation of coal mining waste on the foreshore at Easington, County Durham, UK (site C2 – Site locations can be seen in Figure 5.2). (Image A: Durham Heritage Coast. Image B: Durham Heritage Coast/Credit Mike Smith)

Whilst the macro-diversity associated with kelp forest habitats is well understood, an often-overlooked aspect of the overall biodiversity that kelp forests support is the bacterial microbiome. Kelp-associated microbes can directly benefit plant fitness through the supply of nutrients and CO_2 (Abraham and Rohde, 2014), providing defence against diseases (reviewed by Singh and Reddy, 2016) and possibly facilitating the transfer of organic matter in the form of kelp-derived carbon to higher trophic levels (Newell, Field and Griffiths, 1982). However, the structure of kelp-associated microbial assemblages can be altered when kelp-hosts are exposed to stressful conditions (Newell, Field and Griffiths, 1982; Paix et al., 2021), such as increased temperature leading to alterations to the functions that the microbiome provides to the kelp (Minich et al., 2018). Although not well studied, recent research indicates that exposure to heavy metals, such as those contained in mining wastes, can alter the kelp microbiome and therefore potentially impact the functioning of kelp forest ecosystems (Paix et al., 2021). Consequently, our understanding of the factors underlying the health and functioning of kelp forests requires further research into the ecology of microbes and their interactions with macroalgal hosts when exposed to a variety of stressors.

In the northeast Atlantic, subtidal rocky reefs on exposed coastlines are dominated by the stipitate kelp *Laminaria hyperborea* (Gunnerus) Foslie, 1884. Its distribution extends from northern Portugal, at its equatorward range edge, to northern Norway and northwest Russia

at its poleward range edge (Sjøtun et al., 1993; Schoschina, 1997; Müller et al., 2009). Individuals have been recorded to live up to 18 years, however previous studies at our sampling sites indicate the kelp occupying these areas are generally between 4 and 6 years old, up to a maximum sampled age of 9 years old (Chapter 3). The basic anatomy of *L. hyperborea* consists of a holdfast, stipe and blade. The holdfast is an attachment structure and is perennial, persisting for several years. The stipe holds the photosynthetic blade towards the light and is also perennial, but its epicortex is shed annually to allow for growth and girth extension (Dieck, 1992). Finally, the blade is an annual structure that erodes from the distal end continuously throughout the year with new blade material growing from the meristematic junction between the blade and the stipe during late winter into spring (Kain and Jones, 1976). This anatomy and growth strategy creates a gradient of tissue ages. From the microbiome point of view, it has been shown that this leads to different successional trajectories across the kelp resulting in variation in the microbial assemblage structure across a single individual (Lemay et al., 2021). This, therefore, creates an ideal system for investigating how microbial structure varies across perennial versus annual tissues and against a background of historic mining pollution. Using 16s rDNA bacterial sequencing, this study aims to gain an understanding of the effects of historic pollution on the diversity and assemblage structure of the kelp-associated bacterial microbiome and determine whether microbial structuring takes place over a gradient of tissue ages.

5.2 Methods

5.2.1 Sampling

Sampling took place at 2 sites within each of 3 locations (Figure 5.2) along the northeast England coastline during August 2022. Locations were chosen based on areas of coal mining waste disposal activity, with locations A and C having been heavily polluted between the early 1900s and early 1990s and buried under spoil for much of this time, and location B representing an area where no waste disposal took place. An asymmetrical design was employed (with two impacted and one unimpacted location) as there were no locations both unaffected by historic mine waste disposal and with the presence of kelp along the north

Durham coastline. Within each of the locations, two sites were chosen, ensuring there was dense forests of the dominant canopy forming kelp, *L. hyperborea*. Sites within a location were separated by a distance of between 1 km and 3 km, with locations separated by a distance of between 20 km and 50 km. Five mature canopy forming individuals of *L. hyperborea* were selected at random from each site at a depth of approximately 0-0.3 m below chart datum (BCD) during spring low tides. Individuals were collected at a minimum distance of 2 m from each other within a continuous patch of kelp forest.

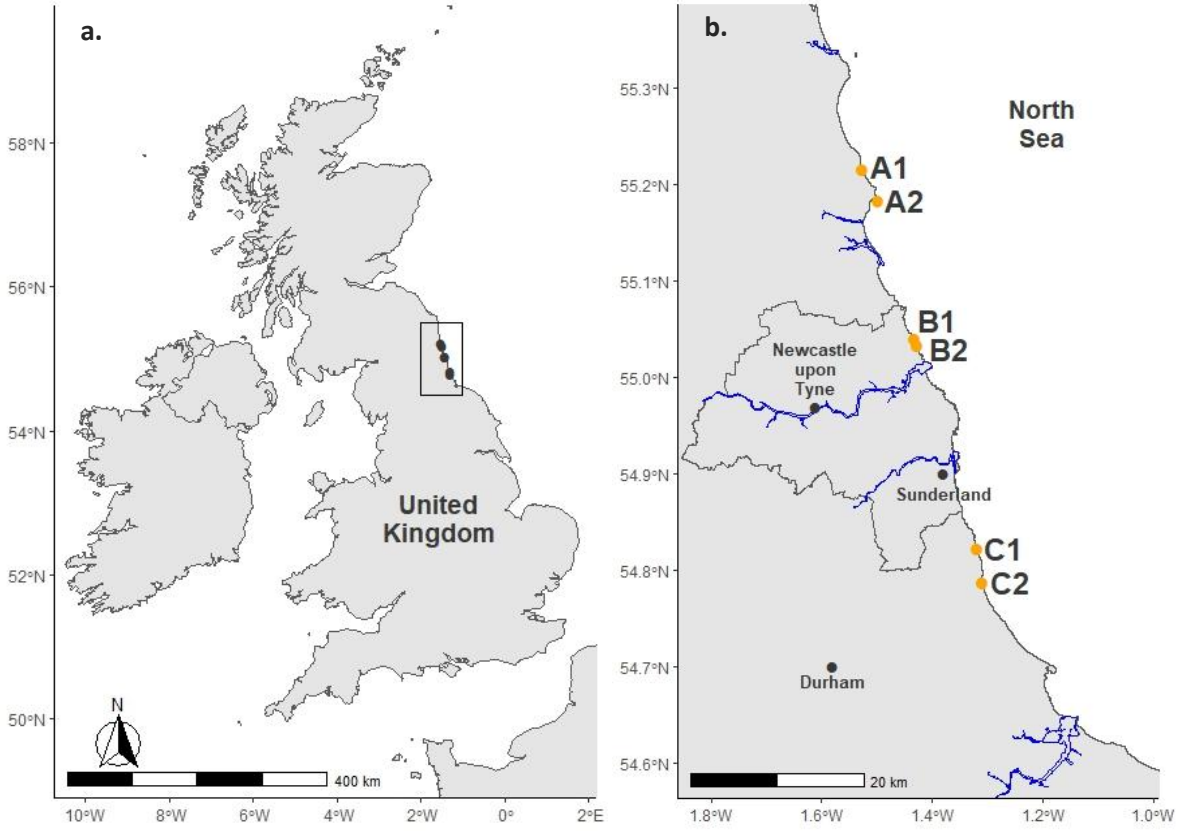

Figure 5.2. Study area (a) showing the position of the two sites (1 and 2) within each of three sampling locations (A, B and C) (b). With A and C representing sites impacted by mining waste disposal and site C not affected by mining waste disposal

A sterile sample bag was placed over the blades of each individual in situ. A cut was made below the stipe meristem junction, separating the blades from the stipe. The stipe was then removed by cutting above the holdfast stipe junction and discarded. A further sample bag was placed over the holdfast prior to the holdfast being dislodged from the substrate. Sample bags containing holdfasts and blades were returned to the shore, where they were washed with

sterile sea water to remove seawater DNA contamination and then swabbed with a sterile cotton swab. Swabbing took place over an area of 25 cm^2 for a period of 30 seconds, occurring above the meristematic tissue area for blade samples and along clean fully formed haptera for holdfast samples.

Environmental controls were also taken at each study site to distinguish between bacteria found in the environment and those of the kelp microbiome. From each patch of kelp forest, rock controls were collected in which five rocks roughly 10 – 15 cm in diameter with biofilm growth but no macroalgal growth were collected from within the kelp forest and swabbed using the same protocol as the blade and holdfast samples. Additionally, seawater controls were taken by collecting five replicate 250ml samples of seawater from each site in a sterile sample pot. These were subsequently filtered through a 0.22 µm syringe filter. Syringe filter elements and cotton swab heads were then removed and placed into 1.5 ml Eppendorf tubes to be stored at -80°C. DNA was extracted using Qiagen DNeasy PowerSoil kits following manufacturer's instructions. Library preparation and sequencing (MiSeq, Illumina, San Diega, CA, USA) of the V4 region of the 16s rDNA gene were carried out following the optimised protocol of Kozich et al. (2013). Sequencing used the primer pair 515f—GTGCCAGCMGCCGCGGTAA and 806r—GGACTACHVHHHTWTCTAAT to give broad bacterial coverage and was conducted by StarSEQ (StarSEQ GmbH, Mainz, DE). At least one negative PCR control was run on each plate, and demonstrated runs were free from contamination.

5.2.2 Sequence processing

Sequence processing was carried out in R (RStudio Team, 2022). Paired end reads were processed following the BIOCONDUCTOR workflow (Callahan et al., 2016) and the "filterAndTrim" function in DADA2 was used for trimming and truncating sequences to remove primers and low-quality reads using the following parameters: truncLen, f = 240, r = 160; truncQ = 2; trimLeft, f = 20, r = 19. Reads were then clustered into amplicon sequence variants (ASVs) using DADA2. Chimeric sequences were removed in DADA2 using the "removeBimeraDenovo" function. The resulting bacterial ASVs were assigned taxonomy using

the SILVA 132 database (Quast et al., 2013) against the RDP naïve Bayesian classifier using the "assignTaxonomy" function in DADA2.

The R package "PHYLOSEQ" was then used to assemble sequence read counts, taxonomic assignments and metadata into an object to be used in further downstream analysis (McMurdie and Holmes, 2013). Samples containing <10,000 reads, taxa contributing <0.01% of the reads in the dataset and ASVs identified as mitochondria or chloroplast were then removed from the PHYLOSEQ object. Sequence counts were expressed as relative abundance (in proportion to total sample count).

5.2.3 Statistical analysis

The "rarefy_even_depth" function in "PHYLOSEQ" was used to rarefy the minimum sample depth of the dataset in order to account for differences in sequence depth between samples in alpha diversity estimates. For each sample, alpha diversity was then estimated using the Chao1 index (Chao, 1984) and Shannon-Weiner diversity index using the "estimate_richness" function in "PHYLOSEQ". All further statistical analysis was carried out on PRIMER (Clarke and Gorley, 2015).

Analyses were conducted on the full and core microbiome, with the core microbiome defined as comprising taxa present in at least 95% of samples, based on thresholds established in previous studies of the kelp microbiome (King et al., 2022). This threshold is commonly used to identify consistently associated microbial taxa that are likely to play important and functional roles in host biology. Each tissue type was analysed separately, and relative sample abundance thresholds were set at 0.1%. Core assemblages were based at the ASV level and compositional datasets were used in their determination. Variation in the diversity of both the full and core microbiome were compared using three-way nested permutational univariate analysis of variance (PERMANOVA) using the model factors of tissue (fixed factor, 4 levels: rock, holdfast, blade, water), pollution (fixed factor, 2 levels: polluted, non-polluted) and site (random factor, 4 levels nested in polluted, 2 levels nested in non-polluted). For each analysis,

permutations (9,999 under a reduced model) were based on Euclidean distance similarity matrices derived from untransformed data. Where the number of permutations was low (i.e. <100) p values derived from Monte Carlo simulations were used. Where significant differences were detected, pairwise Post-Hoc tests were carried out to identify where these differences lay.

Variation in assemblage structure of both the full and core microbiome was analysed using permutational multivariate analysis of variance (PERMANOVA) (Anderson, 2001) using the same statistical model and parameters described above. The homogeneity of within-group multivariate dispersion was tested using PERMDISP, and where significant variation was detected, significance thresholds for the specific factors was set at $p<0.01$ (as opposed to $p<0.05$, as used for all other analyses) (Leclerc et al., 2023; Earp et al., 2024). A similarity of percentages procedure (SIMPER) was carried out to identify the taxa that contributed the most to the observed dissimilarities.

5.3 Results

Sequencing of the V4 region of the 16s rDNA gene produced a total paired-end read count of 3,775,806, with an average coverage of 31,465 reads per sample. Subsequent filtering of these resulted in a total of 6,521 bacterial ASVs for use in downstream analysis. This included ASVs from 36 phyla, 84 classes, 194 orders and 273 families. The taxonomy of 58.6% of ASVs was not resolved down to the genus level, and 28.3% not resolved to family level, although 35% of bacterial abundance was made up of only eleven genera within five families. Almost 92% of bacterial abundance was made up of just 6 classes, Alphaproteobaceria (27.4%), Gammaproteobacteria (21.6%), Bacteroidia (20.4%), Planctomycetacia (13.2%), Acidimicrobiia (4.6%) and Verrucomicrobiae (4.2%) (Figure 5.3). Small differences aside, the relative abundance of taxa was broadly similar across most tissue types and control samples, with the exception of blade tissue samples which had considerably greater proportional abundance of Planctomycetacia and Alphaproteobacteria than other sample types (Figure 5.3).

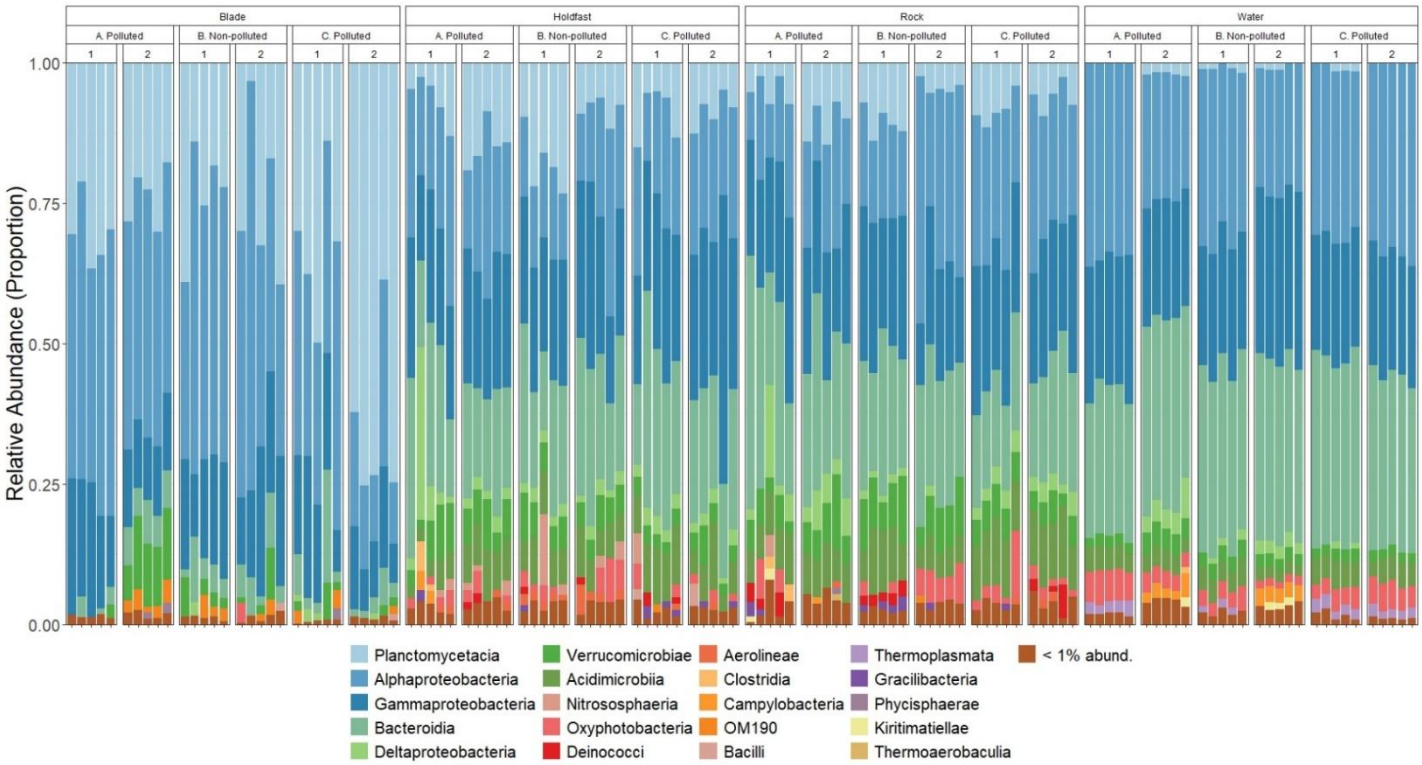

Figure 5.3. Relative abundance of bacterial microbiome classes found on the surface microbiome of *Laminaria hyperborea* blade and holdfast tissues, rock biofilms and seawater controls from two sites within each of three locations. Sites and locations can be seen in Figure 5.2. Classes contributing to <1% abundance were merged into a single category.

5.3.1 Shared ASVs

Across all tissue types (including controls), 51.2% of the 6,521 ASVs were found in the non-polluted sites, and 79.3% were found in polluted sites. Just 1,986 of the total ASVs (30.5%) were shared between non-polluted and polluted sites. Of the total ASVs, 53.3% (3,477) were found on biological samples (kelp blade and holdfasts). Of these ASVs, 33.7% were shared between polluted and non-pollutes sites, and 66.3% were not shared (Figure 5.4a-b). Within blade tissue only, 487 ASVs were found in non-polluted sites and 594 ASVs in polluted sites, with just 305 of these being shared (Figure 5.4a). Holdfast tissues contained a much greater number of ASVs, with 1,661 ASVs identified at non-polluted sites and 2,397 ASVs at polluted sites, with just 948 ASVs being shared (Figure 5.4b). It is important to note that there are twice as many polluted sites as non-polluted.

Across both blade and holdfast samples, non-polluted region B consistently had the greatest number of unshared ASVs, whilst polluted region C consistently had the lowest (Figure 5.4a-b). Although several region-specific ASV groups comprised a greater number of taxa, those shared among all three regions exhibited markedly higher abundances in both blade and holdfast tissues, with the 166 ASVs shared between regions in blade tissues, and the 499 ASVs in holdfast tissues (Figure 5.4a-b), accounting for the majority of ASV abundance in our samples (Figure 5.4c-d). Interestingly, the ASVs shared only between two regions did not account for a proportionate amount of the overall ASV abundance (Figure 5.4).

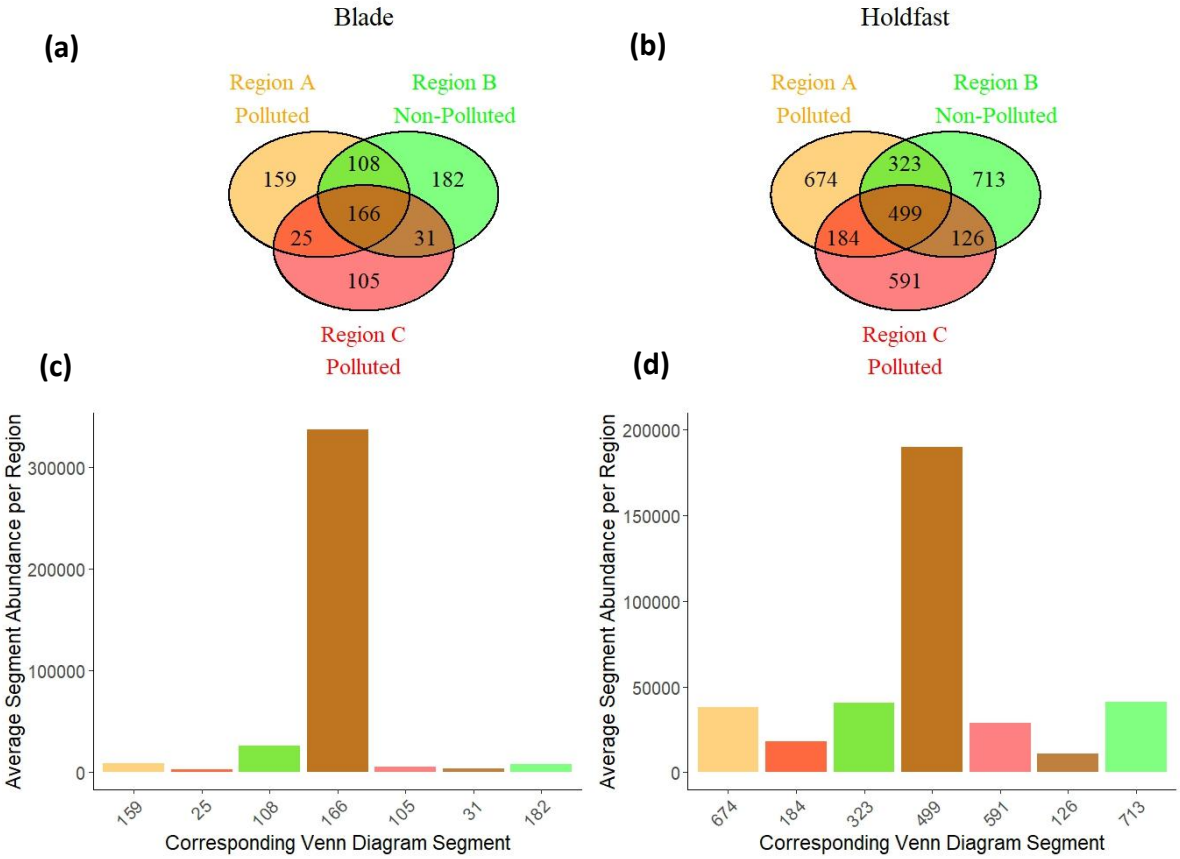

Figure 5.4. Overlap of bacterial ASVs from the surface microbiome of *Laminaria hyperborea* blade (a) and holdfast (b) tissue samples from polluted and non-polluted sites. Total abundance of Venn diagram segments for blade samples (c) and holdfast samples (d) standardised by number of regions represented in each Venn diagram segment.

When comparing taxa shared with the environment, across both levels of pollution, holdfast tissue and seawater samples had 645 shared ASVs, with holdfast samples having almost 1.8 times the number of ASVs than seawater samples (3,110 & 1,767 respectively). Blade tissue samples had considerably fewer ASVs than seawater samples with just 776, with only 234 being shared. Rocky biofilm and holdfast tissue samples had a very similar number of ASVs (3,609 & 3,110 respectively) and interestingly a large proportion of these were shared (47%) (Table S5.1). Rocky biofilm and blade tissue samples shared 327 ASVs.

5.3.2 Diversity and assemblage structure

Bacterial ASV diversity (both Chao1 and Shannon-Weiner) demonstrated considerable small-scale variability, with significant differences at the level of tissue x site nested in pollution (Table 5.1). There were no significant differences in diversity measures between levels of pollution (Table 5.1). Both diversity measures followed the same pattern across all sites and tissue types, with non-polluted site B1 consistently having the highest diversity across both holdfast tissue and rocky biofilm samples, and polluted site A2 having the highest diversity across both blade tissue and seawater samples (Figure 5.5). Non-polluted site B2 had the lowest Shannon-Weiner diversity in holdfast tissue and rocky biofilm samples, and Chao1 diversity was also lowest at site B2 for rocky biofilms, however, the bacterial diversity of holdfast tissue at polluted site C1 was slightly lower than it was at site B2 (Figure 5.5). For blade tissue and water samples, polluted site C2 consistently had the lowest diversity for both measures (Figure 5.5). Across the study, mean Chao1 diversity was 291.74 ± 2.98 SE and mean Shannon-Weiner diversity was 4.62 ± 0.09 SE (Figure 5.5). The most obvious pattern observed was that blade tissues had significantly lower Chao1 and Shannon-Weiner diversity in comparison with other tissue types sampled, whilst holdfasts and rocky biofilm samples had the greatest diversity, with the exception of water samples from site A2 (Table 5.1; Figure 5.5).

PERMANOVA detected significant small-scale differences in assemblage structure at the level of tissue x site nested in pollution (Table 5.2). Pairwise comparisons showed significant differences between all tissue types, as well as between all sites apart from polluted sites C1

and C2, which only displayed significant differences among seawater samples. Interestingly, while significantly different, holdfast and rock assemblages were more similar to each other than they were to water or blade samples. These differences were clearly depicted in the MDS plots, which show clustering of individual tissue samples (Figure 5.6a), as well as clustering by site in seawater samples (Figure 5.6e), and some clustering by levels of pollution in rock samples (Figure 5.6d). SIMPER analysis revealed the observed differences between all sites were primarily being driven by similar ASVs, with ASV2: *Blastopirellula sp.* being the highest contributor to the observed dissimilarity across all sites (Table S5.2). While ASV2: *Blastopirellula sp.* was the highest contributor to overall dissimilarity observed between sites, its contribution was inconsistent across replicates within respective sites (Table S5.2). ASV2: *Blastopirellula sp.* was also the greatest contributor to the observed dissimilarity between blade tissue and all other sample types, being found in considerably greater abundances on blade tissue than on the other sampled surfaces (Table S5.3). In contrast to the dissimilarity observed between sites, ASV2: *Blastopirellula sp.* contributed evenly and consistently to the differences seen between blade tissues and other sample types (Table S5.3).

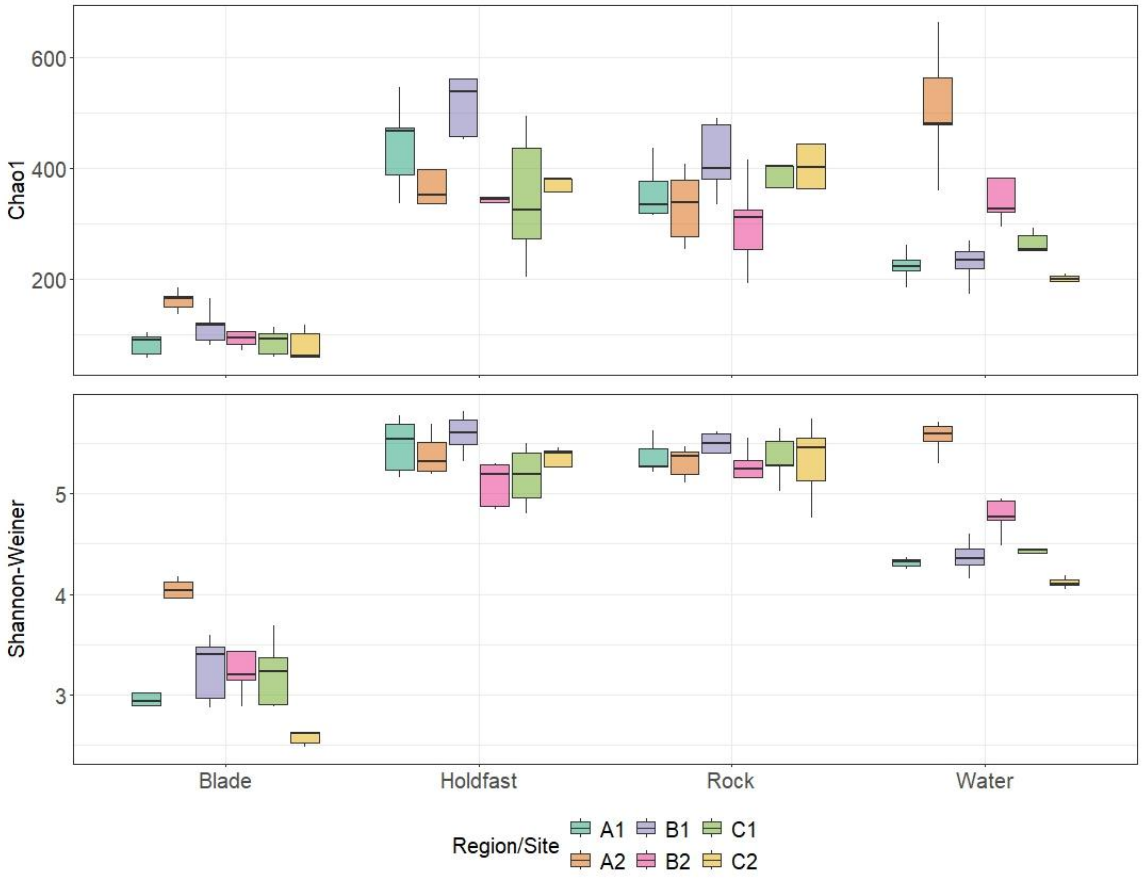

Figure 5.5. Bacterial microbiome alpha diversity metrics (Chao1 (top) and Shannon-Weiner (bottom)) sampled from *Laminaria hyperborea* holdfast and blade tissues, and rock biofilms and seawater controls from two sites within each of three locations. Site locations can be seen in Figure 5.2.

5.3.3 Core assemblage

The number of core ASVs present in each tissue and control type varied greatly, with blades having 8 core ASVs, holdfasts 13, rocky biofilm controls 4 and seawater controls 47 (Figure 5.7). All four of the core ASVs identified in the rocky biofilm, ASV21: *Illuminobacter nomiensis*, ASV51: *Filomicrobium sp.,* ASV66: *Granulosicoccus sp.,* ASV69: *Arcticiflavibacter sp.,* were also present in the core holdfast microbiome which had an additional 9 ASVs (Figure 5.7). Blade tissue samples had ASVs present in considerably greater abundances than holdfast tissues, and water controls had the greatest abundance of ASVs across all sample types (Figure 5.7),

however this is to be expected since seawater forms the pool of bacterial for colonisation of tissue types to take place from (Dang and Lovell, 2016).

Table 5.1. Univariate PERMANOVA testing variation in bacterial microbiome alpha diversity indices (Chao1 and Shannon-Weiner) between tissue types, different levels of pollution and sites nested within pollution. Results indicated with 'ŧ' are derived from Monte-Carlo simulations due to the low number of unique permutations. Significant results are indicated in **bold.**

	Chao1 index			Shannon index		
	df	*Pseudo-F*	*p*(perm)	df	*Pseudo-F*	*p*(perm)
Tissue	3	13.36	**0.0007**	3	45.03	**0.0001**
Pollution	1	0.09	0.7902ŧ	1	0.01	0.9306ŧ
Site(Pollution)	4	7.04	**0.0002**	4	16.81	**0.0001**
Tissue x Pollution	3	0.12	0.9525	3	0.06	0.9794
Tissue x Site(Pollution)	12	8.04	**0.0001**	12	5.95	**0.0001**
Residual	96			96		

Table 5.2. Multivariate PERMANOVA testing variation in bacterial microbiome assemblage structure between tissue types, level of pollution and sites nested in pollution. Results indicated with 'ŧ' are derived from Monte-Carlo simulations due to the low number of unique permutations. Significant results are indicated in **bold.**

	Bacterial Assemblage Structure (PERMANOVA)		
	df	*F*	*p*
Tissue*	3	13.99	**0.0001**
Pollution	1	1.46	0.0777ŧ
Site(Pollution)*	4	4.69	**0.0001**
Tissue x Pollution	3	1.44	**0.0430**
Tissue x Site(Pollution)	12	3.54	**0.0001**
Residual	96		

Within each tissue type, the same ASVs contributed to the core bacterial assemblages across all individuals, sites and pollution levels, however, these were present in different proportions between individuals and sites (Figure 5.7). Bacterial ASV diversity was therefore highly variable across small spatial scales, with the Chao1 diversity index demonstrating significant differences at the level of tissue x site nested in pollution (Table 5.4; Figure 5.8). Pairwise comparisons showed the differences driving this significance to lie within seawater samples between sites B1 & B2, and A2 & C1. Comparison of Shannon-Weiner diversity indicated a significant effect of tissue x pollution (Table 5.4), with pairwise comparisons showing significant differences between all tissue types apart from between blade and holdfast tissues in non-polluted areas, as well as showing that differences in holdfast bacterial diversity between polluted and non-polluted areas approached significance (p(MC)=0.0569). Whilst the bacterial diversity of holdfasts and blades were quite dissimilar in the full microbiome, core diversity values were much more alike, however, the diversity of holdfasts was still slightly greater than blades (Figure 5.8).

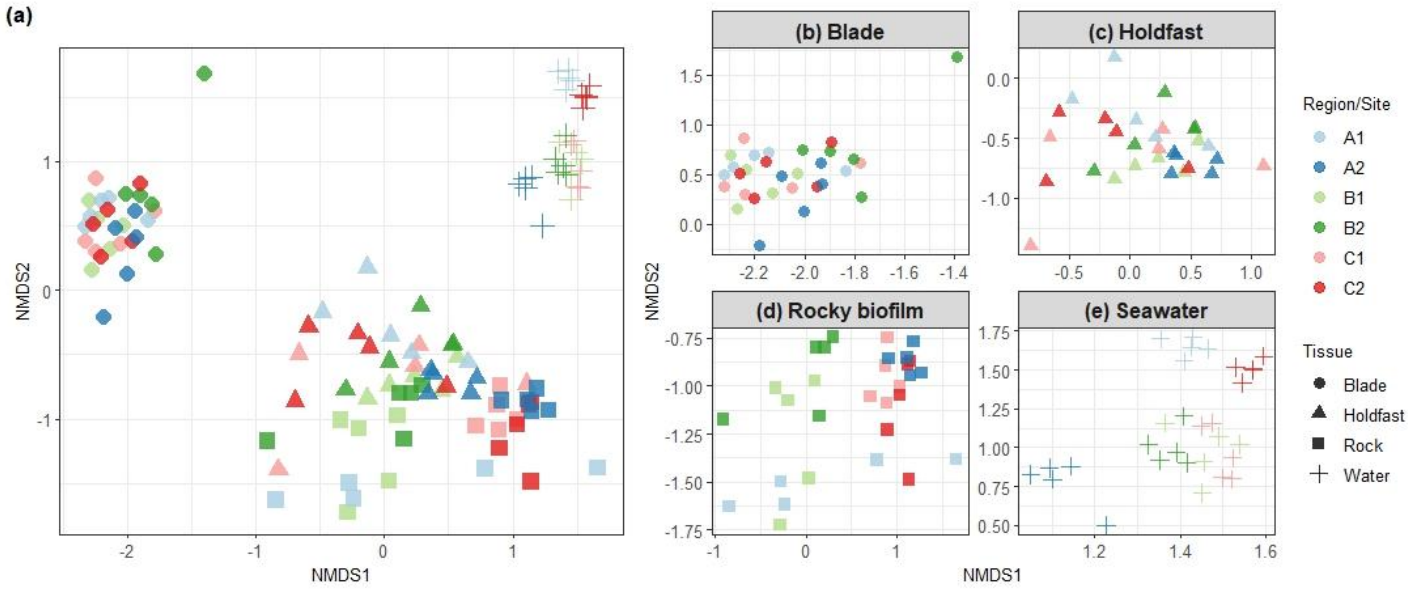

Figure 5.6. Bacterial microbiome assemblage structure associated with *Laminaria hyperborea* (a), as well as for blade (b), holdfast (c), rock biofilms (d) and seawater controls (e) from two sites within each of three locations. Sites and locations can be seen in Figure 5.2. Data based on Bray-Curtis similarity. Each point represents a sample taken from an individual kelp, rock biofilm or water sample.

PERMANOVA showed core assemblage structure varied significantly at the level of tissue x site nested in pollution (Table 5.4; Figure 5.9). Pairwise comparisons highlighted significant

differences between all sample types, although rock and holdfasts were more similar to each other than the other sample types. There were also significant differences between all sites for blade and seawater samples. However, there was no significant difference between holdfast samples in non-polluted sites, and no significant difference in holdfast and rocky biofilm samples between sites within polluted location C. SIMPER analysis revealed the ASVs driving the difference to be similar across tissue types, with ASV2: *Blastopirellula sp.* being present across many of the blade tissue samples and contributing largely to the differences between blade and other sample types (Table S5.4). ASV44: *Blastopirellula sp.* was abundant across many holdfast tissue samples, yet of very low abundance in environmental control samples, therefore acting as a strong contributor to the observed differences between these tissue types (Table S5.4).

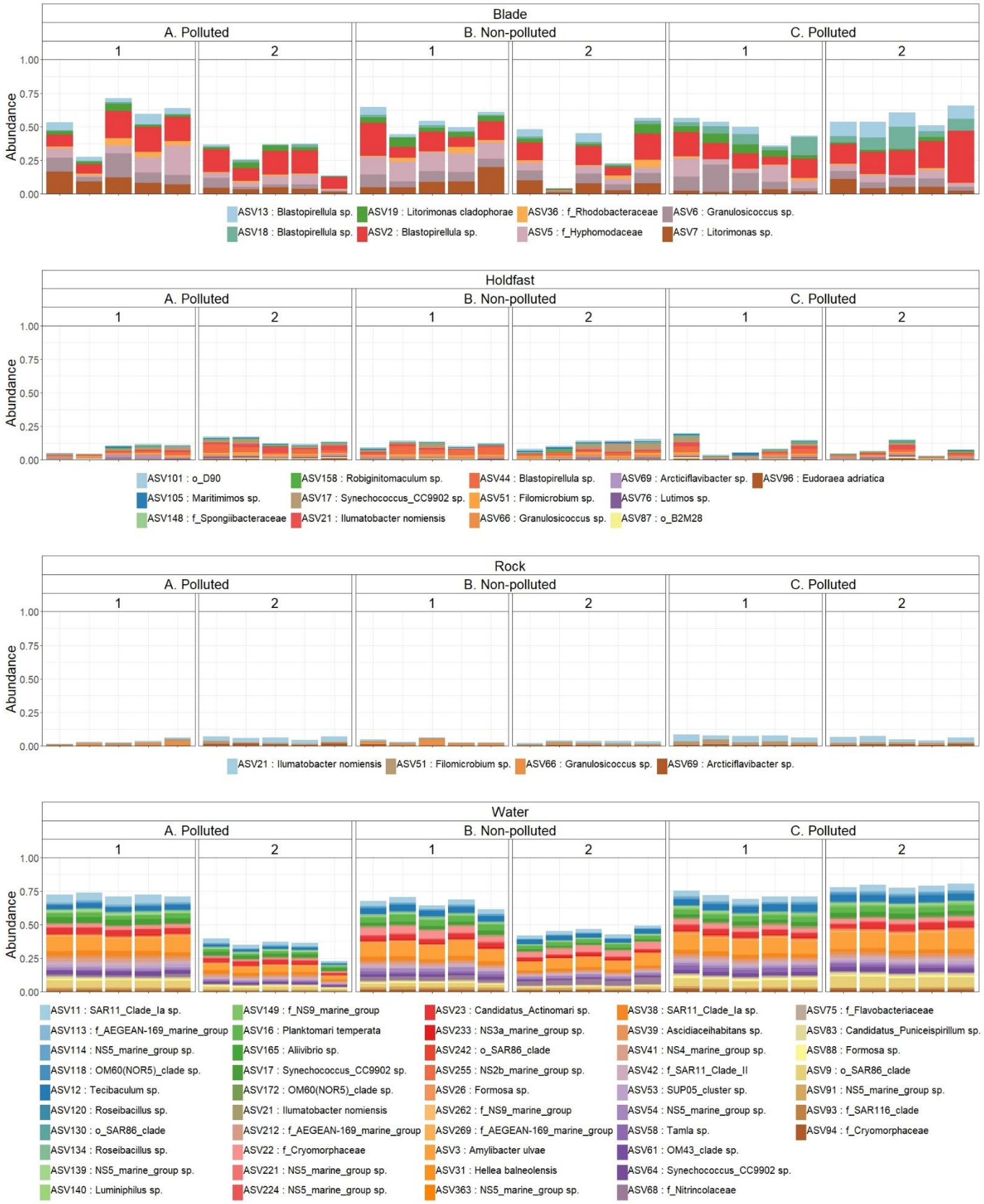

Figure 5.7. Relative abundance of the bacteria within the core bacterial surface microbiome of *Laminaria hyperborea* blade and holdfast tissues, rock biofilms and seawater controls from two sites within each of three locations. Sites and locations can be seen in Figure 5.2. Core bacterial assemblages are defined as taxa present in >95% of samples at a relative abundance of >0.1%. Taxonomic classification given as precursor (f_ = Family, o_ = Order) in the legend. Where no precursor is given, taxonomic classification is to genus or species level. Where "sp." is given, taxonomic classification is to genus level. Abundance is relative to whole bacterial assemblage.

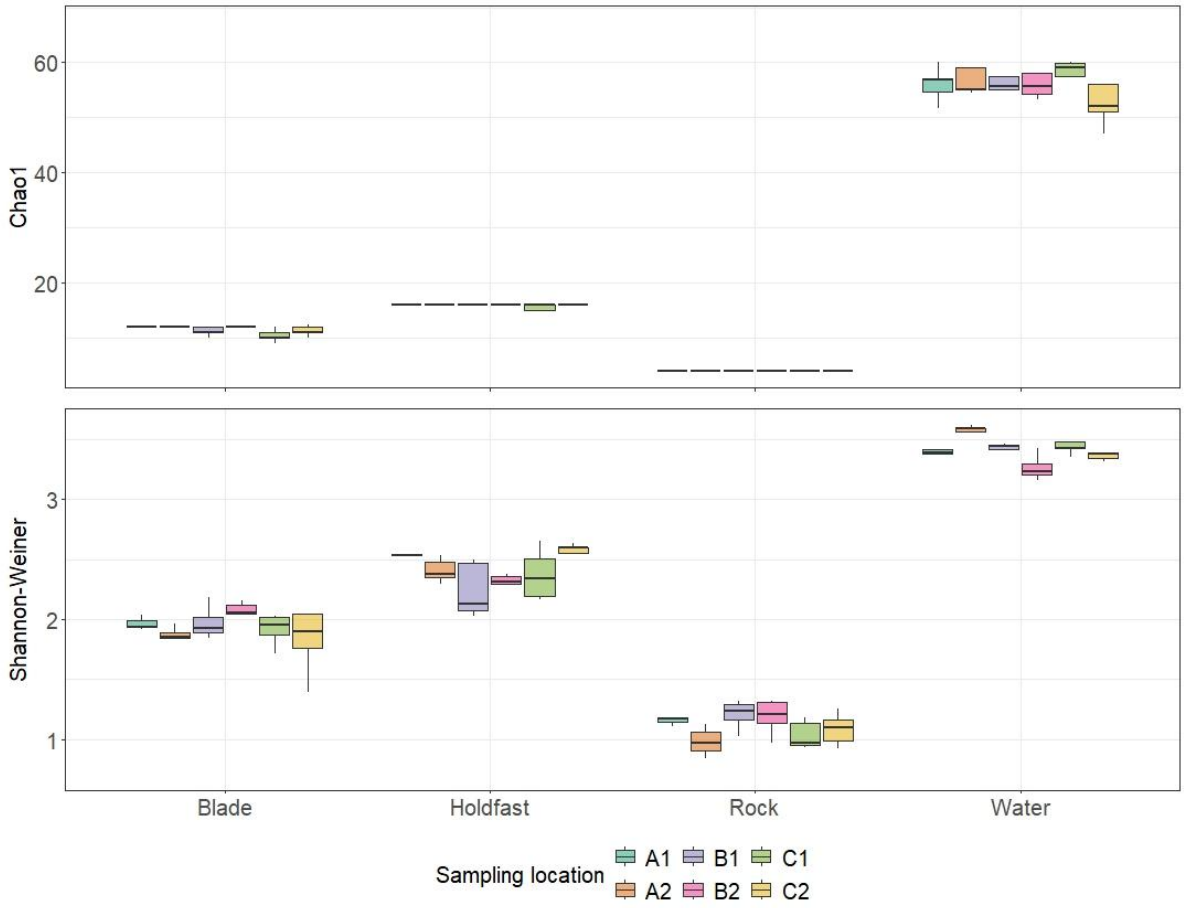

Figure 5.8. Core bacterial microbiome alpha diversity metrics (Chao1 (top) and Shannon-Weiner (bottom)) from *Laminaria hyperborea* holdfast and blade tissues, rock biofilms and seawater controls from two sites within each of three locations. Sites and locations can be seen in Figure 5.2. Core bacterial assemblages are defined as taxa present in >95% of samples at a relative abundance of >0.1%.

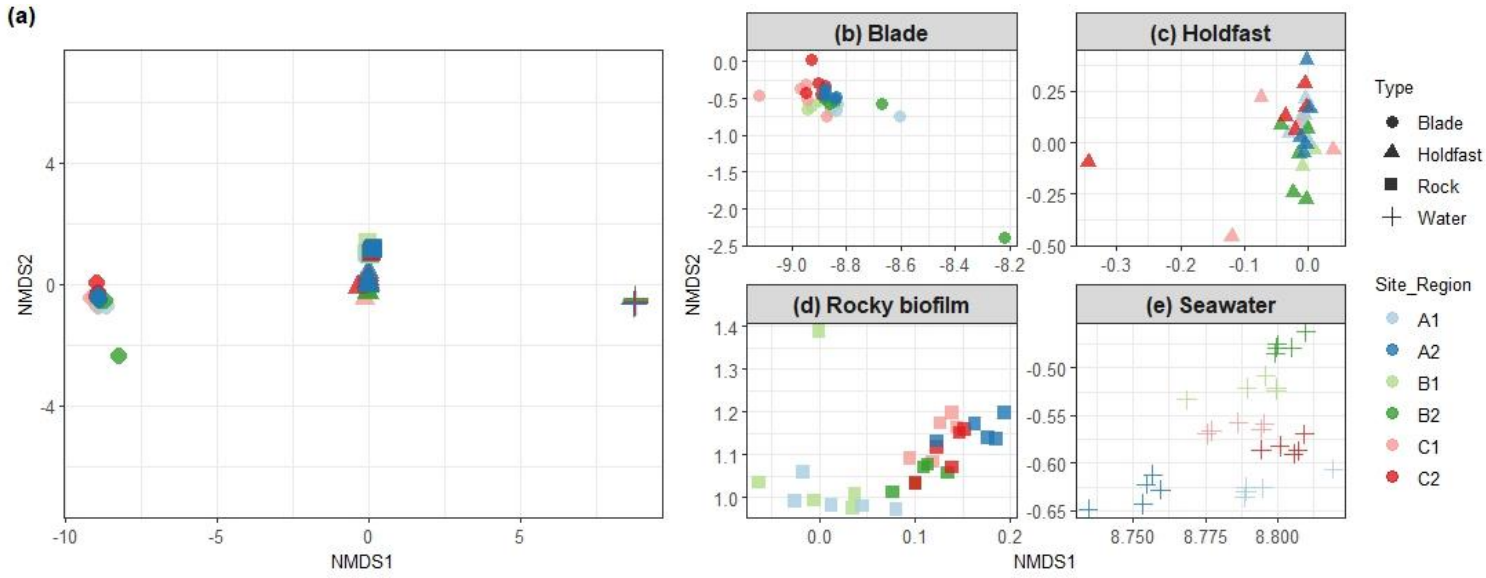

Figure 5.9. Core bacterial microbiome assemblage structure associated with *Laminaria hyperborea* (a), as well as for blade (b), holdfasts (c), rock biofilms (d) and seawater controls (e) from two sites within each of three locations. Sites and locations can be seen in Figure 5.2. Core bacterial assemblages are defined as taxa present in >95% of samples at a relative abundance of >0.1%. Each point represents a sample taken from an individual kelp, rock or water sample.

Table 5.3. Multivariate PERMANOVA testing variation in core bacterial microbiome assemblage structure between tissue type, level of pollution and site nested in pollution. Results indicated with 'ŧ' are derived from Monte-Carlo simulations due to the low number of unique permutations. Significant results are indicated in **bold.**

	Core Bacterial Assemblage Structure (PERMANOVA)		
	df	*F*	*p*
Tissue*	3	20.46	**0.0001**
Pollution	1	1.25	0.2924ŧ
Site(Pollution)	4	5.66	**0.0001**
Tissue x Pollution	3	1.05	0.3939
Tissue x Site(Pollution)	12	5.65	**0.0001**
Residual	96		

Table 5.4. Univariate PERMANOVA testing variation in core bacterial microbiome alpha diversity indices (Chao1 and Shannon-Weiner) between tissue types, levels of pollution and sites nested within pollution. Results indicated with 'ŧ' are derived from Monte-Carlo simulations due to the low number of unique permutations. Significant results are indicated in **bold.**

	Core Microbiome Alpha Diversity (ANOVA)					
	Chao1 index			Shannon index		
	df	*Pseudo-F*	*p*(perm)	df	*Pseudo-F*	*p*(perm)
Tissue	3	2675.3	**0.0001**	3	499.61	**0.0001**
Pollution	1	0.06	0.9556ŧ	1	0.42	0.5957ŧ
Site(Pollution)	4	7.02	**0.0390**	4	1.08	0.3720
Tissue x Pollution	3	0.23	0.9589	3	0.01	**0.0117**
Tissue x Site(Pollution)	12	2.01	**0.0049**	12	0.72	0.7198
Residual	96			96		

5.4 Discussion

The important role that microbiome assemblages play in influencing the health and functioning of kelp is becoming increasingly well understood (reviewed in Singh and Reddy, 2016) as well as how this can influence the wider ecosystem including kelp resilience to anthropogenic stressors (Stratil et al., 2013; Minich et al., 2018; Coclet et al., 2020). In order to further our understanding of the dynamics of kelp forest systems and the impacts of anthropogenic influences it is important for us to understand the bacterial assemblages within their holobiont. Through 16s metabarcoding of kelp tissues the composition and diversity of bacterial assemblages associated with *L. hyperborea* blades and holdfasts, as well as rocky biofilms and seawater as environmental controls was investigated. Specifically, I was interested in understanding whether historic coal mining waste disposal practices, and the likely elevated heavy metal concentrations, influenced bacterial assemblages. Kelp tissues supported distinct bacterial assemblages that were different to those found on rocky biofilm and seawater controls. Interestingly, while kelp holdfasts and rocky biofilms supported different assemblages, they were more similar to each other than they were to blade assemblages. No impact of historic pollution was found in our study, with only evidence of spatial variation between sites nested within pollution levels. Our results suggest that kelp-associated microbial assemblages are selected for across a range of spatial scales, with significant differences between tissue types just tens of centimetres apart, and variation between sites located tens of kilometres apart.

The results of this study align with previous research that shows structuring of bacterial assemblages associated with seaweeds to vary over a range of spatial scales, from microns (Ramírez-Puebla et al., 2022) to thousands of kilometres (Bonthond et al., 2020). However, even when large scale variation is exhibited, variation over smaller scales can still be more dominant, and therefore processes operating at local scales are determined to be the most important sources of variation (Bonthond et al., 2020). Similar to previous studies on *L. hyperborea* (Bengtsson et al., 2012) and other kelp species (Weigel and Pfister, 2019), between-site variation over distances as low as one kilometre in both the kelp tissues sampled was observed. The forces driving the observed level of variation is, however, somewhat speculative. Over larger spatial scales, differences in environmental drivers such as seawater

temperature can, for example, favour psychrophilic strains over mesophilic strains (Laycock, 1974). Genotypic differences (Griffiths et al., 2019) and unique lipidomic signatures (Monteiro et al., 2020) can also be responsible for shifts in bacterial assemblage structure over larger spatial scales. However, these factors are unlikely to be drivers of variation over smaller spatial scales such as those investigated here. Across these smaller scales, factors that vary locally such as exposure to weather elements (rain, wind and UV) during emersion that can lead to cellular stress and potential senescence (Burgunter-Delamare et al., 2023) are more likely to be drivers of observed variation. Anthropogenic pollutants in the form of trace metals have also been highlighted as stressors that shape prokaryotic assemblages. For example, copper and lead contamination in the bay of Toulon have been linked to structural differences of bacterial assemblages in seawater samples (Coclet et al., 2020), biofilms (Coclet et al., 2021), and the Mediterranean seaweed *Taonia atomaria* (Paix et al., 2021). Here, however, although structuring was observed between sites, the effects of pollution were not found to impact bacterial assemblage structure.

The lack of differences observed between polluted and non-polluted sites in both the full and core microbiome may be because the introduction of pollutants at the affected sites ceased more than 30 years ago. This period may have allowed pollutants to disperse throughout the marine environment or settle into sediments over time (Eagle et al., 1979). The concentration of heavy metal pollutants in any one area is subject to gradual reduction over time through factors such as their solubility and atomic weight (Furness and Rainbow, 2018), water currents (Eagle et al., 1979), and bioavailability within the ecosystem (Ansari, Marr and Tariq, 2003). That said, the same mines responsible for historic pollution continue to introduce present-day contaminants through groundwater pumping. At one study site (C1), this process releases in the region of 6 million litres per day of groundwater containing trace metals into the local marine habitat (Alderton, 2012). Although these discharges may contribute to local pollutant levels, their influx is variable, and therefore their impact on kelp microbiomes may only be detectable very close to discharge points. Consequently, bacterial assemblages on kelp at the studied sites may be exposed to pollutant concentrations too low to significantly affect microbiome structure or diversity. However, despite the lack of statistical differences between polluted and non-polluted areas, certain observations were noteworthy. In particular, the observed differences in the numbers of non-shared ASVs between polluted and non-polluted

sites, in which a greater number of unique ASVs were found in non-polluted sites than in polluted sites. Whilst these non-shared ASVs were of very low abundance, the presence of some ASVs was of particular interest. For example, dissimilatory reducing iron bacteria such as those in the generas *Desulfuromusa* and *Pelobacter* were found to be present in holdfast tissue samples in polluted sites yet were absent from non-polluted sites. These bacteria are capable of utilising iron [Fe(III)] to perform anaerobic respiration (Aromokeye et al., 2021) and are able to outcompete sulphate reducing bacteria (that are commonly found on seaweeds) under elevated iron concentration conditions (Vandieken et al., 2012) such as in areas of glacial melt (Vandieken et al., 2012) and those impacted by mine spoil pollution (Alderton, 2012). The presence of these bacteria in polluted sites and their absence in non-polluted sites provides evidence to suggest there may be increased Fe levels at the sampled polluted sites. Additionally, Site C2, historically the most impacted area with up to 2.5 million tonnes of waste deposited annually (Eagle et al., 1979; Cooper et al., 2017), showed the lowest bacterial diversity in both blade tissues and seawater controls. Blade samples from this site also contained a notably higher proportion of Planctomycetacia, a bacterial class associated with bacterial decomposition (Wegner et al., 2013; Parrot et al., 2019). This suggests that background pollution levels at site C2 may still be sufficient to induce minor shifts in microbial diversity, yet not strong enough to cause substantial structural changes to the microbiome.

While pollution may not have significantly altered the microbiome structure, some specific differences in bacterial composition were observed, particularly between different tissues. The blades of *L. hyperborea* are regularly eroded as part of their growth strategy (Kain and Jones, 1976) and are subject to mechanical stress in the exposed environment they occupy. This, therefore, makes them more vulnerable to bacterial decomposition, which creates new ecological niches for bacteria to colonise (Bengtsson and Øvreås, 2010). This could, in part, be responsible for the high abundance of Planctomycetes (in particular the genus *Blastopirellula*) found on blade tissue in comparison to other tissues that we sampled. Planctomycetes are found commonly across seaweeds and biofilms globally (Bengtsson and Øvreås, 2010; Burke et al., 2011; Bondoso et al., 2017), and although their role is not fully understood, they do contain sulfatase genes which degrade sulphated polysaccharides (Wegner et al., 2013). This function makes them able to degrade polysaccharides in the extracellular matrix of biofilms, and therefore useful for degrading tissues that are subject to bacterial decomposition (Parrot

et al., 2019). Unlike blade tissues, *L. hyperborea* holdfast tissues do not decompose or erode as part of their natural growth strategy and aren't subject to the mechanical stress that blades are. Holdfasts would therefore be less likely to have the high abundances of Planctomycetes in their microbiome assemblage as blades do, as our results show. As well as high abundance of Planctomycetes, blade tissues were also found to harbour a greater abundance of Alphaproteobacteria (in particular the family Hyphomonadaceae) than on holdfast tissues. Interestingly, Hyphomonadaceae has been demonstrated to be found in greater abundance in metal contaminated seawater (Coclet et al., 2020), and is commonly found associated with anthropogenically disturbed biofilm communities (Briand et al., 2017). However, Hyphomonadaceae was found across all the study sites, with no differences in its abundance between polluted and non-polluted areas.

Variation over small scales has been described previously, for example, King et al. (2022) found variability even within individual plants, possibly attributed to sampling areas of newer and older growth on kelp blades. Sampling areas of newer growth over older growth, as was done here with blades and holdfasts, would capture earlier stages of bacterial succession which naturally harbours greater bacterial variation between individuals and lower diversity, since less selection and competition has taken place to establish a dominant community (Lee et al., 2008; Dang and Lovell, 2016). Indeed, studies have shown structuring of bacterial assemblages along the blades of a single individual seaweed (Burgunter-Delamare et al., 2023). The likely cause of this is down to the unique growth strategy of certain kelp species. For example, *Laminaria hyperborea* blades grow from the meristematic junction between the stipe and blades (Kain and Jones, 1976). In this area of growth, tissues are younger and therefore less colonised by bacteria, subsequently exhibiting lower bacterial diversity (Staufenberger et al., 2008; Ihua et al., 2019; Lemay et al., 2021). Moving towards the distal tips of the blades, tissues are older and have had greater time to establish a dominant bacterial assemblage with a greater species richness and diversity (Weigel and Pfister, 2019; Lemay et al., 2021). As blades grow longer, they are also more likely to come into contact with the benthos or other individuals, and with water movement manipulating the blades they have greater access to bacterial communities from the broader environment, giving them the potential to further enhance bacterial diversity. Whilst we only sampled one region of blade tissue, we did sample different tissues of different ages within the same individual. With no loss and regrowth of

tissues taking place in the perennial holdfasts, *L. hyperborea* holdfast tissues can be as old as the individual (average age 5.3 ± 0.1 years, n=120, Chapter 2), compared to blades that are annual structures. This gradient of different aged tissues along a single individual resulted in a high degree of structuring in microbial assemblages over very short spatial scales of just metres and has been shown to take place in other kelp species such as *Laminaria setchellii* (Lemay et al., 2021). Whilst blade and holdfast associated bacterial assemblages were very different from each other, holdfast assemblages were of considerably greater similarity to rocky biofilms than to other sample types. Furthermore, holdfasts tissues harboured greater bacterial diversity than blades, possibly due to their perennial nature and the extended period available for bacteria to colonise. Since holdfast tissues are generally several years old, it is likely that a dominant bacterial assemblage has formed on both the holdfast surface and that of the surrounding rock. Given their extremely close proximity to each other, it is unsurprising that the bacterial assemblages found on holdfasts and those on rocky biofilms are structurally similar in comparison to blade tissues. These similarities also carried through to the core microbiome assemblage structure, whereby all rocky biofilm ASVs were also present on holdfast tissues, which still had greater diversity than blades.

Whilst we do not know the functional roles of most of the sampled kelp microbiome, by looking at the core microbiome we can identify taxa that are common and therefore likely to be functionally important. Core bacterial assemblages in both blade and holdfast tissues were remarkably distinct from one another, sharing no ASVs between them. Each tissues core assemblage also showed a high degree of stability among sites, with every site sharing the majority of ASVs within each core assemblage. The core assemblage of blade tissues consisted of 8 ASVs and had high relative abundance, making up 46.6% of the whole bacterial assemblage found on the blade. That said, the ASVs present on the blade only represented 1% of the total ASVs found on the average individual, indicating the presence of a large number of ASVs that have low abundance. No ASVs present in the core assemblage of blade tissues were found in environmental control samples, suggesting a distinct assemblage whose ASVs may have functional roles within the bacterial microbiome. Interestingly, the relative abundance of the core assemblage associated with blade tissues was much greater than previous estimates for *L. hyperborea*, where the core assemblage consisted of only 5 ASVs and made up just 25.4% of the total abundance (King et al., 2022). The 13 ASVs belonging to the

core assemblage of holdfast tissues was considerably lower in abundance, making up just 10.8% of the whole holdfast assemblage relative abundance, and just 0.4% of the total ASVs found in an average individual. All the ASVs identified in rocky biofilm controls were present in core holdfast assemblages, which had an additional 9 ASVs. Two of these additional ASVs were also present in seawater controls, suggesting a distinct core holdfast assemblage of 7 ASVs that may be involved in functional processes.

Whilst blade core assemblage relative abundance was greater than found by King et al. (2022), there were similarities in the composition of the core in terms of shared taxa. Both *Blastopirellula sp.* (Planctomycetes) and *Litorimonas sp.* (Alphaproteobacteria) were found in high abundances in both studies, with the remainder of the core taxa identified here belonging to the common (between studies) classes of Alpha- and Gammaproteobacteria. Indeed, many of our core taxa have been found on seaweeds across the world (Bengtsson and Øvreås, 2010; Burke et al., 2011; Lemay et al., 2018; Parrot et al., 2019; Phelps et al., 2021), suggesting there could be a more general core bacterial assemblage across larger geographic scales, with particular bacterial taxa being associated with a diverse range of macroalgal hosts. These shared core taxa often have important functional roles. For example, Rhodobactereaceae (1 core ASV in blade assemblage) are commonly found in macroalgae (Dogs et al., 2017), as well as in algal core communities (Bonthond et al., 2020), and along with *Granulosicoccus sp.* (1 core ASV in blade assemblage), play a key role in metabolising algal osmolytes such as dimethylsulfoniopropionate (Moran et al., 2012; Kang, Lim and Cho, 2018). Hyphomonodaceae (3 core ASVs in blade assemblage in our study) have also been associated with a wide range of seaweeds and are known to detoxify O_2 produced by photosynthetic hosts and create a closed carbon cycle whereby exudates from photosynthetic hosts are oxidated to form CO_2 which is immediately reutilised by the host (Abraham and Rohde, 2014). Whilst algal holdfasts have been sampled for microbiome analysis considerably less than blades, the few studies available also show similarities in the bacterial taxa present, including *Granulosicoccus sp.* (1 core ASV in holdfast assemblage) (Ihua et al., 2020; Lemay et al., 2021). Once again, suggesting the possibility of globally consistent taxa that are responsible for certain functional roles.

This study examined the bacterial assemblages associated with *Laminaria hyperborea,* surveying across a range of polluted and non-polluted sites and across kelp holdfasts and blades. Whilst we expected to find an impact of pollution from historic coal mining waste disposal practices on the structure and diversity of the host associated microbiome, this was not the case. Although there was significant natural variation between sites, probably driven by localised environmental conditions, we found significant structuring of the kelp microbiome between tissue types. Functional requirements coupled with tissue age are likely to be responsible for the differences observed. Indeed, the high level of shared taxa between here and previous studies on macroalgal species globally suggest the possibility of a generalised core seaweed microbiome, further research is required to give greater functional insight in order to understand the dynamics that underpin microbial assemblages in kelp forests.

Chapter 6. General discussion

6.1 Overview

This thesis aimed to characterise the structure of kelp forests along the northeast coastline of the United Kingdom and explore their functioning in industrialised areas historically impacted by coal mining waste disposal. The research focuses specifically on kelp forests dominated by *Laminaria hyperborea*, the large canopy-forming species prevalent along much of the UK's coastline. Chapter 2 addresses a critical knowledge gap by examining the structure of *L. hyperborea* forests and their variation across depth gradients. While this information is well-documented for many other regions in the UK where kelp forests are abundant, this study is the first to focus on this particular geographic area. The findings reveal that kelp forests in this region exhibit high variability across spatial scales and depth gradients, consistent with observations from other parts of the UK (Smale et al., 2016; Smith et al., 2022). Variation of kelp forest structure over short spatial scales is driven by a number of interacting environmental variables that vary on a local scale. Wave exposure is a key driver of kelp forest structure and was shown in Chapter 2 to vary between sites surveyed here. Increased water motion driven by wave exposure enhances rates of photosynthesis and nutrient uptake (Hurd, 2000), leading to greater growth and productivity rates (Pedersen et al., 2012) and therefore larger individuals. Being photosynthetic organisms, light availability also influences kelp forest structure, and although bigger differences in annual light budgets are seen over large latitudinal gradients, smaller local scale variation in light availability can be driven by differences in water clarity. This can have an impact on kelp growth and productivity and limit the depth to which kelp forests extend (Tsiamis et al., 2020; Smith et al., 2022). Looking over larger spatial gradients, data collected from two regions - northeast England and southeast Scotland - indicate the presence of some of the tallest *L. hyperborea* individuals and highest carbon standing stock estimates within the species' range. These results suggest that these areas provide optimal habitat and growth conditions. Other metrics of individual morphology and kelp forest structure align with previously documented patterns along large-scale gradients of environmental conditions, such as those associated with the UK's latitude (Smale et al., 2016; Smale and Moore, 2017; Smith et al., 2022). Chapter 3 builds on these findings by highlighting structural differences in kelp forests occupying shallow subtidal zones compared

to those recorded at greater depths in Chapter 2. In the shallow subtidal zone (0-0.3 m below chart datum, BCD), kelps were smaller in size but occurred at higher densities than those observed at 2 m, 5 m, and 7-10 m BCD.

Building on the characterisation of kelp forest structure in Chapter 2, Chapters 3 through 5 examine the potential impacts of historic coal mining waste disposal along the Durham and Northumberland coastlines. In these locations, mine waste was directly disposed onto shores between 1899 and 1993, causing severe negative impacts on coastal habitats and the smothering of kelp forest habitats. These chapters explore various aspects of kelp forest ecology, ranging from broad-scale habitat structure and productivity (Chapter 3) to the macroinvertebrate communities inhabiting kelp holdfasts and stipes (Chapter 4), and finally to the bacterial microbiomes that occupy kelp tissue surfaces (Chapter 5). The primary aim was to compare these ecological variables between areas directly affected by historic coal mining waste disposal that were buried under coal mining spoil for decades, and unaffected areas – treating affected sites as proxies for pollution. While the hypothesized effects of historic mine waste on kelp forest ecology were generally not observed, the results suggest that subtle, lingering impacts may persist in some aspects of the ecosystem.

Although no significant effects of historic pollution were detected across most aspects of kelp forest structure or function, consistent patterns were observed in the data from site C2. This site, the location of Easington Colliery waste disposal, was among the most heavily affected areas in this region, receiving over 2.5 million tonnes of waste per year at the peak of mining activity (Eagle et al., 1979; Cooper et al., 2017). At this site, the structure of kelp forests differed notably from other sites. Kelp forests had greater densities but were consistently younger, with less variation in age and a lower maximum age compared to other sites. Additionally, the stipes of kelp at this site lacked epiphytic algae, which typically provides habitat for macroinvertebrate fauna; consequently, no macroinvertebrates were found on the stipes of kelp from site C2. Similarly, the bacterial microbiome on kelp blade surfaces at this site exhibited the lowest diversity (as measured by both Chao1 and Shannon-Weiner indices) and showed the highest proportional abundance of Planctomycetaceae, a bacterial class associated with decomposition processes (Wegner et al., 2013; Parrot et al., 2019). These

consistent observations at site C2 may be attributed to the magnitude and duration of mine waste disposal at this site compared to neighbouring affected sites. Here, kelp forests were buried under coal spoil and smothered for multiple decades, resulting in prolonged physical disturbance and high input of pollutant laden sediments. These conditions likely facilitated the long-term accumulation of heavy metals and other contaminants in surrounding sediments and within biological tissues. Elevated levels of such pollutants have been associated with reduced kelp survivability, contributing to the dominance of younger age classes in affected populations (Vásquez et al., 2000) Similarly, the concentration of heavy metals in the surface of kelp tissues has been shown to inhibit the settlement of epiphytic algae (Contreras et al., 2007; Oyarzo-Miranda et al., 2020) and may be responsible for the lack of epiphytic algae seen on stipes here and in previous studies in polluted areas (Jara-Yáñez et al., 2021). The consistency of these patterns across multiple ecological variables suggests that coal mine waste disposal at site C2 may still be having a lasting negative impact, possibly linked to the greater volume of waste historically deposited in this area.

6.2 Recovery of kelp forests and persistent impacts of historical mine wastes

Aside from the differences observed at site C2, as well as a pattern of smaller holdfasts in polluted areas, very few other differences were found between polluted and non-polluted locations. Polluted sites had been buried under colliery spoil for extended periods of time, leading to habitat degradation through smothering and considerable alterations to benthic habitat conditions. The lack of differences between polluted and non-polluted areas could indicate that the effects of mine waste are no longer significantly impacting kelp forests and that impacted sites have recovered to a point where they are indistinguishable from unaffected sites. However, it is also possible that the non-polluted location, while situated away from areas directly affected by coal mining activities, has still experienced some influence from mine waste pollution. Historically, mine wastes disposed of into the coastal environment contained high concentrations of toxic heavy metals (Eagle et al., 1979), which likely dispersed quickly in the marine environment. Given that mining and waste disposal activity occurred to the north of the non-polluted site (location B), it is plausible that diffuse pollutants were transported southward via the prevailing southerly current (Eagle et al., 1979). Coal mine waste material continues to wash ashore today and is frequently observed on beaches near

non-polluted sites in location B (Figure 6.1) providing further evidence that waste materials and associated pollutants could have reached kelp forests in this area. However, while the influx of waste, its impact on turbidity, and the concentration of any potential pollutants at location B are not documented, it is reasonable to assume that these factors would have been considerably lower compared to the polluted sites that were directly impacted by mining waste disposal and that the experimental design used here still offers a gradient to observe possible effects along.

Figure 6.1. Coal mine waste washed ashore in Northumberland near to location B. Locations can be seen in Figure 5.2.

The polluted sites sampled in this study were located either directly within, or in very close proximity to historical mine waste disposal areas. These sites were therefore buried under vast quantities of mine waste, in some cases exceeding 10 m in depth (Cooper et al., 2017). Figure 1.2, showing the location of sampling at site C1, provides clear evidence of the pressures these kelp forests faced for many decades. Although no formal records exist, photographic evidence strongly suggests that the nearshore kelp forests surveyed as ‘polluted sites’ in this thesis were absent for at least several decades. The recovery of these kelp forests since the cessation of mining activities has, therefore, been remarkable. Studies conducted during the years of active

mining (e.g. Sheppard et al., 1980) indicate that populations of *Laminaria hyperborea* were not completely absent from the coastline. It is quite likely that patches of kelp forest habitat, located in areas not directly impacted by mine waste, persisted and played a crucial role in the recovery of kelp forests after mining activities ceased. These surviving populations may have released spores that colonised newly uncovered bedrock and boulder habitats previously buried under mine waste. However, the broader ecological impacts of mine waste on these surviving kelp forests remain poorly understood. Sheppard et al. (1980) reported shifts in the macroinvertebrate communities associated with kelp holdfasts, attributed to increased turbidity in the surrounding waters, however beyond this, any impacts of mine waste are not well known. The potential genetic consequences of reseeding populations from small, fragmented source populations have not been studied on this coastline and warrants further investigation. Given that *L. hyperborea* has a relatively short dispersal distance of approximately 200 m under normal conditions (Fredriksen et al., 1995), it is likely that recolonisation occurred predominantly from these nearby remnant populations in a stepping-stone pattern (Assis et al., 2018). This could potentially result in low genetic diversity in these recently established kelp forests which may make them more susceptible to future stressors such as climate change (Schoenrock et al., 2020).

6.3 Limitations of thesis and suggestions for future work

Although this thesis revealed few effects of historic pollution, they underscore the need for further research to understand the potential lingering impacts of pollutants at historically affected sites. In Chapter 4, significant differences in macroinvertebrate assemblages between polluted and non-polluted areas were observed, which were attributed primarily to the significantly larger holdfast volumes at non-polluted sites. This raises the possibility that pollution, or associated factors such as increased sedimentation from mine waste disposal, may inhibit growth or development of kelp holdfasts. Similar effects have been documented in *Macrocystis pyrifera*, where heavy metal pollutants negatively impacted holdfast development (Jara-Yáñez et al., 2021). However, other studies indicate that the response to heavy metal exposure can be highly species-specific (Leal et al., 2018). Thus, further research is needed to improve our understanding on how pollution exposure affects *Laminaria*

hyperborea growth, particularly with respect to holdfast development and its subsequent effect on biodiversity.

While historic studies provide quantitative data on the concentrations of heavy metal pollutants introduced into marine environments along the Durham and Northumberland coastlines, there is a notable lack of information available on current pollution levels or the extent of bioaccumulation in local organisms. This thesis included efforts to quantify heavy metal concentrations in kelp tissues using inductively coupled plasma optical emission spectroscopy and mass spectrometry; however, extreme variability in metal concentrations was discovered over short spatial scales of just millimetres on a single individual. Although some level of intra-individual variability was anticipated based on previous research (Burger et al., 2007), the extent of variation observed here was unexpectedly high and occurred over much smaller spatial scales than previously reported. Older kelp tissues, such as the stipe and holdfast, are expected to accumulate higher concentrations of heavy metals due to longer exposure, while younger, seasonally replaced blades typically contain lower concentrations. However, the observed variability far exceeded these expected patterns. More recent studies have found variability of potentially toxic elements over nanoscales in brown seaweeds, suggesting the ability to sequester pollutants into specialised organelles called physodes (Vázquez-Arias et al., 2024). This mechanism, if present in *L. hyperborea*, could be responsible for the large variation observed here over such small spatial scales. Financial, logistical, and time constraints limited further investigation, and consequently, these data were not included in the thesis. Understanding current levels of heavy metal pollution and their distribution is critical for identifying specific drivers of the few pollution effects observed here. Additionally, understanding the mechanisms of heavy metal accumulation and their variability in kelp tissues would advance our understanding of kelps ability to persist in unfavourable environmental conditions. Future work should focus on developing standardised protocols for quantifying heavy metals in kelp tissues and investigating the causes and implications of intra-individual variability. These advancements would greatly enhance the reliability of future pollution studies on *Laminaria hyperborea* and other kelp species. For future studies where intra-individual variability is not a focus, homogenisation of whole individuals and subsequent subsampling from this material for analysis may be a useful method for quantifying broader

levels of metal concentrations stored in kelp tissues, and would remove the element of variability over small scales that was measured here.

Smale et al. (2016)Smith et al. (2022)The data presented in Chapters 2 and 3 offer a valuable foundation for future monitoring of kelp forest health and recovery from historic pollution impacts along the Durham and Northumberland coasts. Simple, low-cost methods such as measuring kelp density and morphological traits (e.g. length and biomass) proved effective in detecting subtle yet consistent site differences, and are well-suited for long-term monitoring at both fine and broad spatial scales. These approaches align with methodologies currently used in national initiatives, including the marine Natural Capital and Ecosystem Assessment (mNCEA) programme and ground-truthing efforts by the Environment Agency (EA) and Natural England (NE), making them ideal for integration into standardised monitoring protocols and national datasets. While comparisons between Chapters 2 and 3 revealed differences in kelp forest structure, these likely reflect the deeper survey depths in Chapter 2. To fully assess the effects of historic pollution, further data collection at consistent depths across sites is essential. This would facilitate robust comparisons with national studies (Smale et al., 2016; Smith et al., 2022) and clarify how local kelp forest dynamics have responded to historic mining pollutants. Regular, temporally spaced surveys incorporating both structural and in-situ environmental data would enhance detection of long-term ecological changes and improve understanding of the drivers behind them. Moreover, increased replication of sites representing polluted and non-polluted conditions would significantly strengthen assessments of persistent pollution effects

6.4 Conclusions

This thesis provides a baseline for the structure of *Laminaria hyperborea* kelp forests on the United Kingdom's northeast coastline and provides valuable insights into their structure and functioning in historically industrialised regions. The findings highlight the remarkable recovery of *Laminaria hyperborea* forests in areas previously impacted by coal mining waste, while also suggesting the potential for lingering subtle effects at heavily affected sites, such as C2. Despite the limited observed impacts of historic pollution, the consistent patterns of

reduced biodiversity and altered kelp forest structure at site C2 underscore the need for further investigation into the long-term ecological consequences of industrial waste exposure. Additionally, this work highlights significant gaps in our understanding of pollution dynamics, including heavy metal bioaccumulation in kelp tissues and its variability, as well as the potential genetic and ecological implications of recolonisation from fragmented populations. Addressing these gaps through future research will not only enhance our understanding of kelp forest resilience and recovery but also provide critical information for managing these vital ecosystems in the face of increasing environmental pressures.

Importantly, the findings of this thesis demonstrate that even habitats once severely degraded by industrial activity are capable of remarkable natural recovery. Several sites that were historically barren, buried under coal spoil for decades, and heavily polluted now support healthy, functioning kelp forests that are in many ways indistinguishable from those in unaffected regions. This resilience offers a hopeful outlook for the restoration of marine ecosystems more broadly and underlines the importance of continued conservation, monitoring, and support for natural recovery processes.

References

ABDULLAH, M.I., FREDRIKSEN, S. and CHRISTIE, H. (2017) The impact of the kelp (Laminaria hyperborea) forest on the organic matter content in sediment of the west coast of Norway. *Marine Biology Research*, 13(2), pp. 151–160.

ABRAHAM, W. and ROHDE, M. (2014) The Prokaryotes. In: pp. 283–299.

ADAIR, K.L. and DOUGLAS, A.E. (2017) Making a microbiome: the many determinants of host-associated microbial community composition. *Current Opinion in Microbiology*, 35, pp. 23–29.

ALDERTON, S. (2012) *Heavy Metal Contamination Along the Coast of North-East England*.

ALLEN, C.D., BRESHEARS, D.D. and MCDOWELL, N.G. (2015) On underestimation of global vulnerability to tree mortality and forest die-off from hotter drought in the Anthropocene. *Ecosphere*, 6(8), pp. 1–55.

DE ALMEIDA RODRIGUES, P. et al. (2022) A Systematic Review on Metal Dynamics and Marine Toxicity Risk Assessment Using Crustaceans as Bioindicators. *Biological Trace Element Research*, 200(2), pp. 881–903.

ANDERSEN, G.S. et al. (2011) Seasonal Patterns of Sporophyte Growth, Fertility, Fouling, and Mortality of Saccharina latissima in Skagerrak, Norway: Implications for Forest Recovery. *Journal of Marine Biology*, 2011, pp. 1–8.

ANDERSON, M.J. (2001) Austral Ecology - 2001 - Anderson - A new method for non-parametric multivariate analysis of variance.pdf.

ANDERSON, M.J. et al. (2005) Consistency and variation in kelp holdfast assemblages: Spatial patterns of biodiversity for the major phyla at different taxonomic resolutions. *Journal of Experimental Marine Biology and Ecology*, 320(1), pp. 35–56.

ANDERSON, M.J. (2008) PERMANOVA+ for PRIMER: guide to software and statistical methods. *PRIMER-E, Plymouth Marine Laboratory*.

ANDERSON, M.J., ELLINGSEN, K.E. and MCARDLE, B.H. (2006) Multivariate dispersion as a measure of beta diversity. *Ecology Letters*, 9(6), pp. 683–693.

ANDERSON, M.J., GORLEY, R.N. and CLARKE, K.R. (2008) PERMANOVA+ Primer V7: User Manual. *Primer-E Ltd., Plymouth, UK*, p. 93.

ANSARI, T.M., MARR, I.L. and TARIQ, N. (2003) Heavy Metals in Marine Pollution Perspective–A Mini Review. *Journal of Applied Sciences*, 4(1), pp. 1–20.

ARAFEH-DALMAU, N. et al. (2019) Extreme Marine Heatwaves alter kelp forest community near its equatorward distribution limit. *Frontiers in Marine Science*, 6(JUL), pp. 1–18.

ARKEMA, K.K., REED, D.C. and SCHROETER, S.C. (2009) Direct and indirect effects of giant kelp determine benthic community structure and dynamics. *Ecology*, 90(11), pp. 3126–3137.

ARNOLD, M. et al. (2016) The structure of biogenic habitat and epibiotic assemblages associated with the global invasive kelp Undaria pinnatifida in comparison to native macroalgae. *Biological Invasions*, 18(3), pp. 661–676.

AROMOKEYE, D.A. et al. (2021) Macroalgae degradation promotes microbial iron reduction via electron shuttling in coastal Antarctic sediments. *Environment International*, 156(April), [Online] Available from: doi.org/10.1016/j.envint.2021.106602.

ASSIS, J., TYBERGHEIN, L., et al. (2018) Bio-ORACLE v2.0: Extending marine data layers for bioclimatic modelling. *Global Ecology and Biogeography*, 27(3), pp. 277–284.

ASSIS, J., SERRÃO, E.Á., et al. (2018) Past climate changes and strong oceanographic barriers structured low-latitude genetic relics for the golden kelp Laminaria ochroleuca. *Journal of Biogeography*, 45(10), pp. 2326–2336.

BEAUMONT, N.J. et al. (2008) Economic valuation for the conservation of marine biodiversity. *Marine Pollution Bulletin*, 56(3), pp. 386–396.

BEKKBY, T. et al. (2014) Length, strength and water flow: Relative importance of wave and current exposure on morphology in kelp Laminaria hyperborea. *Marine Ecology Progress Series*, 506, pp. 61–70.

BEKKBY, T. et al. (2009) Spatial predictive distribution modelling of the kelp species Laminaria hyperborea. *ICES Journal of Marine Science*, 66(10), pp. 2106–2115.

BEKKBY, T. et al. (2019) The abundance of kelp is modified by the combined impact of depth, waves and currents. *Frontiers in Marine Science*, 6(JUL), pp. 1–10.

BELL, M. and WALKER, M.J.C. (2014) Late Quaternary Environmental Change. *Late Quaternary Environmental Change*, [Online] Available from: doi.org/10.4324/9781315847740.

BENGTSSON, M.M. et al. (2012) Bacterial diversity in relation to secondary production and succession on surfaces of the kelp Laminaria hyperborea. *ISME Journal*, 6(12), pp. 2188–2198.

BENGTSSON, M.M. and ØVREÅS, L. (2010) Planctomycetes dominate biofilms on surfaces of the kelp Laminaria hyperborea.

DE BETTIGNIES, T. et al. (2013) Contrasting mechanisms of dislodgement and erosion contribute to production of kelp detritus. *Limnology and Oceanography*, 58(5), pp. 1680–1688.

BIRKETT, D.A. et al. (1998) *Infralittoral Reef Biotipes with Kelp Species. An overview of dynamic and sensivity characteristics for conservation management of marine SACs.*

BOLTON, J.J. (2010) The biogeography of kelps (Laminariales, Phaeophyceae): A global analysis with new insights from recent advances in molecular phylogenetics. *Helgoland Marine Research*, 64(4), pp. 263–279.

BOLTON, J.J. and LÜNING, K. (1982) Optimal growth and maximal survival temperatures of Atlantic Laminaria species (Phaeophyta) in culture. *Marine Biology*, 66(1), pp. 89–94.

BONDOSO, J. et al. (2017) Epiphytic Planctomycetes communities associated with three main groups of macroalgae. *FEMS Microbiology Ecology*, 93(3), pp. 1–9.

BONTHOND, G. et al. (2020) How do microbiota associated with an invasive seaweed vary across scales? *Molecular Ecology*, 29(11), pp. 2094–2108.

BRIAND, J.F. et al. (2017) Spatio-Temporal Variations of Marine Biofilm Communities Colonizing Artificial Substrata Including Antifouling Coatings in Contrasted French Coastal Environments. *Microbial Ecology*, 74(3), pp. 585–598.

BUÉ, M. et al. (2020) Multiple-scale interactions structure macroinvertebrate assemblages associated with kelp understory algae. *Diversity and Distributions*.

BURGER, J. et al. (2007) Kelp as a bioindicator: Does it matter which part of 5 m long plant is used for metal analysis? *Environmental Monitoring and Assessment*, 128(1–3), pp. 311–321.

BURGUNTER-DELAMARE, B. et al. (2023) The Saccharina latissima microbiome: Effects of region, season, and physiology. *Frontiers in Microbiology*, 13(January), [Online] Available from: doi.org/10.3389/fmicb.2022.1050939.

BURKE, C. et al. (2011) Composition, uniqueness and variability of the epiphytic bacterial community of the green alga Ulva australis. *ISME Journal*, 5(4), pp. 590–600.

BURROWS, M.T. (2012) Influences of wave fetch, tidal flow and ocean colour on subtidal rocky communities. *Marine Ecology Progress Series*, 445, pp. 193–207.

BURROWS, M.T. (2020) *Wave fetch GIS layers for the UK and Ireland at 200m scale. figshare. Dataset.*

BURTON, M. et al. (2019) Skomer Marine Conservation Zone Distribution & Abundance of. (397), [Online] Available from: https://cdn.naturalresources.wales/media/688718/skomer-eel-grass-zostera-marina-report-2018-final.pdf.

CALLAHAN, B.J. et al. (2016) Bioconductor workflow for microbiome data analysis: From raw reads to community analyses. *F1000Research*, 5(3), pp. 1–48.

CHAO, A. (1984) Nonparametric Estimation of the Number of Classes in a Population. *Scandinavian Journal of Statistics*, 11(4), pp. 265–270.

CHRISTIE, H. et al. (2003) Species distribution and habitat exploitation of fauna associated with kelp (Laminaria hyperborea) along the Norwegian coast. *Journal of the Marine Biological Association of the United Kingdom*, 83(4), pp. 687–699.

CLARKE, K.R. and GORLEY, R.N. (2015) PRIMER v7; PRIMER-E: Plymouth. [Online] Available from: https://www.primer-e.com/our-software/primer-version-7/.

COCLET, C. et al. (2020) Impacts of copper and lead exposure on prokaryotic communities from contaminated contrasted coastal seawaters: The influence of previous metal exposure. *FEMS Microbiology Ecology*, 96(6), pp. 1–11.

COCLET, C. et al. (2021) Trace Metal Contamination Impacts Predicted Functions More Than Structure of Marine Prokaryotic Biofilm Communities in an Anthropized Coastal Area. *Frontiers in Microbiology*, 12(February), pp. 1–16.

COMELY, C.A. and ANSELL, A.D. (1988) Population density and growth of Echinus esculentus L. on the Scottish west coast. *Estuarine, Coastal and Shelf Science*, 27(3), pp. 311–334.

CONNELL, S.D. (2005) Assembly and maintenance of subtidal habitat heterogeneity: Synergistic effects of light penetration and sedimentation. *Marine Ecology Progress Series*, 289, pp. 53–61.

CONNELL, S.D. et al. (2008) Recovering a lost baseline: Missing kelp forests from a metropolitan coast. *Marine Ecology Progress Series*, 360, pp. 63–72.

CONTRERAS, L. et al. (2007) Effects of copper on early developmental stages of Lessonia nigrescens Bory (Phaeophyceae). *Environmental Pollution*, 145(1), pp. 75–83.

CONTRERAS-PORCIA, L. et al. (2023) Expansion of marine pollution along the coast: Negative effects on kelps and contamination transference to benthic herbivores? *Marine Environmental Research*, 192(October), [Online] Available from: doi.org/10.1016/j.marenvres.2023.106229.

COOPER, N. et al. (2017) Changing coastlines in NE England: A legacy of colliery spoil tipping and the effects of its cessation. *Proceedings of the Yorkshire Geological Society*, 61(3), pp. 217–229.

DANG, H. and LOVELL, C.R. (2016) Microbial Surface Colonization and Biofilm Development in Marine Environments. *Microbiology and Molecular Biology Reviews*, 80(1), pp. 91–138.

DAYTON, P.K. (1985) Ecology of kelp communities. *Annual review of ecology and systematics. Vol. 16*, (63), pp. 215–245.

DEREGIBUS, D. et al. (2023) Potential macroalgal expansion and blue carbon gains with northern Antarctic Peninsula glacial retreat. *Marine Environmental Research*, 189(April), p. 106056.

DESMOND, M.J., PRITCHARD, D.W. and HEPBURN, C.D. (2015) Light limitation within southern New Zealand kelp forest communities. *PLoS ONE*, 10(4), pp. 1–18.

DIECK, I.T. (1992) North Pacific and North Atlantic digitate Laminaria species (Phaeophyta): hybridization experiments and temperature responses. *Phycologia*, 31(2), pp. 147–163.

DOGS, M. et al. (2017) Rhodobacteraceae on the marine brown alga Fucus spiralis are abundant and show physiological adaptation to an epiphytic lifestyle. *Systematic and Applied Microbiology*, 40(6), pp. 370–382.

DREW, A. (1983) Physiology of Laminaria. *Marine Ecology*, 4(3), pp. 227–250.

DUARTE, C.M. et al. (2013) The role of coastal plant communities for climate change mitigation and adaptation. *Nature Climate Change*, 3(11), pp. 961–968.

DUARTE, C.M. and CEBRIÁN, J. (1996) The fate of marine autotrophic production. *Limnology and Oceanography*, 41(8), pp. 1758–1766.

DURUCAN, S., JOZEFOWICZ, R. and BRENKLEY, D. (2010) Extracting the Science. A Century of Mining Research. In: JURGEN, B. (ed.) Colorado: Society for Mining, Mettalurgy, and Exploration, Inc. (SME), pp. 10–22.

EAGLE, R.A. et al. (1979) The Field Assessment of Effects of Dumping Wastes at Sea: 5 The disposal of solid wastes off the north-east coast of England. Fisheries Research Tehcnical Report No. 51.

EARP, H.S., SMALE, D.A., KING, N.G., et al. (2024) Spatial and temporal variation in the diversity and structure of understorey macrofaunal assemblages within Laminaria hyperborea forests in the northeast Atlantic. *Journal of Experimental Marine Biology and Ecology*, 578(March), p. 152034.

EARP, H.S., SMALE, D.A., ALMOND, P.M., et al. (2024) Temporal variation in the structure, abundance, and composition of Laminaria hyperborea forests and their associated understorey assemblages over an intense storm season. *Marine Environmental Research*, 200(July), p. 106652.

EDWARDS, A. (1980) Ecological studies of the kelp, laminaria hyperborea, and its associated fauna in south-west Ireland. *Ophelia*, 19(1), pp. 47–60.

EDWARDS, P. (1975) An assessment of possible pollution effects over a century on the benthic marine algae of Co. Durham, England. *Botanical Journal of the Linnean Society*, 70(4), pp. 269–305.

EGAN, S. and GARDINER, M. (2016) Microbial dysbiosis: Rethinking disease in marine ecosystems. *Frontiers in Microbiology*, 7(JUN), pp. 1–8.

ELLIOTT SMITH, E.A. and FOX, M.D. (2022) Characterizing energy flow in kelp forest food webs: a geochemical review and call for additional research. *Ecography*, 2022(6), pp. 1–16.

ELLIS, D. V. and HOOVER, P.M. (1990) Benthos on tailings beds from an abandoned coastal mine. *Marine Pollution Bulletin*, 21(10), pp. 477–480.

EVANS, L.K. and EDWARDS, M.S. (2011) Bioaccumulation of copper and zinc by the giant kelp Macrocystis pyrifera. *Algae*, 26(3), pp. 265–275.

FILBEE-DEXTER, K. et al. (2024) Carbon export from seaweed forests to deep ocean sinks. *Nature Geoscience*, 17(6), pp. 552–559.

FILBEE-DEXTER, K. et al. (2018) Movement of pulsed resource subsidies from kelp forests to deep fjords. *Oecologia*, 187(1), pp. 291–304.

FILBEE-DEXTER, K., FEEHAN, C.J. and SCHEIBLING, R.E. (2016) Large-scale degradation of a kelp ecosystem in an ocean warming hotspot. *Marine Ecology Progress Series*, 543, pp. 141–152.

FILBEE-DEXTER, K. and WERNBERG, T. (2018) Rise of Turfs: A New Battlefront for Globally Declining Kelp Forests. *BioScience*, 68(2), pp. 64–76.

FOX, J., WEISBERG, S. and PRICE, B. (2001) car: Companion to Applied Regression. *CRAN: Contributed Packages*, [Online] Available from: doi.org/10.32614/CRAN.package.car.

FREDRIKSEN, S. et al. (1995) Spore dispersal in Laminaria hyperborea (Laminariales, Phaeophyceae). *Sarsia*, 80(1), pp. 47–53.

FURNESS, R.W. and RAINBOW, P.S. (2018) *Heavy metals in the marine environment*.

GARRARD, S.L. and BEAUMONT, N.J. (2014) The effect of ocean acidification on carbon storage and sequestration in seagrass beds; a global and UK context. *Marine Pollution Bulletin*, 86(1–2), pp. 138–146.

GORMAN, D. et al. (2013) Modeling kelp forest distribution and biomass along temperate rocky coastlines. *Marine Biology*, 160(2), pp. 309–325.

GOURAGUINE, A. et al. (2024) Temporal and spatial drivers of the structure of macroinvertebrate assemblages associated with Laminaria hyperborea detritus in the northeast Atlantic. *Marine Environmental Research*, 198(February), [Online] Available from: doi.org/10.1016/j.marenvres.2024.106518.

GRIFFITHS, S.M. et al. (2019) Host genetics and geography influence microbiome composition in the sponge Ircinia campana. *Journal of Animal Ecology*, 88(11), pp. 1684–1695.

GUNDERSEN, H. et al. (2021) Variation in Population Structure and Standing Stocks of Kelp Along Multiple Environmental Gradients and Implications for Ecosystem Services. *Frontiers in Marine Science*, 8(April), pp. 1–19.

GUTT, W. et al. (1974) Survey of the Locations, Disposal and Prospective Uses of the Major Industrial By-Products and Waste Materials. *Building Research Establishment*.

HAGEN, N.T. (1983) Destructive grazing of kelp beds by sea urchins in Vestfjorden, Northern Norway. *Sarsia*, 68(3), pp. 177–190.

HARFOOT, M.B.J. et al. (2018) Present and future biodiversity risks from fossil fuel exploitation. *Conservation Letters*, 11(4), pp. 1–13.

HARGRAVE, M.S. et al. (2017) The effects of warming on the ecophysiology of two co-existing kelp species with contrasting distributions. *Oecologia*, 183(2), pp. 531–543.

HARLEY, C.D.G. et al. (2012) Effects Of Climate Change On Global Seaweed Communities. *Journal of Phycology*, 48(5), pp. 1064–1078.

HARROLD, C., WATANABE, J. and LISIN, S. (1988) Spatial Variation in the Structure of Kelp Forest Communities Along a Wave Exposure Gradient. *Marine Ecology*, 9(2), pp. 131–156.

HILL, R. et al. (2015) Can macroalgae contribute to blue carbon? An Australian perspective. *Limnology and Oceanography*, 60(5), pp. 1689–1706.

HISCOCK, K. (1992) The ecology and conservation of sublittoral hard substratum ecosystems in Scotland. *Proceedings - Royal Society of Edinburgh, Section B*, 100(May 2015), pp. 95–112.

HJORLEIFSSON, E., KASSA, O. and GUNNARSSON, K. (1995) Grazing of kelp by green sea urchins in Eyyjafjordu, North Iceland. *Ecology of fjords and coastal waters*, pp. 593–597.

HOBBS, R.J., HIGGS, E. and HARRIS, J.A. (2009) Novel ecosystems: implications for conservation and restoration. *Trends in Ecology and Evolution*, 24(11), pp. 599–605.

HOBDAY, A.J. (2000) Macrocystis pyrifera rafts in the Southern California Bight. *Journal of Experimental Marine Biology and Ecology*, 253(1), pp. 75–96.

HOPKIN, R. and KAIN, J.M. (1978) The effects of some pollutants on the survival, growth and respiration of Laminaria hyperborea. *Estuarine and Coastal Marine Science*, 7(6), pp. 531–553.

HOWARD, J. et al. (2017) Clarifying the role of coastal and marine systems in climate mitigation. *Frontiers in Ecology and the Environment*, 15(1), pp. 42–50.

HUOVINEN, P., LEAL, P. and GMEZ, I. (2010) Interacting effects of copper, nitrogen and ultraviolet radiation on the physiology of three south Pacific kelps. *Marine and Freshwater Research*, 61(3), pp. 330–341.

HURD, C.L. (2000) Water motion, marine macroalgal physiology, and production. *Journal of Phycology*, 36(3), pp. 453–472.

HYDRAULICS RESEARCH STATION (1970) Colliery waste on the Durham coast. A study of the effect of tipping colliery waste on the coastal processes (EX 521).

HYSLOP, B.T. et al. (1997) Effects of colliery waste on littoral communities in north-east England. *Environmental Pollution*, 96(3), pp. 383–400.

IHUA, M.W. et al. (2020) Diversity of bacteria populations associated with different thallus regions of the brown alga Laminaria digitata. *PLoS ONE*, 15(11 November), pp. 1–15.

IHUA, M.W. et al. (2019) Microbial population changes in decaying ascophyllum nodosum result in macroalgal- polysaccharide-degrading bacteria with potential applicability in enzyme-assisted extraction technologies. *Marine Drugs*, 17(4), pp. 1–20.

IPCC (2023) Sections. In: Climate Change 2023: Synthesis Report. Contribution of Working Groups I, II and III to the Sixth Assessment Report of the Intergovernmental Panel on Climate Change [Core Writing Team, H. Lee and J. Romero (eds.)]. *Climate Change 2023: Synthesis Report*, IPCC(Geneva, Switzerland), pp. 35–115.

JACKSON-BUE, M. et al. (2023) Spatial variability in the structure of fish assemblages associated with Laminaria hyperborea forests in the NE Atlantic. *Journal of Experimental Marine Biology and Ecology*, 564(March), [Online] Available from: doi.org/10.1016/j.jembe.2023.151899.

JARA-YÁÑEZ, R. et al. (2021) Negative consequences on the growth, morphometry, and community structure of the kelp macrocystis pyrifera (Phaeophyceae, ochrophyta) by a short pollution pulse of heavy metals and pahs. *Toxics*, 9(8), [Online] Available from: doi.org/10.3390/toxics9080190.

JAYATHILAKE, D.R.M. and COSTELLO, M.J. (2021) Version 2 of the world map of laminarian kelp benefits from more Arctic data and makes it the largest marine biome. *Biological Conservation*, 257(April), [Online] Available from: doi.org/10.1016/j.biocon.2021.109099.

JOHNSON, L.J. and FRID, C.L.J. (1995) The recovery of benthic communities along the County Durham coast after cessation of colliery spoil dumping. *Marine Pollution Bulletin*, 30(3), pp. 215–220.

JOHNSON, M. and HART, P. (2001) Preliminary report of the coastal fisheries around the coasts of the British Isles 1950–1999. Fisheries impacts on North Atlantic ecosystems: catch, effort and national/regional datasets. *Fisheries Centre Research Reports*, pp. 135–140.

JONES, A.A. and ELLIS, D. V (1976) Sub-Obliterative Effects of Mine-Tailing on Marine Infaunal Benthos. 5, pp. 299–307.

JONES, D.J. (1972) Changes in the ecological balance of invertebrate communities in kelp holdfast habitats of some polluted North Sea waters. *Helgoländer Wissenschaftliche Meeresuntersuchungen*, 23(2), pp. 248–260.

JONES, D.J. (1973) Variation in the trophic structure and species composition of some invertebrate communities in polluted kelp forests in the North Sea. *Marine Biology*, 20(4), pp. 351–365.

JONES, N.S. and KAIN, J.M. (1967) Subtidal algal colonisation following removal of Echinus. *Helgoland Marine Research*, 15, pp. 460–466.

JUPP, B.P. and DREW, E.A. (1974) Studies on the growth of LAminaria hyperborea (Gunn.) Fosl. I. Biomass and productivity. *Journal of Experimental Marine Biology and Ecology*, 15(2), pp. 185–196.

KAIN, J.M. (1971) Aspects of the biology of Laminaria hyperborea. *Journal of Invertebrate Pathology*, 18(3), p. 430.

KAIN, J.M. and JONES, N.S. (1963) Aspects of the Biology of Laminaria Hyperborea : II. Age, Weight and Length. *Journal of the Marine Biological Association of the United Kingdom*, 43(1), pp. 129–151.

KAIN, J.M. and JONES, N.S. (1976) The biology of laminaria hyperborea ix. growth pattern of fronds. *Journal of the Marine Biological Association of the United Kingdom*, 56(3), pp. 603–628.

KAIN, J.M. and JONES, N.S. (1977) The biology of laminaria hyperborea x. The effect of depth on some populations. *Journal of the Marine Biological Association of the United Kingdom*, 57(3), pp. 587–607.

KANG, I., LIM, Y. and CHO, J.C. (2018) Complete genome sequence of Granulosicoccus antarcticus type strain IMCC3135T, a marine gammaproteobacterium with a putative dimethylsulfoniopropionate demethylase gene. *Marine Genomics*, 37(November 2017), pp. 176–181.

KASSAMBARA, A. (2016) ggpubr: 'ggplot2' Based Publication Ready Plots. *CRAN: Contributed Packages*, [Online] Available from: doi.org/10.32614/CRAN.package.ggpubr.

KASSAMBARA, A. (2019) rstatix: Pipe-Friendly Framework for Basic Statistical Tests. *CRAN: Contributed Packages*, [Online] Available from: doi.org/10.32614/CRAN.package.rstatix.

KING, N.G. et al. (2022) Consistency and Variation in the Kelp Microbiota: Patterns of Bacterial Community Structure Across Spatial Scales. *Microbial Ecology*, (0123456789), [Online] Available from: doi.org/10.1007/s00248-022-02038-0.

KING, N.G. et al. (2020) Ecological performance differs between range centre and trailing edge populations of a cold-water kelp: implications for estimating net primary productivity. *Marine Biology*, 167(9), pp. 1–12.

KING, N.G. et al. (2021) Multiscale spatial variability in epibiont assemblage structure associated with stipes of kelp Laminaria hyperborea in the northeast Atlantic. *Marine Ecology Progress Series*, 672(Stachowicz 2001), pp. 33–44.

KOZICH, J.J. et al. (2013) Development of a dual-index sequencing strategy and curation pipeline for analyzing amplicon sequence data on the miseq illumina sequencing platform. *Applied and Environmental Microbiology*, 79(17), pp. 5112–5120.

KRAUSE-JENSEN, D. and DUARTE, C.M. (2016) Substantial role of macroalgae in marine carbon sequestration. *Nature Geoscience*, 9(10), pp. 737–742.

KRUMHANSL, K.A. et al. (2016) Global patterns of kelp forest change over the past half-century. *Proceedings of the National Academy of Sciences of the United States of America*, 113(48), pp. 13785–13790.

KRUMHANSL, K.A., LEE, J.M. and SCHEIBLING, R.E. (2011) Grazing damage and encrustation by an invasive bryozoan reduce the ability of kelps to withstand breakage by waves. *Journal of Experimental Marine Biology and Ecology*, 407(1), pp. 12–18.

KRUMHANSL, K.A. and SCHEIBLING, R.E. (2012) Production and fate of kelp detritus. *Marine Ecology Progress Series*, 467, pp. 281–302.

LAYCOCK, R.A. (1974) The detrital food chain based on seaweeds. I. Bacteria associated with the surface of Laminaria fronds. *Marine Biology*, 25(3), pp. 223–231.

LEAL, P.P. et al. (2018) Copper pollution exacerbates the effects of ocean acidification and warming on kelp microscopic early life stages. *Scientific Reports*, 8(1), pp. 1–13.

LEBLANC, M. et al. (2000) 4,500-year-old mining pollution in southwestern Spain: Long-term implications for modern mining pollution. *Economic Geology*, 95(3), pp. 655–661.

LECLERC, J. et al. (2023) Distribution of functionally distinct native and non-indigenous species within marine urban habitats. *Diversity and Distributions*, 29(11), pp. 1445–1457.

LECLERC, J.C. et al. (2015) Community, trophic structure and functioning in two contrasting Laminaria hyperborea forests. *Estuarine, Coastal and Shelf Science*, 152, pp. 11–22.

LEE, J.W. et al. (2008) Bacterial communities in the initial stage of marine biofilm formation on artificial surfaces. *Journal of Microbiology*, 46(2), pp. 174–182.

LELIAERT, F. et al. (2000) Subtidal understorey algal community structure in kelp beds around the Cape Peninsula (Western Cape, South Africa). *Botanica Marina*, 43(4), pp. 359–366.

LEMAY, M.A. et al. (2018) Alternate life history phases of a common seaweed have distinct microbial surface communities. *Molecular Ecology*, 27(17), pp. 3555–3568.

LEMAY, M.A. et al. (2021) Kelp-Associated Microbiota are Structured by Host Anatomy. *Journal of Phycology*, 57(4), pp. 1119–1130.

LI, Z. et al. (2014) A review of soil heavy metal pollution from mines in China: Pollution and health risk assessment. *Science of the Total Environment*, 468–469, pp. 843–853.

LING, S.D. et al. (2009) Overfishing reduces resilience of kelp beds to climate-driven catastrophic phase shift. *Proceedings of the National Academy of Sciences of the United States of America*, 106(52), pp. 22341–22345.

LIU, Y. et al. (2021) A review of water pollution arising from agriculture and mining activities in Central Asia: Facts, causes and effects. *Environmental Pollution*, 291(September), p. 118209.

MALIK, A., LAN, J. and LENZEN, M. (2016) Trends in Global Greenhouse Gas Emissions from 1990 to 2010. *Environmental Science and Technology*, 50(9), pp. 4722–4730.

MANN, K.H. (1973) Seaweeds: Their productivity and strategy for growth. *Science*, 182(4116), pp. 975–981.

MCMURDIE, P.J. and HOLMES, S. (2013) Phyloseq: An R Package for Reproducible Interactive Analysis and Graphics of Microbiome Census Data. *PLoS ONE*, 8(4), [Online] Available from: doi.org/10.1371/journal.pone.0061217.

MINICH, J.J. et al. (2018) Elevated temperature drives kelp microbiome dysbiosis, while elevated carbon dioxide induces water microbiome disruption. *PLoS ONE*, 13(2), pp. 1–23.

MONTEIRO, J.P. et al. (2020) The unique lipidomic signatures of saccharina latissima can be used to pinpoint their geographic origin. *Biomolecules*, 10(1), [Online] Available from: doi.org/10.3390/biom10010107.

MOORE, P.G. (1972) Particulate matter in the sublittoral zone of an exposed coast and its ecological significance with special reference to the fauna inhabiting kelp holdfasts. *Journal of Experimental Marine Biology and Ecology*, 10(1), pp. 59–80.

MOORE, P.G. (1973) THE KELP FAUNA OF NORTHEAST BRITAIN. II. MULTIVARIATE CLASSIFICATION: TURBIDITY AS AN ECOLOGICAL FACTOR. *J. exp. mar. Biol. Ecol.,* 13, pp. 127–163.

MORAN, M.A. et al. (2012) Genomic insights into bacterial DMSP transformations. *Annual Review of Marine Science*, 4, pp. 523–542.

MORRIS, D.J. et al. (2018) Over 10 million seawater temperature records for the United Kingdom Continental Shelf between 1880 and 2014 from 17 Cefas (United Kingdom government) marine data systems. *Earth System Science Data*, 10(1), pp. 27–51.

MORRIS, R.L. et al. (2020) Kelp beds as coastal protection: Wave attenuation of Ecklonia radiata in a shallow coastal bay. *Annals of Botany*, 125(2), pp. 235–246.

MOY, F.E. and CHRISTIE, H. (2012) Large-scale shift from sugar kelp (Saccharina latissima) to ephemeral algae along the south and west coast of Norway. *Marine Biology Research*, 8(4), pp. 309–321.

MUDD, G.M. (2007) Sustainability and Mine Waste Management – A Snapshot of Mining Waste Issues. *Waste Management & Infrastructure Conference - IIR Conferences*, (January), pp. 1–12.

MÜLLER, R. et al. (2009) Impact of oceanic warming on the distribution of seaweeds in polar and cold-temperate waters. *Botanica Marina*, 52(6), pp. 617–638.

NEWELL, R., FIELD, J. and GRIFFITHS, C. (1982) Energy Balance and Significance of Microorganisms in a Kelp Bed Community. *Marine Ecology Progress Series*, 8, pp. 103–113.

NORDERHAUG, K.M. et al. (2012) Does the diversity of kelp forest macrofauna increase with wave exposure? *Journal of Sea Research*, 69, pp. 36–42.

NORDERHAUG, K.M. et al. (2005) Fish-macrofauna interactions in a kelp (Laminaria hyperborea) forest. *Journal of the Marine Biological Association of the United Kingdom*, 85(5), pp. 1279–1286.

NORDERHAUG, K.M., FREDRIKSEN, S. and NYGAARD, K. (2003) To Kelp Forest Consumers and the Importance of Bacterial Degradation To Food Quality. *Marine Ecology Progress Series*, 255, pp. 135–144.

OJEDA, F.P. and SANTELICES, B. (1984) Invertebrate communities in holdfasts of the kelp Macrocystis pyrifera from southern Chile. 16(1), pp. 65–73.

ORLAND, C. et al. (2016) Application of computer-aided tomography techniques to visualize kelp holdfast structure reveals the importance of habitat complexity for supporting marine biodiversity. *Journal of Experimental Marine Biology and Ecology*, 477, pp. 47–56.

OTERO-FERRER, F. et al. (2020) Effect of depth and seasonality on the functioning of rhodolith seabeds. *Estuarine, Coastal and Shelf Science*, 235(December 2019), p. 106579.

OVERNELL, J. and YOUNG, S. (1995) Sedimentation and carbon flux in a scottish sea loch, loch linnhe. *Estuarine, Coastal and Shelf Science*, 41(3), pp. 361–376.

OYARZO-MIRANDA, C. et al. (2020) Coastal pollution from the industrial park Quintero bay of central Chile: Effects on abundance, morphology, and development of the kelp Lessonia spicata (Phaeophyceae). *PLoS ONE*, 15(10 October), pp. 1–24.

PAIX, B. et al. (2021) Integration of spatio-temporal variations of surface metabolomes and epibacterial communities highlights the importance of copper stress as a major factor shaping host-microbiota interactions within a Mediterranean seaweed holobiont. pp. 1–19.

PALUMBO-ROE, B. and COLMAN, T. (2010) The nature of waste associated with closed mines in England and Wales Minerals & Waste Programme. *British Geolofical Survey Open Report.*

PARROT, D. et al. (2019) Mapping the Surface Microbiome and Metabolome of Brown Seaweed Fucus vesiculosus by Amplicon Sequencing, Integrated Metabolomics and Imaging Techniques. *Scientific Reports*, 9(1), pp. 1–17.

PEDERSEN, M.F. et al. (2020) Detrital carbon production and export in high latitude kelp forests. *Oecologia*, 192(1), pp. 227–239.

PEDERSEN, M.F. et al. (2012) Effects of wave exposure on population structure, demography, biomass and productivity of the kelp Laminaria hyperborea. *Marine Ecology Progress Series*, 451(Kain 1971), pp. 45–60.

PÉREZ-MATUS, A. et al. (2007) Community structure of temperate reef fishes in kelp-dominated subtidal habitats of northern Chile. *Marine And Freshwater Research*, pp. 1069–1085.

PESSARRODONA, A. et al. (2018) Carbon assimilation and transfer through kelp forests in the NE Atlantic is diminished under a warmer ocean climate. *Global Change Biology*, 24(9), pp. 4386–4398.

PESSARRODONA, A., FOGGO, A. and SMALE, D.A. (2019) Can ecosystem functioning be maintained despite climate-driven shifts in species. *Journal of Ecology*, (107), pp. 91–104.

PFISTER, C.A., ALTABET, M.A. and WEIGEL, B.L. (2019) Kelp beds and their local effects on seawater chemistry, productivity, and microbial communities. *Ecology*, 100(10), pp. 1–15.

PHELPS, C.M. et al. (2021) The surface bacterial community of an Australian kelp shows cross-continental variation and relative stability within regions. *FEMS Microbiology Ecology*, 97(7), pp. 1–14.

PINHO, D. et al. (2016) Spatial and temporal variation of kelp forests and associated macroalgal assemblages along the Portuguese coast. *Marine and Freshwater Research*, 67(1), pp. 113–122.

PINSKY, M.L., GUANNEL, G. and ARKEMA, K.K. (2013) Quantifying wave attenuation to inform coastal habitat conservation. *Ecosphere*, 4(8), [Online] Available from: doi.org/10.1890/ES13-00080.1.

POSFORD DUVIVIER (1993) Durham Coast Management Plan – Issues Statement. Report to the Durham Coast Management Plan Steering Committee, 1993.

PROVOST, E.J. et al. (2017) Climate-driven disparities among ecological interactions threaten kelp forest persistence. *Global Change Biology*, 23(1), pp. 353–361.

QUAST, C. et al. (2013) The SILVA ribosomal RNA gene database project: Improved data processing and web-based tools. *Nucleic Acids Research*, 41(D1), pp. 590–596.

QUEIRÓS, A.M. et al. (2023) Identifying and protecting macroalgae detritus sinks toward climate change mitigation. *Ecological Applications*, 33(3), pp. 1–16.

RAMIREZ-LLODRA, E. et al. (2016) A snap shot of the short-term response of crustaceans to macrophyte detritus in the deep Oslofjord. *Scientific Reports*, 6(0349), pp. 1–5.

RAMÍREZ-PUEBLA, S.T. et al. (2022) Spatial organization of the kelp microbiome at micron scales. *Microbiome*, 10(1), pp. 1–20.

RASSWEILER, A. et al. (2018) Improved estimates of net primary production, growth, and standing crop of Macrocystis pyrifera in Southern California. *Ecology*, 99(9), p. 2132.

REED, D.C. and BRZEZINSKI, M.A. (2009) *Kelp forests. In D. Laffoley & G. Grimsditch (Eds.), The Management of Natural Coastal Carbon Sinks*. Gland, Sweden: IUCN.

RINDE, E. and SJØTUN, K. (2005) Demographic variation in the kelp Laminaria hyperborea along a latitudinal gradient. *Marine Biology*, 146(6), pp. 1051–1062.

RSTUDIO TEAM (2022) RStudio: Integrated Development Environment for R. [Online] Available from: http://www.rstudio.com/.

SAGARIN, R.D., GAINES, S.D. and GAYLORD, B. (2006) Moving beyond assumptions to understand abundance distributions across the ranges of species. *Trends in Ecology and Evolution*, 21(9), pp. 524–530.

SCHEIBLING, R.E. and HATCHER, B.G. (2013) Strongylocentrotus droebachiensis. *Developments in Aquaculture and Fisheries Science*, 38, pp. 381–412.

SCHEIBLING, R.E., HENNIGAR, A.W. and BALCH, T. (1999) Destructive grazing, epiphytism, and disease: The dynamics of sea urchin - kelp interactions in Nova Scotia. *Canadian Journal of Fisheries and Aquatic Sciences*, 56(12), pp. 2300–2314.

SCHERNER, F., BONOMI BARUFI, J. and HORTA, P.A. (2012) Photosynthetic response of two seaweed species along an urban pollution gradient: Evidence of selection of pollution-tolerant species. *Marine Pollution Bulletin*, 64(11), pp. 2380–2390.

SCHIEL, D.R., STEINBECK, J.R. and FOSTER, M.S. (2014) Ten Years of Induced Ocean Warming Causes Comprehensive. *Ecology*, 85(7), pp. 1833–1839.

SCHIENER, P. et al. (2015) The seasonal variation in the chemical composition of the kelp species Laminaria digitata, Laminaria hyperborea, Saccharina latissima and Alaria esculenta. *Journal of Applied Phycology*, 27(1), pp. 363–373.

SCHOENROCK, K.M. et al. (2020) Genetic diversity of a marine foundation species, Laminaria hyperborea (Gunnerus) Foslie, along the coast of Ireland. *European Journal of Phycology*, 55(3), pp. 310–326.

SCHOSCHINA, E. V. (1997) On laminaria hyperborea (laminariales, phaeophyceae) on the murman coast of the barents sea. *Sarsia*, 82(4), pp. 371–373.

SHEPPARD, C. (1976) The holdfast ecosystem of laminaria hyprborea (gunn ,) fosl . and environmental monitoring : an ecological study.

SHEPPARD, C., BELLAMY, D.J. and SHEPPARD, A.L.S. (1980) Study of the fauna inhabiting the holdfasts of Laminaria hyperborea (gunn.) fosl. along some environmental and geographical gradients. *Marine Environmental Research*, 4(1), pp. 25–51.

SINGH, R.P. and REDDY, C.R.K. (2016) Unraveling the functions of the macroalgal microbiome. *Frontiers in Microbiology*, 6(JAN), pp. 1–8.

SIVERTSEN, K. (1997) Geographic and environmental factors affecting the distribution of kelp beds and barren grounds and changes in biota associated with kelp reduction at sites along the Norwegian coast. *Canadian Journal of Fisheries and Aquatic Sciences*, 54(12), pp. 2872–2887.

SJØTUN, K. et al. (1993) Population studies of Laminaria hyperborea from its northern range of distribution in Norway. *Hydrobiologia*, 260–261(1), pp. 215–221.

SJØTUN, K., CHRISTIE, H. and FOSSÅ, J.H. (2006) The combined effect of canopy shading and sea urchin grazing on recruitment in kelp forest (Laminaria hyperborea). *Marine Biology Research*, 2(1), pp. 24–32.

SJØTUN, K. and FREDRIKSEN, S. (1995) Growth allocation in Laminaria hyperborea. *Marine Ecology Progress Series*, 126(1971), pp. 213–222.

SJØTUN, K., FREDRIKSEN, S. and RUENESS, J. (1998) Effect of canopy biomass and wave exposure on growth in laminaria hyperborea (laminariaceae: Phaeophyta). *European Journal of Phycology*, 33(4), pp. 337–343.

SMALE, D.A. et al. (2020) Environmental factors influencing primary productivity of the forest-forming kelp Laminaria hyperborea in the northeast Atlantic. *Scientific Reports*, 10(1), pp. 1–12.

SMALE, D.A., PESSARRODONA, A., et al. (2022) Examining the production, export, and immediate fate of kelp detritus on open-coast subtidal reefs in the Northeast Atlantic. *Limnology and Oceanography*, 67(S2), pp. S36–S49.

SMALE, D.A. (2020) Impacts of ocean warming on kelp forest ecosystems. *New Phytologist*, 225(4), pp. 1447–1454.

SMALE, D.A. et al. (2016) Linking environmental variables with regionalscale variability in ecological structure and standing stock of carbon within UK kelp forests. *Marine Ecology Progress Series*, 542, pp. 79–95.

SMALE, D.A. et al. (2019) Marine heatwaves threaten global biodiversity and the provision of ecosystem services. *Nature Climate Change*, 9(4), pp. 306–312.

SMALE, D.A., KING, N.G., et al. (2022) Quantifying use of kelp forest habitat by commercially important crustaceans in the United Kingdom. *Journal of the Marine Biological Association of the United Kingdom*, 102(8), pp. 627–634.

SMALE, D.A. et al. (2015) The rise of Laminaria ochroleuca in the Western English Channel (UK) and comparisons with its competitor and assemblage dominant Laminaria hyperborea. *Marine Ecology*, 36(4), pp. 1033–1044.

SMALE, D.A. et al. (2013) Threats and knowledge gaps for ecosystem services provided by kelp forests: A northeast Atlantic perspective. *Ecology and Evolution*, 3(11), pp. 4016–4038.

SMALE, D.A. and MOORE, P.J. (2017) Variability in kelp forest structure along a latitudinal gradient in ocean temperature. *Journal of Experimental Marine Biology and Ecology*, 486, pp. 255–264.

SMALE, D.A. and VANCE, T. (2016) Climate-driven shifts in species' distributions may exacerbate the impacts of storm disturbances on North-east Atlantic kelp forests. *Marine and Freshwater Research*, 67(1), pp. 65–74.

SMITH, K.E. et al. (2022) Examining the influence of regional-scale variability in temperature and light availability on the depth distribution of subtidal kelp forests. *Limnology and Oceanography*, 67(2), pp. 314–328.

SMITH, S.D.A. (1996a) The effects of domestic sewage effluent on marine communities at Coffs Harbour, New South Wales, Australia. *Marine Pollution Bulletin*, 33(7–12), pp. 309–316.

SMITH, S.D.A. (1996b) The macrofaunal community of Ecklonia radiata holdfasts: Variation associated with sediment regime, sponge cover and depth. *Austral Ecology*, 21(3), pp. 144–153.

STAUFENBERGER, T. et al. (2008) Phylogenetic analysis of bacteria associated with Laminaria saccharina. *FEMS Microbiology Ecology*, 64(1), pp. 65–77.

STENECK, R.S. et al. (2002) Kelp forest ecosystems: Biodiversity, stability, resilience and future. *Environmental Conservation*, 29(4), pp. 436–459.

STRATIL, S.B. et al. (2013) Temperature-driven shifts in the epibiotic bacterial community composition of the brown macroalga F ucus vesiculosus. *MicrobiologyOpen*, 2(2), pp. 338–349.

TANAKA, K. et al. (2012) Warming off southwestern japan linked to distributional shifts of subtidal canopy-forming seaweeds. *Ecology and Evolution*, 2(11), pp. 2854–2865.

TEAGLE, H. et al. (2018) Spatial variability in the diversity and structure of faunal assemblages associated with kelp holdfasts (Laminaria hyperborea) in the northeast Atlantic. *PLoS ONE*, 13(7), pp. 1–25.

TEAGLE, H. et al. (2017) The role of kelp species as biogenic habitat formers in coastal marine ecosystems. *Journal of Experimental Marine Biology and Ecology*, 492, pp. 81–98.

TEAM, R.C. (2022) R: A language and environment for statistical computing. R Foundation for Statistical Computing, Vienna, Austria. *URL https://www.R-project.org/.*

TREVATHAN-TACKETT, S.M. et al. (2015) Comparison of marine macrophytes for their contributions to blue carbon sequestration. *Ecology*, 96(11), pp. 3043–3057.

TSIAMIS, K. et al. (2020) Macroalgal vegetation on a north European artificial reef (Loch Linnhe, Scotland): biodiversity, community types and role of abiotic factors. *Journal of Applied Phycology*, 32(2), pp. 1353–1363.

TYLER-WALTERS, H. (2007) Laminaria hyperborea. Tangle or cuvie. *MARLIN*.

UNITED NATIONS (2022) World Populaton Prospects: The 2022 Revision. *Population Divison*.

VANDIEKEN, V. et al. (2012) Three manganese oxide-rich marine sediments harbor similar communities of acetate-oxidizing manganese-reducing bacteria. *ISME Journal*, 6(11), pp. 2078–2090.

VÁSQUEZ, J.A. et al. (2000) The effects of mining pollution on subtidal habitats of northern Chile. *International Journal of Environment and Pollution*, 13(1–6), pp. 2–25.

VÁZQUEZ-ARIAS, A. et al. (2024) Nanoscale distribution of potentially toxic elements in seaweeds revealed by synchrotron X-ray fluorescence. *Journal of Hazardous Materials*, 480, p. 136454.

WATANABE, J.M. and HARROLD, C. (1991) Destructive grazing by sea urchins Strongylocentrotus spp. in a central California kelp forest: potential roles of recruitment, depth, and predation. *Marine Ecology Progress Series*, 71(2), pp. 125–141.

WEGNER, C.E. et al. (2013) Expression of sulfatases in Rhodopirellula baltica and the diversity of sulfatases in the genus Rhodopirellula. *Marine Genomics*, 9, pp. 51–61.

WEIGEL, B.L. and PFISTER, C.A. (2019) Successional dynamics and seascape-level patterns of microbial communities on the canopy-forming kelps Nereocystis luetkeana and Macrocystis pyrifera. *Frontiers in Microbiology*, 10(FEB), pp. 1–17.

WERNBERG, T. et al. (2013) An extreme climatic event alters marine ecosystem structure in a global biodiversity hotspot. *Nature Climate Change*, 3(1), pp. 78–82.

WERNBERG, T. et al. (2015) Climate-driven regime shift of a temperate marine ecosystem. *Science*, 353(6295), pp. 169–172.

WERNBERG, T. et al. (2024) Impacts of Climate Change on Marine Foundation Species. *Annual Review of Marine Science*, 16, pp. 247–282.

WERNBERG, T. (2021) Marine Heatwave Drives Collapse of Kelp Forests in Western Australia. In: *Ecosystem Collapse and Climate Change*. pp. 325–343.

WHITTICK, A. (1983) Spatial and temporal distributions of dominant epiphytes on the stipes of Laminaria hyperborea (Gunn.) Fosl. (Phaeophyta:Laminariales) in S.E. Scotland. *Journal of Experimental Marine Biology and Ecology*, 73(1), pp. 1–10.

WHITTOCK, A. (1969) *The kelp forest ecosystem at Petticoe Wick Bay lat 55 55'N. Long 2 09'W: an ecological study*. Thesis. Durham University.

WICKHAM, H. (2016) ggplot2: Elegant Graphics for Data Analysis. *Springer-Verlag New York*, ISBN 978-3.

WILDING, C.M. et al. (2023) British Kelp Forest Restoration: Feasibility Report.

WILLIAMS, C. and DAVIES, W. (2019) Valuing the ecosystem service benefits of kelp bed recovery off West Sussex. Report for Sussex IFCA. (September), pp. 1–68.

WILSON, R.J. and HEATH, M.R. (2019) Increasing turbidity in the North Sea during the 20th century due to changing wave climate. *Ocean Science*, 15(6), pp. 1615–1625.

YESSON, C. et al. (2015) The distribution and environmental requirements of large brown seaweeds in the British Isles. *Journal of the Marine Biological Association of the United Kingdom*, 95(4), pp. 669–680.

YOUNGER, P.L. (1993) Possible Environmental Impact of the Closure of Two Collieries in County Durham. *Water and Environment Journal*, 7(5), pp. 521–531.

ZAHN, L.A. et al. (2016) The biogeography and community structure of kelp forest macroinvertebrates. *Marine Ecology*, 37(4), pp. 770–785.

ZOZAYA-VALDÉS, E. et al. (2017) Microbial community function in the bleaching disease of the marine macroalgae Delisea pulchra. *Environmental Microbiology*, 19(8), pp. 3012–3024.

Supplementary materials

Table S2.1. DISTLM testing the relationship between population and individual level kelp metrics and wave fetch in kelp forests at a depth of 5 m BCD between two regions of the UK (A and B; Figure 2.1). Significant values ($p < 0.05$) are indicated in **bold**. Mean wave fetch values can be seen in Table 2.1.

Response Variable	SS	p	R^2
Per m^2			
Canopy density	8.6848	0.2681	0.0271
Total density	1.1369	**0.0015**	0.1938
Total canopy biomass	0.2403	0.1210	0.0422
Per canopy-forming individual			
Stipe length	1.9855	**0.0001**	0.2276
Total length	1.5707	**0.0001**	0.5643
Canopy plant biomass	4.6805	**0.0001**	0.5280
Age	0.8142	0.5275	0.0071

Table S2.2. Maximum depth penetration of kelp forest and individual plants surveyed at sloping gradient sites in two regions of the UK (A and B; Figure 2.1).

Region	Site code	Site name	Max forest depth (m)	Max plant depth (m)
NE England	**A2**	**Northern Hares**	13	15
	A3	**Crumstone**	11	12
SE Scotland	**B2**	**Pettico Wick**	7	8
	B3	**White Heugh**	10	12

Table S2.3. DISTLM testing the relationship between maximum kelp forest depth and urchin (*Echinus esculentus)* density at sloping gradient sites in two regions of the UK (A and B; Figure 2.1).

Response Variable	SS	P	R^2
Maximum kelp forest depth (m)	15.309	0.0709	0.1367

Table S3.1. The number of individuals retrieved during each sampling period. '-' indicates no sampling took place for that month due to inaccessibility.

Site	Sampling Month								
	October	November	December	February	March	April	May	June	August
A1	-	9	-	-	-	-	7	-	4
A2	-	10	9	8	-	7	7	6	7
B1	-	-	-	-	8	-	-	8	-
B2	-	-	-	8	8	-	6	4	9
C1	9	9	5	-	15	-	19	-	10
C2	10	-	-	-	-	-	10	10	10

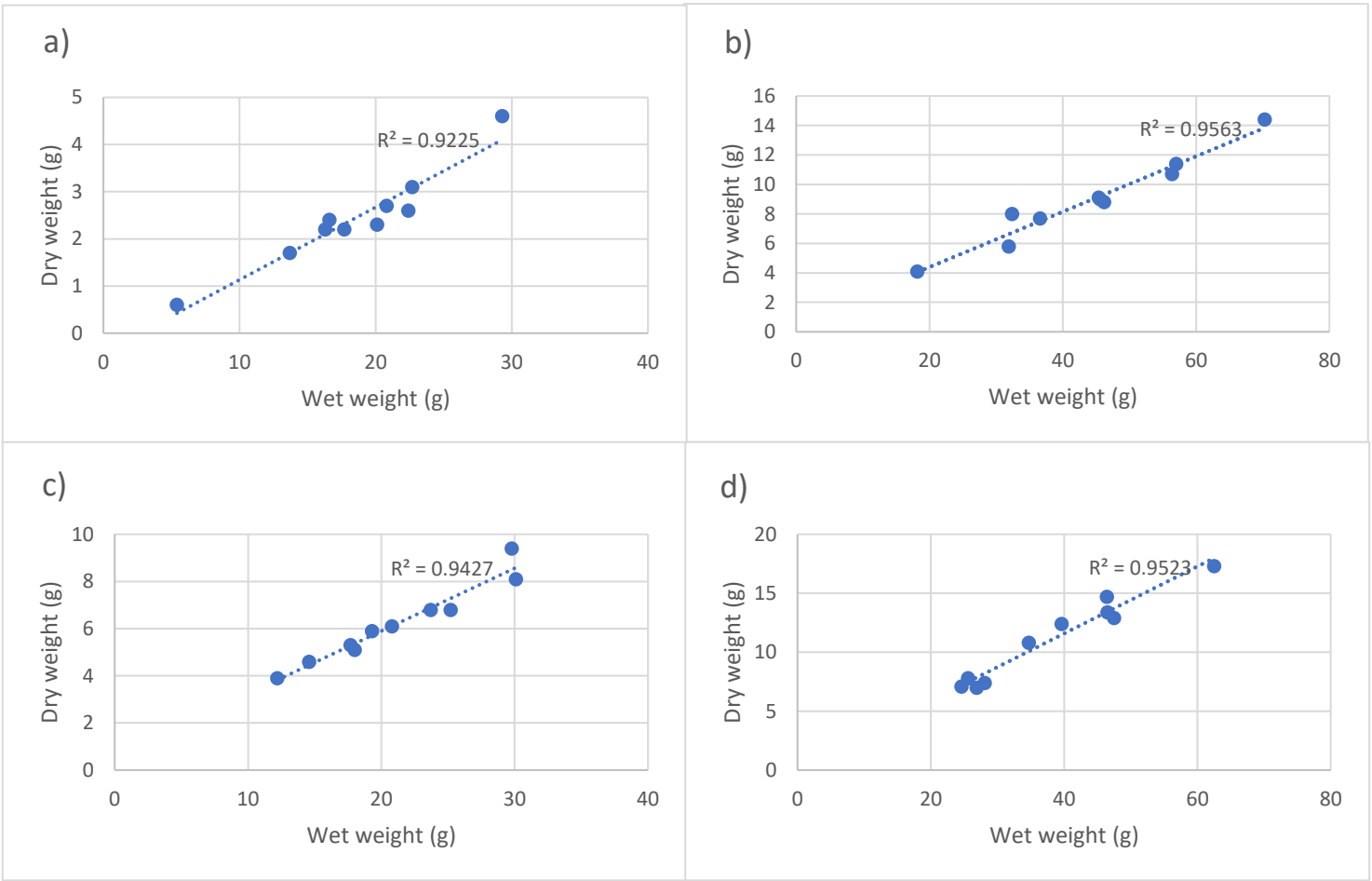

Figure S3.1. Relationship between fresh weight and dry weight of distal (a & c) and basal (b & d) segments of kelp blades from sites B1 (c & d) and B2 (a & b). Sites and locations can be seen in Figure 3.1.

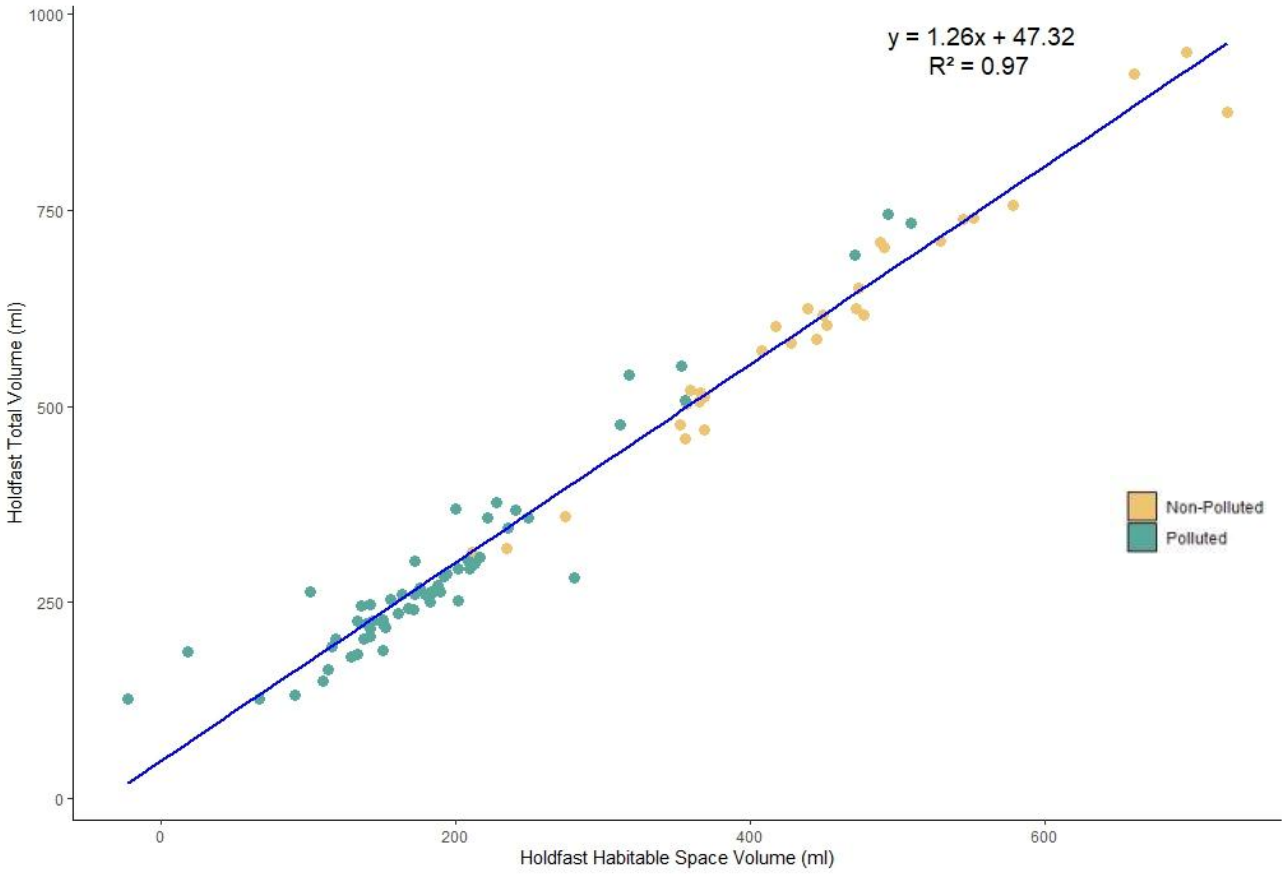

Figure S4.1. Correlation between total holdfast volume and the volume of habitable space n = 90.

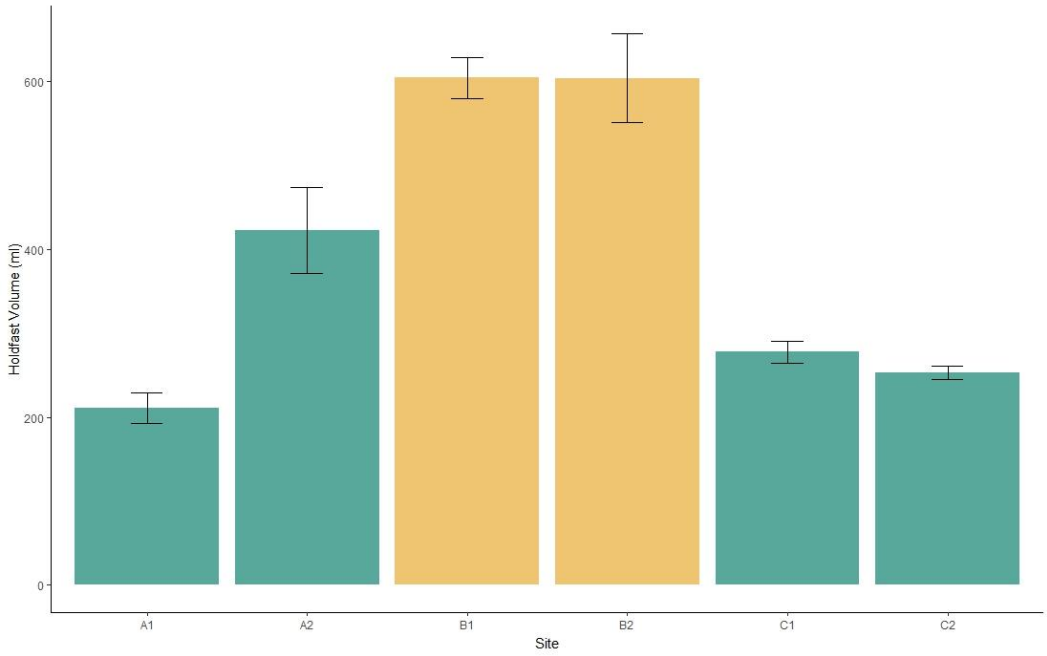

Figure S4.2. Holdfast volume (ml) measured by displacement of water.

Table S4.1. Univariate PERMANOVA testing variation in holdfast volume between sites and levels of pollution. Results indicated with 'ŧ' are derived from Monte-Carlo simulations due to a low number of unique permutations. Significant results are indicated in **bold**.

		Holdfast Volume	
	df	*F*	p
Pollution	1	20.70	**0.0092**ŧ
Site(Pollution)	4	1.69	0.1788
Res df	24		

Table S4.2. Top 5 taxa contributing to the observed dissimilarity of kelp holdfast associated macroinvertebrate assemblages. Percentage contributions determined by SIMPER analysis carried out on significant pairwise comparisons at the site level identified by PERMANOVA analysis.

Taxa	Average abundance		Average dissimilarity	Dissimilarity / SD	Contribution to dissimilarity (%)	Cumulative contribution to dissimilarity (%)
Average dissimilarity = 73.40%	**A1**	**C2**				
Modiolus modiolus	0.75	13.98	17.17	4.10	23.40	23.40
Verruca stroemia	3.58	8.83	8.55	1.95	11.65	35.05
Nemertea	0.00	5.05	6.26	1.85	8.52	43.57
Balanus crenatus	1.08	5.15	5.24	1.29	7.14	50.71
Hiatella arctica	0.73	3.09	3.08	1.87	4.20	54.91
Average dissimilarity = 68.24%	**A1**	**C1**				
Verruca stroemia	3.58	10.37	12.36	2.30	18.12	18.12
Anomia ephippium	3.01	4.99	5.85	1.82	8.57	26.69
Nemertea	0.00	3.46	5.35	1.07	7.84	34.53
Modiolus modiolus	0.75	3.16	4.81	1.40	7.05	41.59
Sabellaria spinulosa	2.26	1.38	3.14	1.12	4.60	46.19

Average dissimilarity = 58.25%	**A2**	**C2**				
Modiolus modiolus	3.30	13.98	10.45	2.97	17.94	17.94
Verruca stroemia	4.10	8.83	6.64	1.61	11.40	29.34
Nemertea	0.45	5.05	4.48	1.59	7.69	37.03
Balanus crenatus	3.69	5.15	2.47	0.94	4.25	41.28
Sabellaria spinulosa	3.40	1.21	2.29	1.43	3.93	45.20

Average dissimilarity = 59.03%	**A2**	**C1**				
Verruca stroemia	4.10	10.37	8.56	1.66	14.51	14.51
Nemertea	0.45	3.46	3.82	1.09	6.47	20.98
Balanus crenatus	3.69	0.75	3.63	1.93	6.14	27.13
Anomia ephippium	5.52	4.99	3.40	1.48	5.76	32.89
Sabellaria spinulosa	3.40	1.38	2.62	1.27	4.45	37.34

Average dissimilarity = 54.37%	**C2**	**C1**				
Modiolus modiolus	13.98	3.16	11.11	2.48	20.44	20.44
Verruca stroemia	8.83	10.37	4.60	1.41	8.46	28.91
Balanus crenatus	5.15	0.75	4.51	1.34	8.29	37.19
Nemertea	5.05	3.46	3.91	1.35	7.20	44.39
Anomia ephippium	4.93	4.99	2.43	1.90	4.47	48.86

Average dissimilarity = 50.70%	**B2**	**B1**				
Anomia ephippium	5.68	8.60	2.21	1.62	4.35	4.35
Nemertea	0.57	3.46	1.99	1.62	3.92	8.27
Verruca stroemia	3.86	5.31	1.73	1.60	3.41	11.69
Pododesmus patelliformis	2.42	0.00	1.54	1.14	3.03	14.72
Ophiothrix fragilis	2.68	0.60	1.32	1.93	2.60	17.32

Table S4.3. Top 5 (or the highest number available) taxa contributing to the observed dissimilarity of kelp stipe associated macroinvertebrate assemblage. Percentage contributions determined by SIMPER analysis carried out on significant pairwise comparisons at the site level identified by PERMANOVA analysis.

Taxa	Average abundance		Average dissimilarity	Dissimilarity / SD	Contribution to dissimilarity (%)	Cumulative contribution to dissimilarity (%)
Average dissimilarity = 85.43%	**A1**	**A2**				
Modiolus modiolus	0.00	2.52	17.81	2.20	20.85	20.85
Patella pellucida	2.51	1.06	14.71	1.74	17.22	38.07
Lacuna vincta	2.18	0.35	14.02	1.99	16.41	54.48
Amphipholis squamata	0.00	0.75	6.04	1.03	7.07	61.55
Porcellana platycheles	0.00	0.80	5.91	1.44	6.92	68.47
Average dissimilarity = 51.54%	**A1**	**C1**				
Lacuna vincta	2.18	4.99	15.84	1.58	30.73	30.73
Patella pellucida	2.51	4.30	10.84	1.03	21.03	51.76
Corophiidae	0.60	1.86	7.46	1.43	14.47	66.23
Modiolus modiolus	0.00	0.97	4.91	1.63	9.52	75.75
Average dissimilarity = 76.23%	**A2**	**C1**				
Lacuna vincta	0.35	4.99	22.71	3.17	29.79	29.79
Patella pellucida	1.06	4.30	15.97	2.25	20.95	50.74
Corophiidae	0.40	1.86	7.29	1.85	9.56	60.30
Modiolus modiolus	2.52	0.97	6.76	1.09	8.87	69.17
Ampithoe rubricata	0.00	1.06	4.01	0.79	5.26	74.43

Table S5.1. The number of unique bacterial ASVs identified on the surface of different *Laminaria hyperborea* tissue types and rocks and within the water column.

Tissue	**No. of ASVs**
Blade	776
Holdfast	3110
Rock	3609
Water	1767
Total	6521

Table S5.2. SIMPER analysis for sites based on significant pairwise comparisons identified by PERMANOVA analysis. Taxa presented are top 3 contributors to observed dissimilarity between sites within the whole bacterial microbiome. Sites can be seen in Figure 5.2.

Taxa	Average abundance		Average dissimilarity	Dissimilarity / SD	Contribution to dissimilarity (%)	Cumulative contribution to dissimilarity (%)
Average dissimilarity = 85.06%	**C1**	**A1**				
ASV2: *Blastopirellula sp.*	0.03	0.04	2.76	0.81	3.25	3.25
ASV6: *Granulosicoccus sp.*	0.03	0.03	2.10	0.73	2.47	5.72
ASV3: *Amylibacter ulvae*	0.03	0.03	1.99	0.85	2.35	8.06
Average dissimilarity = 83.04%	**B1**	**B2**				
ASV2: *Blastopirellula sp.*	0.04	0.03	2.57	0.75	3.09	3.09
ASV5: *Hyphomonadaceae* (F)	0.03	0.01	1.94	0.72	2.34	5.43
ASV3: *Amylibacter ulvae*	0.02	0.02	1.68	0.83	2.02	7.46
Average dissimilarity = 86.05%	**A1**	**A2**				
ASV2: *Blastopirellula sp.*	0.04	0.04	2.88	0.81	3.35	3.35
ASV7: *Litorimonas sp.*	0.03	0.01	1.60	0.73	1.86	5.21
ASV5: *Hyphomonadaceae* (F)	0.03	0.01	1.52	0.60	1.77	6.98
Average dissimilarity = 81.02%	**C1**	**C2**				
ASV2: *Blastopirellula sp.*	0.03	0.06	3.52	0.73	4.35	4.35
ASV4: *Blastopirellula sp.*	0.01	0.04	2.32	0.61	2.86	7.21
ASV3: *Amylibacter ulvae*	0.03	0.03	2.23	0.86	2.75	9.96
Average dissimilarity = 84.70%	**A1**	**C2**				
ASV2: *Blastopirellula sp.*	0.04	0.06	3.73	0.76	4.40	4.40
ASV4: *Blastopirellula sp.*	0.02	0.04	2.40	0.65	2.83	7.24
ASV3: *Amylibacter ulvae*	0.03	0.03	2.19	0.85	2.58	9.82
Average dissimilarity = 83.30%	**C2**	**A2**				
ASV2: *Blastopirellula sp.*	0.03	0.04	2.67	0.83	3.21	3.21
ASV3: *Amylibacter ulvae*	0.03	0.01	1.59	0.80	1.91	5.12
ASV6: *Granulosicoccus sp.*	0.03	0.01	1.55	0.60	1.86	6.97
Average dissimilarity = 83.30%	**C1**	**A2**				
ASV2: *Blastopirellula sp.*	0.03	0.04	2.67	0.83	3.21	3.21
ASV3: *Amylibacter ulvae*	0.03	0.01	1.59	0.80	1.91	5.12
ASV6: *Granulosicoccus sp.*	0.03	0.01	1.55	0.60	1.86	6.97

Table S5.3. SIMPER analysis for sample type based on significant pairwise comparisons identified by PERMANOVA analysis. Taxa presented are top 3 contributors to observed dissimilarity between tissue types within the whole microbiome samples. Sites can be seen in Figure 5.2.

Taxa	Average abundance		Average dissimilarity	Dissimilarity / SD	Contribution to dissimilarity (%)	Cumulative contribution to dissimilarity (%)
Average dissimilarity = 93.24%	**Blade**	**Holdfast**				
ASV2: *Blastopirellula sp.*	0.14	0.01	7.10	2.04	7.62	7.62
ASV5: *Hyphomonadaceae* (F)	0.07	0.00	3.35	1.32	3.59	11.21
ASV6: *Granulosicoccus sp.*	0.07	0.00	3.31	1.41	3.55	14.77
Average dissimilarity = 97.21%	**Blade**	**Rock**				
ASV2: *Blastopirellula sp.*	0.14	0.00	7.31	2.09	7.52	7.52
ASV5: *Hyphomonadaceae* (F)	0.07	0.00	3.42	1.36	3.51	11.03
ASV6: *Granulosicoccus sp.*	0.07	0.00	3.40	1.45	3.50	14.53
Average dissimilarity = 98.56%	**Blade**	**Water**				
ASV2: *Blastopirellula sp.*	0.14	0.00	7.42	2.13	7.52	7.52
ASV3: *Amylibacter ulvae*	0.00	0.09	4.48	3.03	4.55	12.07
ASV6: *Granulosicoccus sp.*	0.07	0.00	3.43	1.46	3.48	15.55
Average dissimilarity = 75.41%	**Holdfast**	**Rock**				
ASV44: *Blastopirellula sp*	0.02	0.00	0.99	1.16	1.31	1.31
ASV21: *Illuminobacter nomiensis*	0.01	0.02	0.89	1.29	1.18	2.49
ASV81: *Perspicuibacter sp.*	0.01	0.00	0.67	0.24	0.89	3.38
Average dissimilarity = 91.61%	**Holdfast**	**Water**				
ASV3: *Amylibacter ulvae*	0.00	0.09	4.30	2.87	4.70	4.70
ASV9: SAR86_clade (O)	0.00	0.04	2.22	1.95	2.43	7.12
ASV11: SAR11_clade_Ia	0.00	0.04	1.90	2.99	2.07	9.19
Average dissimilarity = 93.05%	**Rock**	**Water**				
ASV3: *Amylibacter ulvae*	0.00	0.09	4.47	3.02	4.80	4.80
ASV9: SAR86_clade (O)	0.00	0.04	2.22	1.95	2.39	7.20
ASV11: SAR11_clade_Ia	0.00	0.04	1.90	2.99	2.04	9.23

Table S5.4. SIMPER analysis for sample type on significant pairwise comparisons identified by PERMANOVA analysis. Taxa presented are top 3 contributors to observed dissimilarity between tissue types in the core bacterial microbiome. Core bacterial microbiome is defined as the ASVs present in 95% of samples at a relative abundance of >0.1%.

Taxa	Average abundance		Average dissimilarity	Dissimilarity / SD	Contribution to dissimilarity (%)	Cumulative contribution to dissimilarity (%)
Average dissimilarity = 98.86%	**Blade**	**Holdfast**				
ASV2: *Blastopirellula sp.*	0.28	0.00	13.89	2.27	14.05	14.05
ASV44: *Blastopirellula sp.*	0.00	0.16	8.21	1.55	8.31	22.36
ASV5: *Hyphomonadaceae* (F)	0.13	0.00	6.60	1.61	6.68	29.04
Average dissimilarity = 100.00%	**Blade**	**Rock**				
ASV21: *Illuminobacter nomiensis*	0.00	0.43	21.65	2.18	21.65	21.65
ASV2: *Blastopirellula sp.*	0.28	0.00	13.89	2.27	13.89	35.54
ASV51: *Filomicrobium sp.*	0.00	0.22	11.12	2.17	11.12	46.66
Average dissimilarity = 100.00%	**Blade**	**Water**				
ASV2: *Blastopirellula sp.*	0.28	0.00	13.89	2.27	13.89	13.89
ASV3: *Amylibacter ulvae*	0.00	0.14	6.79	7.42	6.79	20.68
ASV5: *Hyphomonadaceae* (F)	0.13	0.00	6.60	1.61	6.60	27.29
Average dissimilarity = 69.57%	**Holdfast**	**Rock**				
ASV21: *Illuminobacter nomiensis*	0.11	0.43	16.67	1.73	23.95	23.95
ASV44: *Blastopirellula sp.*	0.16	0.00	8.21	1.55	11.81	35.76
ASV66: *Granulosicoccus sp.*	0.07	0.20	7.76	0.93	11.15	46.91
Average dissimilarity = 95.68%	**Holdfast**	**Water**				
ASV44: *Blastopirellula sp.*	0.16	0.00	8.21	1.55	8.59	8.59
ASV3: *Amylibacter ulvae*	0.00	0.14	6.79	7.42	7.10	15.68
ASV21: *Illuminobacter nomiensis*	0.11	0.01	4.98	1.54	5.20	20.89
Average dissimilarity = 99.00%	**Rock**	**Water**				
ASV21: *Illuminobacter nomiensis*	0.43	0.01	21.14	2.13	21.36	21.36
ASV51: *Filomicrobium sp.*	0.22	0.00	11.12	2.17	11.24	32.60
ASV66: *Granulosicoccus sp.*	0.20	0.00	9.77	1.04	9.87	42.46

Table S5.5. SIMPER analysis for site on significant pairwise comparisons identified by PERMANOVA analysis. Taxa presented are top 3 contributors to observed dissimilarity between tissue types in the core bacterial microbiome. Core bacterial microbiome is defined as the ASVs present in 95% of samples at a relative abundance of >0.1%.

Taxa	Average abundance		Average dissimilarity	Dissimilarity / SD	Contribution to dissimilarity (%)	Cumulative contribution to dissimilarity (%)
Average dissimilarity = 31.47%	**B1**	**B2**				
ASV21: *Illuminobacter nomiensis*	0.06	0.14	4.72	0.60	15.01	15.01
ASV66: *Granulosicoccus sp.*	0.13	0.06	4.33	0.63	13.76	28.76
ASV28: *Rhodobacteracea* (F)	0.00	0.06	2.77	0.30	8.79	37.55
Average dissimilarity = 34.74%	**C1**	**A1**				
ASV66: *Granulosicoccus sp.*	0.03	0.11	5.15	0.61	14.82	14.82
ASV21: *Illuminobacter nomiensis*	0.17	0.08	5.12	0.67	14.73	29.55
ASV25: Gammaproteobacteria (C)	0.08	0.08	2.26	0.56	6.50	36.04
Average dissimilarity = 33.28%	**A1**	**A2**				
ASV21: *Illuminobacter nomiensis*	0.08	0.20	6.23	0.75	18.72	18.72
ASV66: *Granulosicoccus sp.*	0.11	0.02	5.00	0.57	15.03	33.75
ASV2: *Blastopirellula sp.*	0.06	0.11	2.68	0.50	8.06	41.81
Average dissimilarity = 24.96%	**C1**	**C2**				
ASV21: *Illuminobacter nomiensis*	0.17	0.18	2.34	0.73	9.39	9.39
ASV2: *Blastopirellula sp.*	0.06	0.09	1.71	0.40	6.83	16.22
ASV6: *Granulosicoccus sp.*	0.05	0.02	1.44	0.43	5.75	21.97
Average dissimilarity = 32.82%	**A1**	**C2**				
ASV21: *Illuminobacter nomiensis*	0.08	0.18	5.14	0.66	15.66	15.66
ASV66: *Granulosicoccus sp.*	0.11	0.04	4.98	0.62	15.17	30.82
ASV51: *Filomicrobium sp.*	0.08	0.06	2.14	0.53	6.53	37.35
Average dissimilarity = 25.92%	**C2**	**A2**				
ASV21: *Illuminobacter nomiensis*	0.18	0.20	2.66	0.74	10.25	10.25
ASV2: *Blastopirellula sp.*	0.09	0.11	1.80	0.47	6.95	17.20
ASV13: *Blastopirellula sp*	0.04	0.01	1.64	0.53	6.35	23.55
Average dissimilarity = 28.29%	**C1**	**A2**				
ASV21: *Illuminobacter nomiensis*	0.17	0.20	2.65	0.67	9.38	9.38
ASV2: *Blastopirellula sp.*	0.06	0.11	2.63	0.49	9.28	18.66
ASV51: *Filomicrobium sp.*	0.08	0.06	2.10	0.57	7.43	26.09